

# Determination of Fatigue Assessment of Monopile - Based Offshore Wind Turbines through Fidelity Quantification

Ioannis Nikiforakis

Master of Science Thesis





# **Determination of Fatigue Assessment of Monopile – Based Offshore Wind Turbines through Fidelity Quantification**

MASTER OF SCIENCE THESIS

For the degree of Master of Science in Sustainable Energy Technology  
at Delft University of Technology

Ioannis Nikiforakis

4412087

June 12, 2017

Faculty of Aerospace Engineering (AE) and Electrical Engineering, Mathematics and  
Computer Science (EEMCS)



DELFT UNIVERSITY OF TECHNOLOGY  
DEPARTMENT OF  
WIND ENERGY, AEROSPACE ENGINEERING

The following academic staff certifies that it has read and recommends to the Faculty of  
Aerospace Engineering (AE) and Electrical Engineering, Mathematics and  
Computer Science (EEMCS) for acceptance a thesis entitled

DETERMINATION OF FATIGUE ASSESSMENT OF MONOPILE – BASED OFFSHORE WIND  
TURBINES THROUGH FIDELITY QUANTIFICATION

by

IOANNIS NIKIFORAKIS

in partial fulfillment of the requirements for the degree of  
MASTER OF SCIENCE SUSTAINABLE ENERGY TECHNOLOGY

Dated: June 12, 2017

Supervisor(s):

Dr. ir. M. Zaaijer

MSc S. Sanchez Perez-Moreno

Reader(s):

Prof. dr. G. van Bussel

Dr. ir. M. Zaaijer

MSc S. Sanchez Perez-Moreno

Dr. ir. G. La Rocca



## Abstract

The application of stability checks in simulated offshore wind structures is performed through tools that are established in the offshore wind industry. In particular, the structure should fulfill certain strength and fatigue criteria among which Fatigue Limit States (FLSs) checks are critical. In terms of the process, fatigue assessment can be carried out in both time (TD) and frequency domain (FD), with the former being more popular in the offshore wind energy sector. Nevertheless, simplified tools in the FD have been suggested, since they yield results similar to those of the TD analysis. In order to decide upon the choice of tool in performing the FLS estimations, a relative comparison should be implemented. Particularly, fatigue assessment in the TD, fatigue assessment in the FD and a simplified type of fatigue assessment in the FD are examined. These types of fatigue assessment are conducted in three respective tools, with the TD type conducted in NREL's FAST v8 and both the FD types simulated within MATLAB tools. The tools are judged upon the desirable levels of Modelling & Simulation (M&S) fidelity. A set of criteria are defined for the particular use case, in an attempt to express that fidelity. The criteria's metrics are additionally provided in the proposed methodology and associated measurements are taken during simulations. Only after conducting further multi-criteria decision analyses (MCDA), the eventual levels of fidelity for the three types of fatigue assessment result to a consequent ranking among the tools. Therefore, the measured criteria lead to the quantification of these levels of fidelity for all three tools and the application of MCDA results to their ranking. The proposed fidelity framework is applied in a case study in order to evaluate the proposed methodology, as well as to select the type of fatigue assessment and consequent tool that should be used within an early design stage. The results indicate that the simplified fatigue assessment in the FD should be preferred over conventional fatigue assessment in both TD & FD. In addition, the criteria included in the fidelity framework seem to provide a multifaceted approach, since none of the tools is favored in all categories. Finally, similarities in results between relevant types of conducted comparisons as well as between different types of MCDA, enhance the consistency of the proposed fidelity methodology and increase its credibility.



## Acknowledgments

I would like to express my gratitude to the individuals that have helped me throughout the compilation of the particular thesis.

Primarily, I would like to thank both my supervisors, Dr. ir. M. Zaaijer and MSc S. Sanchez Perez-Moreno, for the support and guidance they provided through all stages of this thesis. Their constant availability and intention to assist, not only in the biweekly meetings, but whenever needed, greatly contributed to the finalization of this MScThesis.

I would also like to thank Dr. ir. Eliz-Mari Lourens as well as Ir. Pim van der Male, for granting me access to licensed operation of GH Bladed.

Finally, the unconditional support of family and friends was crucial throughout the conduction of this thesis, from beginning to end, and I would like to express my sincere gratitude for everything they offered.

Ioannis Nikiforakis

Delft University of Technology

June 12, 2017



# Nomenclature

$\alpha$	Power Law Exponent
$\log(\alpha)$	Intercept of $\log N$ axis by S-N curve
$\alpha_{JS}$	Parameter in the JONSWAP equation
$\gamma$	Unit Weight Length
$\gamma_{JS}$	Peak Enhancement Factor
$\gamma_f$	Material Factor
$\gamma_p$	Peak Enhancement Parameter
$\lambda_{max}$	Maximum Eigen Value
$\mu$	Tower per meter Mass
$\rho_{air}$	Air density
$\rho_s$	Steel Density
$\rho_w$	Water Density
$\sigma_t$	Wind Speed Standard Deviation
$\Delta\sigma$	Stress Range
$\sigma_{ss}$	Sea Surface Elevation Standard Deviation
$\varphi$	Friction Angle
$\Omega$	Rotor's Rotational Speed
<i>AGARD</i>	Advisory Group of Aerospace and Research Development
<i>AHP</i>	Analytical Hierarchy Process
$[A_i]$	Accuracy Comparison Matrix
$a_{ij}$	Matrix Component
$[A_j]$	Judgmental Matrix
$[A_{jnorm}]$	Normalized Judgmental Matrix
$C_{DP}$	Pile's Drag Coefficient
$C_{DSP}$	Submerged Structure's Drag Coefficient
$C_{DT}$	Tower's Drag Coefficient
<i>CI</i>	Consistency Index
$[C_{ii}]$	Comparison Matrix's Weighting Vector
$C_{MP}$	Pile's Inertia Coefficient
$C_{MSP}$	Submerged Structure's Inertia Coefficient
$C_n$	Fourier Coefficient
$C_{TR}$	Rotor's Thrust Coefficient
$C_u$	Undrained Shear Strength
$d$	Sea Depth
<i>DAF</i>	Dynamic Amplification Factor
<i>Damage</i>	Fatigue Damage
$dd$	Design driver
<i>DEL</i>	Damage Equivalent Load
$dF$	Morrison's Hydrodynamic Load Term
<i>DFT</i>	Discrete Fourier Transform
$[D_i]$	Detail's Comparison Matrix
<i>DIS</i>	Distributed Interactive Simulation
$D_R$	Rotor's Diameter
$D_T$	Tower's Diameter
$D_{Tb}$	Tower's Base Diameter

$D_{TP}$	Diameter of Transition Piece
$D_{Tt}$	Tower's Top Diameter
$D_Y$	Yaw Bearing Diameter
$E$	Young's Module of Elasticity
$EF$	Experimental Frame
$EI$	Bending Stiffness
$f$	Frequency
$f(s)$	Frequency Domain signal
$f(t)$	Time Domain signal
$F[m]$	N-tuple of discrete signal
$FAA$	Federal Aviation Administration
$FD$	Frequency Domain
$FFT$	Fast Fourier Transformation
$F_i$	Fatigue Load Case
$FLOP$	Floating Point Operation
$FLS$	Fatigue Limit State
$f_p$	Wave Spectral Peak Frequency
$FT$	Fourier Transformation
$g$	Acceleration of Gravity
$HLA$	High Level Architecture
$H_s$	Significant Wave Height
$I$	Moment of Inertia
$IEEE$	Institute of Electrical and Electronics Engineers
$IFFT$	Inverse Fast Fourier Transformation
$iv$	Independent variable
$JAA TO$	Joint Aviation Authorities Administration Training Organization
$k$	Stiffness
$L_g$	Grout Length
$L_i$	Velocity Component Integral Scale Parameter
$L_P$	Penetration Length
$L_s$	Scour Length
$m$	Negative Slope of N-S Curve
$M\&S$	Modelling & Simulation
$M_A$	Metric for Accuracy
$MCDA$	Multi-Criteria Decision Analysis
$M_D$	Metric for Detail
$MDAO$	Multidisciplinary Design, Optimization & Analysis
$M_{OT}$	Metric for Operational Time
$m_{RNA}$	Mass of Rotor – Nacelle Assembly
$M_{ST}$	Metric for Time of Simulation
$N_{eq}$	Equivalent Cycles
$N_i$	Cycles to failure
$n_i$	Cycles of signal $f_i$
$N_p$	Number of parameters
$N_r$	Number of referent parameters
$OT$	Operational Time
$OWF$	Offshore Wind Farm
$P_{occ}$	Probability of Occurrence
$PSD$	Power Spectral Density
$RFC$	Rain-Flow Counting

<i>RI</i>	Random Index
<i>r<sub>N</sub></i>	Referent Factor of the N parameter
<i>RNA</i>	Rotor – Nacelle Assembly
<i>S<sub>1</sub></i>	First Set of Simulations
<i>S<sub>2</sub></i>	Second Set of Simulations
<i>SCF</i>	Stress Concentration Factor
<i>S<sub>Ftop</sub></i>	Tower Top Load Spectrum
<i>SISO</i>	Simulation Interoperability Standards Organization
<i>S<sub>JS</sub></i>	JONSWAP Spectrum
<i>S<sub>Kaimal</sub></i>	Kaimal Spectrum
<i>S<sub>Karman</sub></i>	von Karman Spectrum
<i>S-N</i>	Stress – Cycles Curve
<i>ST</i>	Time of Simulation
<i>S<sub>v</sub></i>	Aerodynamic Load Spectrum
<i>TD</i>	Time Domain
<i>t<sub>g</sub></i>	Grout Thickness
<i>TI</i>	Longitudinal Turbulence Intensity
<i>T<sub>p</sub></i>	Wave Peak Period
<i>TP</i>	Transition Piece
<i>t<sub>P</sub></i>	Pile Wall Thickness
<i>T<sub>R</sub></i>	Rotor’s Thrust
<i>TR</i>	Tidal Range
<i>TRF</i>	Transfer Function
<i>t<sub>TP</sub></i>	Transition Piece Wall Thickness
<i>t<sub>Tt</sub></i>	Tower Top Wall Thickness
<i>U</i>	Instantaneous Wind Speed
$\bar{U}$	Average Wind Speed
<i>ULS</i>	Ultimate Limit State
<i>u<sub>w</sub></i>	Water Particle Velocity
<i>v<sub>p</sub></i>	Expected Peak Occurrence Frequency
<i>W</i>	Weighting Vector resulting from Judgmental Matrix
<i>x<sub>CM</sub></i>	Center of Mass Position
<i>Z</i>	Normalized Amplitude
<i>Z<sub>hub</sub></i>	Hub Height
<i>Z<sub>0</sub></i>	Surface Roughness
<i>Z<sub>P</sub></i>	Platform Height
<i>Z<sub>TP</sub></i>	Transition Piece Elevation



# Table of Contents

Abstract .....	i
Acknowledgments.....	iii
Nomenclature .....	v
List of Figures .....	xi
List of Tables .....	xiii
1. Introduction .....	1
1.1 Background Information .....	1
1.2 Problem Analysis .....	3
1.3 Objectives .....	4
1.4 Approach.....	5
1.5 Thesis Outline.....	6
2. Proposed Methodology .....	9
2.1 Conceptualizing Fidelity .....	9
2.2 Fidelity Criteria .....	11
2.2.1 Accuracy .....	13
2.2.2 Time of Simulation.....	14
2.2.3 Operational Time .....	14
2.2.4 Detail .....	15
2.3 Tool Ranking through MCDA.....	22
3. Use case .....	27
3.1 Particularities of the Use Case .....	27
3.2 Tools .....	29
3.2.1 Time & Frequency Domains .....	29
3.2.2 Fatigue Assessment in the Frequency domain - Tool 1 .....	30
3.2.3 Simplified Fatigue Assessment in the Frequency Domain – Tool 2 .....	31
3.2.4 Fatigue Assessment in the Time Domain – Tool 3.....	31
4. Fatigue Specification .....	33
4.1 Fatigue Assessment .....	33
4.2 Aerodynamic Loading .....	34
4.3 Hydrodynamic Loading .....	35
4.4 Soil .....	38

4.5 Additional Variable Loading .....	38
4.6 Fatigue .....	38
4.7 Rain Flow Counting & Dirlik Method .....	39
4.8 S-N curve .....	40
4.9 Fatigue Damage.....	42
4.10 Damage Equivalent Load .....	42
5. Generic Application of the Fidelity Framework .....	43
5.1 Referent Framework of Parameters.....	43
5.2 Implementation of Criteria .....	47
6. Case Study.....	49
6.1 Selection of Location .....	49
6.2 Environmental Data.....	49
6.3 Wind Turbine Selection.....	52
6.4 Support Structure Configuration .....	53
6.5 Scoring of Criteria .....	56
6.5.1 Accuracy .....	56
6.5.2 Time of Simulation.....	57
6.5.3 Operational Time .....	58
6.5.4 Detail .....	59
6.6 Tool Ranking.....	64
6.6.1 AHP .....	64
6.6.2 Monte Carlo Method .....	69
6.7 Discussion.....	71
7. Conclusions & Recommendations.....	75
7.1 Conclusions .....	75
7.2 Recommendations for Future Work.....	77
Bibliography.....	79
Appendix A – Environmental Data .....	83
Appendix B – Sensitivity Analyses Data.....	85
Appendix C – Times of Simulation .....	89
Appendix D – Operational Times .....	91
Appendix E – Alternative Patterns .....	95

# List of Figures

<b>1.1:</b> Modelling and simulation process according to Benjamin P.[2].....	6
<b>2.1:</b> The Fidelity Framework with SOU and SDU [44]. .....	10
<b>2.2:</b> Implementation of Fidelity-Related Concepts [46]. .....	11
<b>2.3:</b> Relationships between Reality, Simuland and Model as illustrated by Roza [45]. .....	12
<b>2.4:</b> Real-World, Conceptual Model & Simulation Model Relations [45].....	16
<b>2.5:</b> Detail, Resolution and Accuracy of the Real-World Referent and Simulation System [45]...	17
<b>2.6:</b> Sensitivity analysis of varying site conditions in respect to DEL [36]. .....	18
<b>2.7:</b> Interaction of Detail for The Fidelity Definition and Metrics (FDM –ISG) [46]. .....	19
<b>2.8:</b> The proposed algorithms in order to acquire the score of a tool for the detail criterion.....	21
<b>2.9:</b> Most preferred alternatives at all possible weight combinations for the 3 attributes [3].....	26
<b>3.1:</b> Part of the Middelgrunden wind farm [1]. .....	27
<b>3.2:</b> Flow Chart of the Design Process an Offshore Wind Support Structure [28].....	28
<b>3.3:</b> Illustration of signals in time(left) and frequency(right) domains. ....	29
<b>3.4:</b> Conversion from both TD to FD via FFT as well as from FD to TD through IFFT [48]. .....	30
<b>3.5:</b> The by-pass of the TRF as proposed in [36]. .....	31
<b>3.6:</b> FAST v8 control volumes (BeamDyn, IceFloe and IceDyn are not shown) [54]. .....	32
<b>4.1:</b> Load sources for a monopile-based offshore wind turbine [27]. .....	33
<b>4.2:</b> JONSWAP (red line) and PM (black dotted line) spectrums for North Sea storm state [18]..	37
<b>4.3:</b> Stress plotted versus time (left), imperfections due to stress concentrations (right) [57]. ...	39
<b>4.4:</b> The emerging half cycles of trough and peak generated stress ranges [55]. .....	40
<b>4.5:</b> Various suggestions on S-N slopes [53]. .....	41
<b>6.1:</b> Site location indicated by the red X sign [60]. .....	49
<b>6.2:</b> Relative wind distribution for the particular location [61]. .....	51
<b>6.3:</b> Several locations among the installation site with their respective soil profiles.....	52
<b>6.4:</b> Qualitative diagram of frequency regions [29].....	53
<b>6.5:</b> Design of the offshore wind structure within the case study.....	55
<b>6.6:</b> Results of Sensitivity Analyses for the 6 parameters of the memorandum in Tool 1. ....	60
<b>6.7:</b> Results of Sensitivity Analyses for the 13 parameters of the memorandum in Tool 2. ....	62
<b>6.8:</b> Enlarged version of Figure 6.7 in the ratios of 0 – 3.5, for fatigue damage ratios.....	62
<b>6.9:</b> The pie charts that display the percentages of 1 <sup>st</sup> , 2 <sup>nd</sup> and 3 <sup>rd</sup> position.....	70
<b>6.10:</b> Illustration of all criteria scores of Detail, Accuracy, ST and OT for all 3 Tools.....	71
<b>6.11:</b> Damage plotted versus pile’s wall thickness in Tools 1 and 2. ....	72
<b>6.12:</b> Illustration of all critetia scores for Detail, Accuracy, ST and OT for Tools 1 and 2. ....	73
<b>A.1:</b> Sea elevations in the installation site, in respect to MSL. ....	84
<b>A.2:</b> The S-N curve used in fatigue assessment [9] .....	84



## List of Tables

<b>2.1:</b> The Fundamental Scale [47].	24
<b>2.2:</b> RI for different values of n [30].	25
<b>5.1:</b> Parameters related to Aerodynamic Loading.	44
<b>5.2:</b> Parameters related to hydrodynamic loading.	45
<b>5.3:</b> Parameters related to soil configuration.	46
<b>5.4:</b> Parameters set by turbine manufacturers	46
<b>5.5:</b> Structural & design parameters.	47
<b>6.1:</b> Final environmental states as resulted from data processing.	50
<b>6.2:</b> Soil properties in depth [m] below mudline.	52
<b>6.3:</b> Basic properties of 5MW NREL offshore wind turbine [22].	53
<b>6.4:</b> Dimensions & Elevations of pile and transition piece.	54
<b>6.5:</b> Values of the proposed Accuracy metric for Tools 1,2 and 3 for the case study.	56
<b>6.6:</b> Values of ST proposed metric for Tools 1 and 2 for the case study.	57
<b>6.7:</b> Values of ST proposed metric for all 3 tools for the case study.	57
<b>6.8:</b> Values of the OT Metric for Tools 1 and 2 in their comparison for the case study.	58
<b>6.9:</b> Values of the OT Metric for all 3 tools in their comparison for the case study.	58
<b>6.10:</b> Detail Metric values for Tools 1 and 2, in their comparison for the case study.	63
<b>6.11:</b> Detail Metric values for Tools 1, 2 and 3, in their comparison for the case study.	64
<b>6.12:</b> Values of all criteria for both Tools 1 and 2 in their comparison for the case study.	66
<b>6.13:</b> Rankings and scores for each alternative between Tools 1 and 2.	67
<b>6.14:</b> Values of all criteria for all Tools 1, 2 and 3 in their comparison for the case study.	68
<b>6.15:</b> Rankings and Scores of Tools 1, 2 and 3 resulting from the AHP.	69
<b>6.16:</b> Rankings and scores of all 3 tools in case of omission of OT for the case study.	73
<b>6.17:</b> Ranking and Scores for Tools 1,2 and 3 after omitting the MCDA.	74
<b>A.1:</b> The 3-D scatter diagram that was used in order to extract initial lumped states.	83
<b>A.2:</b> The lumped environmental states, as resulted from A.1.	84
<b>B.1:</b> Results of Sensitivity Analyses of simulations $S_1$ & $S_2$ in Tool 1.	85
<b>B.2:</b> Results of Sensitivity Analyses of simulations $S_1$ & $S_2$ in Tool 2.	86
<b>C.1:</b> Time of Simulation as measured in Tool 1 for all lumped cases of the case study.	89
<b>C.2:</b> Times of Simulation as measured in Tool 2 for the case study.	89
<b>C.3:</b> Times of Simulation of the first 7 lumped states of the case study in Tool 3.	90
<b>C.4:</b> Times of Simulation of the last 6 lumped states of the case study in Tool 3.	90
<b>D.1:</b> PRT and Operational Time for each of the first 8 lumped states of the use case.	91
<b>D.2:</b> Operational Time for the latter 5 lumped cases and POT of Tool 1 for the case study.	91
<b>D.3:</b> Operational Time as measured in Tool 2 for the case study.	92
<b>D.4:</b> Operational Time for the first 8 lumped cases and PRT in Tool 3 for the case study.	92
<b>D.5:</b> Operational Time for the latter 5 lumped cases and POT in Tool 3 for the case study.	93



# 1.Introduction

This chapter introduces the reader to the concept of model fidelity and addresses the need for its application in the offshore wind industry. In order of presentation, at first background information relating to the offshore wind energy sector is provided, in order to present all incentives that led to the compilation of this thesis. To continue, the problem was identified in the conventional use of a limited number of tools in order to perform stability checks. In addition, the absence of proper justification for their use over similar, more cost-efficient tools, is discussed. Especially in terms of strength & fatigue checks, the use of popular tools that operate in the TD, such as GH Bladed, is established in almost every design stage of offshore wind farms (OWFs) [48]. The assessment of alternatives should be examined and a particular fidelity framework should be established in order to achieve that. Consequently, the adopted approach that should result to the relative comparison between the associated to FLS estimations tools is described. All relevant steps that led to the proposed fidelity framework are provided and an additional description of the following chapters is displayed.

## 1.1 Background Information

Despite the fact that the number of offshore wind farms (OWFs) has significantly increased during the past decade, the offshore wind energy sector has determined that further development would mainly emerge from the reduction of cost per kWh [26]. Therefore, this cost reduction has been acknowledged among absolute priorities in order for the offshore wind industry to compete with other renewable energy sources, as well as fossil fuels, in the near future. Specifically, cost breakdown in offshore wind turbines suggested that the costs of wind turbines and their support structures are among the most significant. Even if the cost of wind turbines in multiple cases consists of more than 40% of the overall investment, the cost of the support structures is additionally significant, as it comprised in certain cases approximately one quarter of the overall wind farm cost [28]. At this point, the fact that the industry is oriented towards installation at larger depths renders the design of support structure and its consequent cost of utter significance [48].

The configuration of support structure consists of a significant part of the early design. The structure has to fulfill, among others, certain strength and fatigue criteria in order to function for the predetermined lifetime of the wind farm, which is nominally 20 years. In further detail, Ultimate Limit States (ULSs) and Fatigue Limit States (FLSs) have been established within the industry in order to assess the relevant structures [17]. Consequently, the determination of fatigue damage is rendered as one of the design drivers of offshore wind structures. Thus fatigue assessment should be thoroughly examined in order to result to the appropriate dimensioning of the structure.

At an early design stage, the structure is modelled and simulated accordingly, in order to determine the preliminary design and move to the detailed analysis [28]. In particular, fatigue assessment is executed in both time and frequency domain (TD and FD), while in the latter a significant number of simplified approaches has been recently suggested [36]. The above fact predisposes the inevitable application of different types of assessment, and thus the use of different tools for the same use case. The above claim is even intensified by the fact that the

selection of tool is not frequently conducted upon a predefined framework of criteria that are relevant to the particularities of the use case [48].

Fatigue assessment in TD is considered the main practice and advanced software is used in the offshore wind industry [36]. Certain tools that operate in the TD are GH Bladed, NREL's FAST and ECN's Phatas, with the first being the most popular. In addition, TD simulations enable the user to take into account all non-linearities of turbine operations, hence are considered more accurate. Nevertheless, that advanced software is associated with timely and thus costly simulations [48]. As a result, alternative ways of assessment should be examined, at least at an early design stage.

FD tools are gaining attention in the determination of fatigue damage of offshore wind structures, with the inclusion of tools that perform simplified types of fatigue assessment. Turbload by Garrad Hassan and ECN's Turbu are the two main frequency domain tools [10] [32]. However the addition of numerous MATLAB models for multiple respective use cases has been recently gaining significant attention. In offshore engineering in particular, FD analysis is recommended due to the effective linearization of wave loads [48]. Moreover, the main advantage of the use of FD tools is associated with the speed of simulation, which is significantly greater than in respective TD tools [36]. In addition, the significant cost of licensed operation of popular TD tools, such as GH Bladed, led to the assessment of other tools that operate in the FD. Overall, wide application of FD analysis in the offshore oil and gas industry [48] encourages the usage of FD tools over the respective of the TD.

In order to decide upon the most adequate tool for the conduction of fatigue assessment, criteria such as time and accuracy, as well as their consequent cost-effectiveness, only commence to illustrate the necessity for the establishment of a relative comparison. In that respect, fidelity-related concepts provide valuable guidelines to the desired correlations. The fidelity of a tool has been given numerous definitions, with the term being characterized as "*nebulous*" and in certain cases "*the subject of heated discussions*" [15] [45]. At this point the definition of fidelity seems a challenging task in itself, and most of the efforts conducted towards that direction verify its complexity [15] [45] [46]. A popular attempt to define fidelity was issued by the Fidelity Definition and Metrics Implementation Group (FDM-ISG) and provided valuable insight on the matter. "*The degree to which a model or simulation reproduces the state and behavior of a real world object, feature, condition or standard in a measurable or perceivable manner*" has been considered a genuine effort to quantitatively define the fidelity of a model or simulation within the modelling and simulation (M&S) community [46]. As a result, at an early attempt to determine the selection of a tool and justify the reasons behind that choice, that tool should primarily implement an accurate reproduction of a real-world structure.

Fidelity frequently involves a set of criteria, the aggregation of which contributes to its quantification. Accuracy, precision, speed and detail are among the most significant criteria involved in fidelity quantification, and multiple definitions have been used to describe them [15] [45] [46]. In brief, accuracy measures the likeness of a set of parameters to reality, while precision expresses "*the level of granularity with which a parameter can be determined*" [45]. Detail however is a relative term in itself, and is associated with the parameters involved in a tool [2]. All of the criteria should be further assessed through multi-criteria decision analysis (MCDA) and constitute the basis of fidelity quantification. The resulting

quantification not only determines the required levels of fidelity for the use case, but also illustrates the suitability of a tool for the required simulations. In other words, quantified fidelity results to a particular ranking of tools according to preset specifications [15].

Considering the above, the fidelity of a model or simulation is intrinsically connected to the specifics of the use case [44]. Each model is designed to serve a particular purpose and the concept of fidelity consequently depends on what the manufacturer has predetermined for its use. The above fact confirms that fidelity is a relative term and thus requires a unique approach, primarily for its definition and eventually for its quantification. To specify, since there is a significant number of tools to choose from in conducting fatigue assessment, the task of determining the best candidate among the tools should be challenging.

## 1.2 Problem Analysis

All of the background information displayed in section 1.1 suggests the existence of an unresolved issue within the offshore wind energy sector. In the words of researchers, *“there has been no clear way for users of a Multidisciplinary Design, Optimization and Analysis (MDAO) framework to know what model fidelity and optimization algorithms have to be included in an offshore wind system assessment”* [42]. In further detail, in the majority of use cases of offshore wind structures, relevant simulations are conducted in particular tools, without proper justification on their choice. In addition, extensive research on offshore wind systems has resulted to the increase of available tools, hence broadening the range of choice. As a result, significant effort should be put in establishing a generic fidelity framework, in order to thoroughly examine the selection of tool. Therefore, fidelity determination and quantification would emerge from the aforementioned framework.

The main purpose of the current project was identified in the assessment of certain frameworks that would contribute to a user’s choice of tool. All relevant alternatives that would determine fatigue damage of an offshore wind structure and at an early design stage should be examined. By considering fatigue damage as the design driver of the offshore structure, fidelity assessment for the given tools was conformed accordingly. This very fact is primarily due to the choice of parameters which would result to the respective framework for fatigue assessment. These parameters should derive from the process of fatigue assessment and constitute the basis of the fidelity framework. Within the boundaries of the current thesis, the framework that includes the parameters that are associated with fatigue damage determination, is addressed as referent framework. Consequently, in order to discern the most significant parameters in the process of fatigue assessment, the establishment of that particular referent framework would facilitate the overall comparison.

Apart from that referent framework, the selection of criteria that would quantify fidelity should constitute the most compelling part of the challenge. The aggregation of those criteria would result to the eventual fidelity metric of all candidate tools. Therefore, all selection, definition and manner of quantification of the criteria, should be crucial to the realization of the required assessment. Speed and accuracy are considered the most popular in tool selection, with their relative trade-offs monopolizing relevant literature [15] [30] [45].

The eventual ranking between a set of tools would emerge through the conduction of multi-criteria decision analyses (MCDA). The criteria are primarily assigned with weighting factors

and in the process a variety of alternatives is assessed. These factors should result from both particularities of the use case, as well as the intention of use for the compared tools. In that respect, the influence the decision-maker would exert on the initial assignment of weighting factors should be limited. That would enhance the credibility of the method and hinder the subjectivity of the user in the assignment of the weighting factors. The process should eventually provide an output ranking of any tools that are involved, resulting to the final tool ranking [30].

The initial fidelity framework should be fitted to the defined use case. In the context of the current thesis, the choice of fatigue assessment for monopile-based offshore wind structures at an early design stage is examined. In addition, the structure should be neither over or under-dimensioned. Hence, the configuration of support structure would prevent over-dimensioning of the overall structure, which is frequently the case in modern OWFs [36]. Towards that end, fatigue damage should be considered as the main design driver within the framework of the current thesis.

### **1.3 Objectives**

The main goal of the thesis was identified in the provision of a fidelity framework according to which the choice of a particular tool among a range of alternatives would be justified. Three types of fatigue assessment and thus three respective tools were examined. In addition, a fidelity framework should be established, according to which a consequent ranking could be eventually derived among the involved tools. In order to identify that ranking, a series of initial objectives should be fulfilled, as shown below:

1. Establish a set of criteria according to which the levels of required fidelity should be determined, in respect to the use case. Which criteria constitute fidelity for fatigue assessment tools for offshore wind structures?
2. Justify the choice of parameters that will be involved in the referent framework for the different types of fatigue assessment. What parameters exactly constitute the referent framework for fatigue and why?
3. Reach an eventual ranking which would result from the application of MCDA to the measured criteria of the fidelity framework. How does the eventual ranking result from the quantified criteria and how is it justified?

In relation to the first objective, Modelling & Simulation (M&S) researchers have linked fidelity to a considerably vast spectrum of criteria. Accuracy, precision, detail and speed are included among others, with varying definitions throughout literature in every respective case [15] [45]. Thus a selection of criteria that would constitute the fidelity framework of the current thesis should be conducted. These criteria should be thoroughly defined and assigned respective metrics in order to reach to eventual fidelity quantification. In addition, their boundaries should be distinct as well as their interrelations should be rigorously assessed.

The second objective required the selection of parameters which are associated to fatigue assessment. These would constitute the referent framework for fatigue that would fit the fidelity framework to the specifications of the defined use case. Fatigue analysis in both TD

and FD, with the inclusion of simplified types of fatigue analysis in the FD, all would apply to the offshore wind structure and provide the user with fatigue damage values. The fitted criteria of the fidelity framework would be measured during the respective simulations and provide the data base to the overall tool comparison.

In terms of the third objective, the relative impact of each criterion to the eventual fidelity metric should be examined through the process of MCDA. Through relevant literature, trade-offs between the established fidelity criteria are subject to further assessment which should require specification to the use case. Especially conventional trade-offs between speed and accuracy that monopolize scientific reports [15] [30] [45] on simulation fidelity, should be directly addressed through the application of MCDA. All respective choices should be implemented judging by the intention of use for the tools, apart from the aforementioned specifications of the selected use case [44]. Evidently, the application of MCDA should be aligned to the current trends of the offshore wind industry.

## **1.4 Approach**

The adopted approach to quantify fidelity and rank models accordingly, should provide insight to any effort towards that direction. The particularities of this approach are associated, to fatigue damage determination of monopile-based offshore wind turbines. However, the process in itself integrates elements and procedures that could potentially apply to similar use cases. All above considered, the different steps that were followed within this approach in order to compare the associated tools should be briefly described.

Initially, a fidelity framework was established in order to quantify the respective magnitude in the tools that were selected to conduct fatigue assessment. As a result, a set of criteria should be decided, rigorously defined and quantified through simulations. These criteria and their respective metrics were selected from a variety of fidelity indicators [25] [42] [45] [46] and were subsequently defined in an effort to best quantify the levels of fidelity in the tools.

A particular use case was defined which, while setting a particular set of initial conditions for the steps that would follow, did not limit the fidelity quantification process. All relevant choices such as the main design driver, the type of support structure and choice of environmental data taken into account, shaped the referent framework of parameters for fatigue. That referent framework should adjust the fidelity framework accordingly, in order to render it applicable to the selected case study.

The relative score of each criterion should collectively emerge from simulations and the objectivity of the method would be enhanced in case all criteria were computed under the same set of conditions. As a result, the fidelity framework should be universally applied in the tools. The metrics of the criteria would be calculated during those simulations and later would be correlated accordingly, in order to acquire the desired fidelity metric.

The scoring of the criteria however should be assessed in a meticulous manner, in which their relative level of influence to the eventual fidelity metric should be analyzed. As a result, the MCDA should provide a relative multifaceted approach and further credit the aforementioned proposition. In that respect, the subjectivity of the decision-maker in the assignment of the initial weighting factors should be limited, as the objectivity of the proposed method would be further intensified. To specify, the Analytical Hierarchy Process (AHP) was selected, as it

comprised of the most common MCDA type. It is worth mentioning, that the hierarchical scheme [30] it suggests should be aligned to the defined use case and therefore to the current trend of the offshore wind energy sector. An additional MCDA method was identified in the Monte Carlo Method, as proposed by Butler J. [3], and was also included in the proposed methodology. The iterative application of Monte Carlo simulations differentiate the method from the AHP and provide a multi-faceted approach, as analyzed in Chapter 2.

The proposed methodology would be assessed through its application to a case study, in which the fidelity framework would be evaluated. The selection of the offshore wind structure should be primarily based upon the credibility of input data, as well as to its applicability in all three in disposal tools [2]. Consequently, a particular site should be selected with thorough environmental data, in which a particular offshore wind structure would be installed, while fatigue damage would comprise of the basic design driver.

Figure 1.1 that was suggested by Benjamin P. [2] includes the steps of the aforementioned approach that was followed in the current thesis. The development of the fidelity framework is identified in the blue boxes and its further evaluation emerges from the application to the case study, as illustrated in the orange boxes.

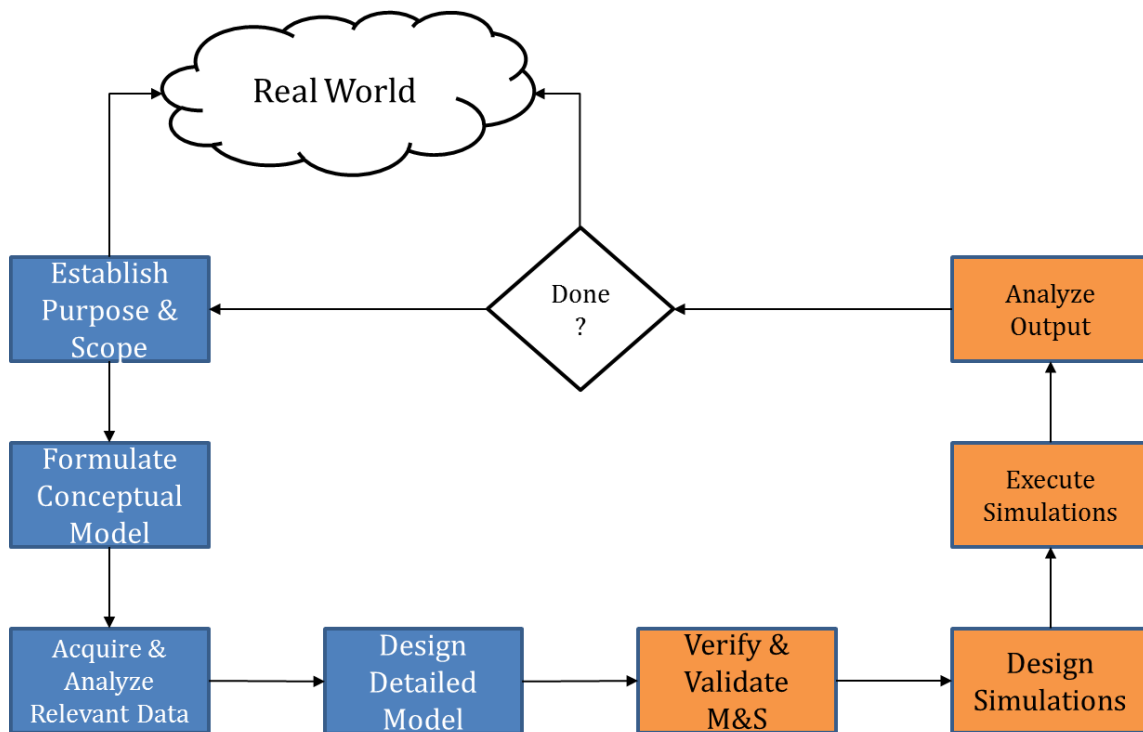


**Figure 1.1:** Modelling and simulation process according to Benjamin P. [2].

## 1.5 Thesis Outline

The current thesis consists of 7 chapters. Chapter 1 introduces the reader to the topic following a particular sequence. Primarily, it provides relevant background information which targets to familiarize the reader to the fidelity concept as well as to the offshore wind

energy sector orientations. By reviewing additional information on the available tools that perform different types of fatigue assessment for offshore wind structures, the need for a fidelity framework to guide the user through tool selection is mainly addressed. A number of objectives accompanied by research questions are stipulated in an effort to develop the purpose of the thesis and partially illustrate the series of steps that should follow.

In Chapter 2 the proposed methodology is suggested in a generic manner. Fidelity-related concepts that emerged through extensive literature review are assessed in order to create the framework upon which tool selection will be justified. A set of criteria is selected to express fidelity and their respective metrics are defined. Additional information on MCDA is displayed, including the types according to which the eventual ranking of the tools will be implemented. All concepts and notions are suggested regardless of specifications of the later defined use case.

In Chapter 3 the use case is specified in order to appropriately adjust the generic fidelity framework of Chapter 2. All particularities are examined and relevant information on available tools in which fatigue assessment is conducted is included. Additional information on the modelled types of fatigue assessment is provided, as well as information associated with TD and FD concepts is analyzed. The tools determine the environment in which the fidelity framework of Chapter 2 will be integrated.

Chapter 4 includes background theory that is mainly related to the process of fatigue assessment. Extended information on environmental loading is provided, as they impact later fatigue damage determination, the design driver of the suggested use case. In addition, all prerequisite steps to compute fatigue damage in monopile-based offshore wind turbines are analyzed, in an attempt to appropriately lay the foundation of the suggested referent framework of Chapter 5.

In Chapter 5 the proposed methodology of Chapter 2 is specified to the particularities of the use case and conformed to the process of fatigue assessment, mainly through the proposition of the referent framework of parameters. All background theory displayed in Chapter 4 justifies the development of the particular framework according to which the proposed fidelity criteria are modified. The metrics of the criteria are specifically determined in order to suitably apply the fidelity framework to the case study of Chapter 6.

Chapter 6 involves the assessment of a case study in order to evaluate the results of the proposed fidelity framework. A particular offshore wind structure is selected and simulated at an installation site situated in the North Sea (Horns Rev). Through simulations, both support structure configuration is identified, as well as scoring of the fidelity criteria is acquired. The three tools are ranked according to their respective levels of fidelity through the application of the MCDA that was presented in Chapter 2.

Chapter 7 reflects on the results of the case study and suggests certain improvements to the proposed framework. This chapter includes the conclusions that were reached during the overall process that was followed and its eventual evaluation in the case study. In addition, parts of the proposed methodology that are subject to alterations are assessed and suggestions on potentially improving the fidelity framework are provided. The latter are presented as recommendations for future work in order to increase the reliability of the methodology .



## 2. Proposed Methodology

Tools should be used after proper evaluation of alternatives. Currently, the use of TD software is identified at almost all design stages for offshore wind structures in the respective industry, with the use of GH Bladed being considered second to none [36] [48]. The need to assess the potential use of other tools instead, at an early design stage at least, should be addressed and resulting methodologies should be developed towards that direction. In order to reach the desired tool comparison, the fidelity of those tools should be quantified and directly compared. The suggestion of criteria comprising the fidelity framework facilitates the process of fidelity quantification in the tools. In addition, the application of MCDA would output the eventual ranking of the tools, and consequently provide the best candidate among them.

### 2.1 Conceptualizing Fidelity

The fidelity term comprises of an abstract concept that has been fundamentally derived from the aerospace community [25]. As briefly described in section 1.3, the fidelity matter primarily originated from pilot - training in 1980 [45], where NATO's Advisory Group of Aerospace and Research Development (AGARD) conducted efforts to assess the level of fidelity needed in the flight simulators in order to achieve the desired level of pilot training. In further detail, high fidelity resulted to higher development and operational costs and as a result researchers attempted to determine the appropriate level of fidelity for the provided training, in order to reduce the aforementioned costs. In a way, they tried to render the program cost-effective by assessing the speed vs accuracy trade-off, which consists of the most popular among relevant literature [15] [30] [45]. In the following years, similar issues rapidly emerged throughout similar domains.

Additionally, the fidelity matter significantly grew in popularity and was addressed by multiple organizations. Both the Federal Aviation Administration (FAA) in 1993 and the Joint Aviation Authorities Administration Training Organization (JAA TO) in 1997 issued requirements and standards for flight simulators, respectively. Moreover, Lane published in 1992 "Fidelity and Validity in Distributed Interacted Simulation: Questions and Answers" in which he developed his insight through a set of seventeen questions and answers concerning fidelity requirements and validity issues in the context of Distributed Interactive Simulations (DIS) based Simulations [45]. To continue, the Institute of Electrical and Electronics Engineers (IEEE) issued a standard in 1995 in an effort to describe fidelity and simulation components for the very same type of models, basically through a fidelity definition taxonomy and a fidelity assessment process [45]. In the following years, the M&S community attempted to develop and validate High Level Architecture (HLA) simulations within the Simulation Interoperability Standards Organization (SISO). In brief, Pace [41], Gross [14], Foster [11], McDonald [33] and Meyer [35] all expressed their perspectives on the HLA fidelity and collectively established sets of fidelity criteria as well as formed patterns for fidelity quantification. However, all aforementioned parties failed in resulting to a unified fidelity framework, given the abstract character of fidelity.

Nevertheless, particular efforts have been attempted in order to establish particular fidelity frameworks of intensified universal character. Roza Z.C. in 2004 [45] suggested a unified

fidelity framework in the PhD Thesis entitled “Simulation Fidelity Theory and Practice”, in which fidelity is rigorously quantified and applied to a set of case studies for evaluation. A set of eight fidelity criteria among which detail, accuracy and precision are included, quantified and constitute the eventual fidelity metric. In addition, Ponnusamy S. S., Albert V. and Thebault P. in “A Simulation Fidelity Assessment Framework” addressed the need for a consistent approach in order to appropriately evaluate fidelity of simulation models along the product development cycle [44]. In their publication they raised matters such as the choice of the most suitable abstraction of reality in relation to fidelity of both model and simulation. In addition they suggested an Experimental Frame (EF), as proposed by Ziegler [59], which would provide a set of acceptance conditions for the model abstractions. Moreover, they proposed a fidelity metric through the measurement of distance to reality for both model and simulation, as was suggested by Gross [14]. In their effort they evidently discerned tool from simulation fidelity, as in certain cases they were conflicting, with the former consisting of an absolute measure while the latter comprised of a relative concept, respectively. In addition, they separated intention of use from the particularities of the use case, with the respective terms of Simulation Objective of Use (SOU) and Simulation Domain of Use (SDU), as shown in Figure 2.1. In brief, they suggested that a solid mathematical framework with assessment of both abstraction of reality as well as simulation objectives would significantly improve product development life cycle quality, while rendering the relevant processes more cost-effective and of reduced risk.

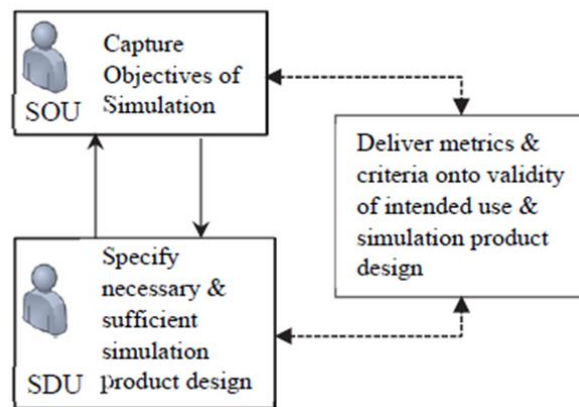


**Figure 2.1:** The Fidelity Framework according to Ponnussamy et al. where SOU and SDU stand for Simulation Objective of Use and Simulation Domain of Use, respectively [44].

All aforementioned researchers that suggested various patterns and raised multiple issues, were stimulated to provide their collective insight which converges in a set of particular points. They all partially agreed to the abstract character of fidelity and Ponnussamy et al. admitted that an “*absolute definition of fidelity is neither feasible nor useful since a model is always abstracted with an objective behind*” [44]. Additionally, they argued that fidelity of a tool or simulation should be referenced to a particular abstraction of reality than reality itself. That very abstraction may be referred to as simuland by Gross and Roza [15], reference abstraction by Ponnussamy et. al. [44] or surjection map by Girard [13]. In any case they collectively claimed that such a concept is vital to the development of a fidelity framework due to the complexity of reality. Moreover, the majority of researchers either stated that fidelity criteria should be established or even defined both criteria and their respective

metrics, in their attempt to render further fidelity quantification feasible. As a result, due to the diversity of the suggested criteria, that are frequently found conflicting, as well as the dependence of fidelity on both M&S objectives and particularities of each use case, further assessment of criteria is required in order to appropriately measure the fidelity metric. Roza suggested Multi-Criteria Analysis in order to assess “simulation systems comparison”, suitability assessment and trade-offs [45] while Loper claimed that the framework’s internal dependencies should be assessed [25]. Therefore further evaluation of criteria should be conducted in order to examine all dependencies of tool and simulation in expressing fidelity.

## 2.2 Fidelity Criteria

In order to appropriately justify the use of a particular tool over another for the same use case, a relative ranking is required among them. In order to achieve that, specific criteria with their consequent metrics should be established. The scoring of the latter would therefore provide the data base to the eventual ranking. Those metrics are associated to the way simulations both depict reality as well as address the goals set by the users of the tools [2]. In addition they should collectively express fidelity in simulations [45] and they would facilitate its quantification. In other words, the metrics of the criteria aggregate to the fidelity metric and thus quantification of fidelity.

The choice of criteria varies as the concepts associated to fidelity are relative. Since extended research has been performed in flight simulators, their findings are widely popular. Considering both nature and predetermined goals of simulations performed in stability checks in the offshore wind energy sector, certain criteria such as timeliness or consistency are not applicable to the fidelity assessment process included in the frame of this thesis. Additionally, SISO suggested a pattern to establish the implementation of criteria, as shown in Figure 2.2 [46]. Naturally, the selected criteria should be determined in both definition and metric before the use of the tools, in order to quantify the level of reality that could be simulated, hence fidelity.

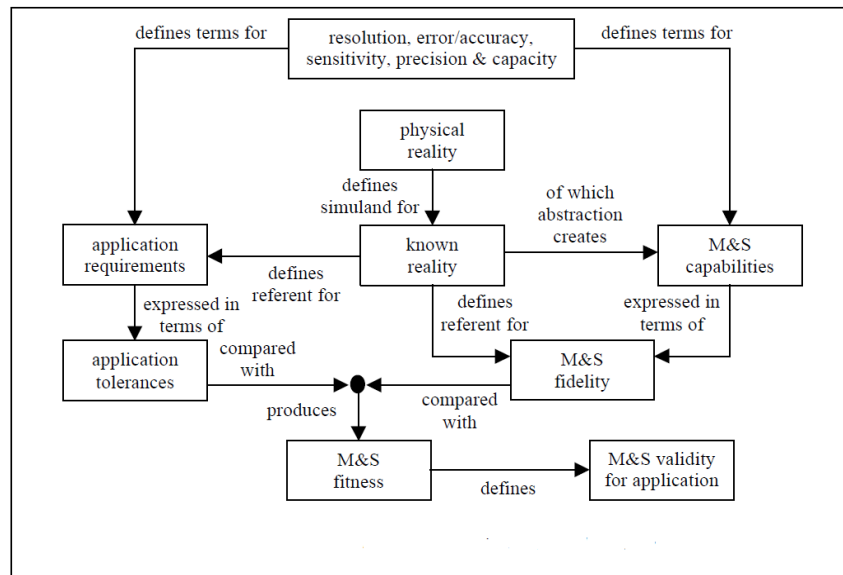
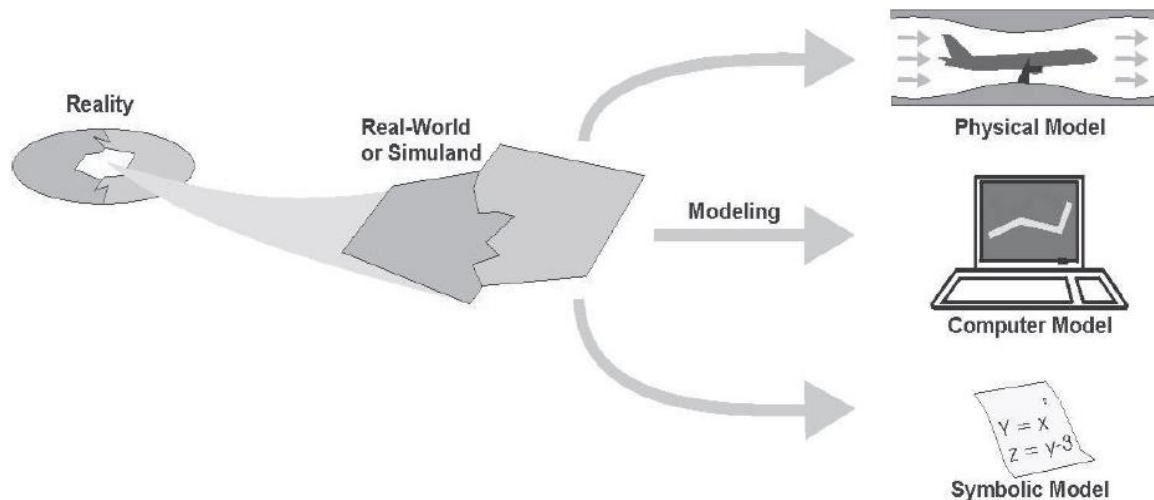


Figure 2.2: Implementation of Fidelity-Related Concepts [46].

The concept of simuland, as illustrated in Figure 2.3 from Roza, in respect to flight simulators [45], is associated to the aforementioned criteria and could also be applicable to offshore wind systems. The stochastic character of certain variables associated to environmental conditions such as wind and waves render any simulation, no matter how advanced or complexed, incapable of simulating absolute reality. As a result, *“the part of the real-world that has been developed”* [46] correlated primarily to how well established the proposed criteria should be, as well as predisposed for the later establishment of the referent framework.



**Figure 2.3:** Relationships between Reality, Simuland and Model as illustrated by Roza [45].

Literature review indicated additional common ground in different kinds of simulations. Accuracy and precision constitute two of the basic fidelity criteria in flight simulators [46], with the former being compared with speed in the most common trade-off [15] [30] [45]. Criteria such as repeatability, in other words *“uncertainties that are relative to generic algorithms and other adoptive programming methods”* [46] which are used in the field of artificial intelligence should not be included in the proposed framework. Nevertheless, the essence of uncertainty should be considered due to the stochastic character of environmental data but also because of the human factor. The latter has been referenced as the user effect and occurs when different users derive to conflicting results for the same simulation [15]. In particular, the human factor should be addressed and potentially be integrated to the foundation of one of the criteria. Partially due to the number of the parameters in the referent framework, the required level of detail should be assessed, as fidelity was defined as a measure of detail by both Gross and McDonald in their respective perspectives [15], [33].

The selection of fidelity criteria that should constitute the proposed fidelity framework were identified during the relevant literature review but comprised of abstract concepts which were overlapping and even contradicting at an extent. As a result the selected criteria should be defined in both definition and metric, while the boundaries between them should be distinct. Eventually, a set of 4 criteria were selected for fidelity quantification: Accuracy, Time of Simulation, Operational Time and Detail, with the reasons behind each choice being analyzed in the following four sub-sections.

### 2.2.1 Accuracy

The accuracy of a model or simulation has been defined in multiple manners by fidelity researchers. Roza suggested that accuracy comprised of “*a measure of how good a parameter or a set of parameters represent the reality simulated*” [45]. Gross suggested that it consists of a measure of correctness of the level of detail and therefore constitutes a dynamic analysis measured through cumulative executions data [14]. Moreover, certain researchers among which are Foster [11] and McDonald [33] have identified accuracy with fidelity, with the latter claiming that fidelity should be defined as the accuracy of abstraction, in comparison to the real world. In contrast, other scientists have implemented distinct separations between the terms. Meyer included accuracy among his four simulation goodness terms, along with detail, resolution and fidelity, stating that accuracy is “*the exactness of a model with respect to the observable characteristics and behaviors of the physical entity*” while fidelity is a measure of convergence of a simulation with apprehensive reality [45]. Nevertheless, in multiple scientific domains as in computer science, accuracy is quantified as the difference in tool output from output trajectories from reality [45]. The most credited however definition was issued by the Simulation Interoperability Workshop in which accuracy was defined as “*the degree to which a parameter or variable or set of parameters or variables within a model or simulation conform exactly to reality or some chosen standard referent*” [15]. The aggregation of the above render accuracy, just as detail and fidelity, abstract, with the respective definitions overlapping and in some cases conflicting with relevant fidelity concepts.

In the framework of the current thesis, accuracy was separated from the concept of fidelity and expressed accordingly. Fidelity as aforementioned was divided to a set of criteria that would lead to its overall quantified expression. Detail is defined in section 2.2.4 as a fidelity criterion and accuracy would aggregate along with detail and the rest of the later proposed criteria to the eventual fidelity metric. As a result, in an attempt to discern accuracy from the other fidelity-related concepts, the following definition and respective metric are suggested.

Accuracy is limited to the comparison to the anticipated value of the design driver in the associated models. As a result, the term comprises of a measurement of correctness to reality or reality referent, mainly as indicated by SISO [15] and Meyer [35]. Consequently, the proposed metric would express the distance from the referent numerical value of the design factor. That distance was quantified in equation 2.1 as:

$$\Delta dd = |dd_s - dd_r| \quad 2.1$$

where  $dd_s$  the value of the design driver at the output of simulation and  $dd_r$  the referent value of the design driver. In that respect, the metric of accuracy would result from equation 2.2.

$$M_A = \frac{\Delta dd_{\max} - \Delta dd}{\Delta dd_{\max} - \Delta dd_{\min}} \quad 2.2$$

where  $\Delta dd_{\max}$  the maximum difference throughout the tools and  $\Delta dd_{\min}$  the respective minimum. The magnitude of accuracy is dimensionless just as detail, as well as the rest of the

suggested metrics of the criteria, in order to collectively quantify fidelity. The potential values of the metric are situated at the respective range [0,1], with 1 being the most accurate.

### 2.2.2 Time of Simulation

The simulation time (ST) expresses the time required within a particular tool to process input and extend to output. The above expression, while being straight-forward, essentially describes the criterion. In other words, it is the time required for a simulation to run in order to yield a particular output. Moreover, the concept of this criterion has been frequently mentioned in speed of execution or simulation in relevant literature [25] [35] [42] [45]. In certain cases, simulational time referred to the simulator’s unique representation of time, and the particular criterion was defined as wall-clock time [15].

Measurement of ST should be conducted under particular circumstances. There are multiple ways to measure simulation time among which are certain model functions, floating point operations (FLOPs) counters as well as computer timers triggered at initiation of the simulations. Overall, measurements should be universal and therefore the same manner of measurement should apply to all tools involved.

The metric for simulation time ( $M_{ST}$ ) is defined in the same manner as accuracy in order to render the metric dimensionless. It consists of the linear mapping of the average simulation time (ST) between the maximum and minimum averages,  $ST_{max}$  and  $ST_{min}$  measured across all simulations, as suggested by MSc Sebastian Sanchez Perez-Moreno [42].

$$M_{ST} = \frac{ST_{max} - ST}{ST_{max} - ST_{min}} \quad 2.3$$

Overall, the specific metric is proportional to the speed of simulation and inversely proportional to time of simulation.. All of the metrics were formed in a manner in which they would range from 0 to 1, 1 being the greatest (Detail – most detailed, Accuracy – most accurate etc.). As a result, in this case 1 is translated to the fastest simulation and thus shortest simulational time

### 2.2.3 Operational Time

Speed in simulation is evidently included among the most popular fidelity criteria in relevant literature [15] [45] [46]. However, apart from time of simulation, the total time that a user consumes while using a model should be evaluated. There are no essential benefits in terms of overall speed, even if a model’s simulation speed is high, in case the time required for input over-exceeds the average anticipated operational time spent in similar tools. The complexity of a tool would stall the user from getting the desired output and potentially even lead the user to input errors. Consequently, the popular among relevant literature human factor[25] [44] [45] is taken under consideration during the operation of a tool. In addition, the way in which the tool’s output is provided, may result in further delay for the user if post-processors are required. As a result, the operational time of a tool is selected among the basic fidelity criteria.

Operational time (OT) is required to be measured in the same manner across simulations, in order to form a standard of comparison. The same use case should be simulated in multiple tools and the amount of time the user consumes to input constitutes the most significant part of the measurement. Post-processing OT should also be taken under consideration, but is of minor importance in relation to pre-processing OT, due to its relatively lower magnitude.

The accuracy of the OT's measurements during simulations is of particular significance, but its precision is not justified decisive to fidelity quantification. That is due to the fact that measurements during comparison vary significantly between the tools involved, and potentially amount to even larger orders of magnitudes than mere seconds. One of the most accurate ways of measuring operational time would be achieved with the use of a software timer that would be triggered when the user commenced tool use and stopped right after the user has received the output. The ST would be subtracted from the measured amount and that would result to operational time's measurement. Another simpler way of measurement would be achieved with the use of a conventional timer. Overall, the metric of operational time is defined dimensionless, as the respective metric of ST, as shown in equation 2.4.

$$M_{OT} = \frac{OT_{max} - OT}{OT_{max} - OT_{min}} \quad 2.4$$

where  $OT$  the average operational time between the maximum and minimum averages,  $OT_{max}$  and  $OT_{min}$  of running time measured across all model simulations. The metric of operational time is by definition dimensionless, as should the rest of the criteria metrics. The respective values range from 0 to 1.

#### 2.2.4 Detail

The primary step in establishing the appropriate fidelity framework comprised of the definition and determination of the desired level of detail that would be required. The reader of the current thesis should by now comprehend the abstract character of fidelity and any relevant concepts. Detail could possibly be placed on top of that list, including the most complex perceptions mainly due to the contradicting definitions throughout literature, as well as due to the absence of a solid fidelity framework in M&S. In that scope, the determination of detail should be associated to both the required level of fidelity as well as to the respective fidelity criterion. The above imply that the particular task was more than challenging and thus a multi-faceted approach should be adopted.

As introduced in section 2.1, the fidelity of M&S is directly connected to the suitable abstraction of reality rather than reality itself, a statement that iterated over research [2], [15], [42], [45]. The Fidelity Implementation Study Group issued in its report in 1999 that the concept of detail was included among accuracy, scope, level of abstraction and repeatability as part of a fidelity description, the metric of which would contribute to eventual fidelity quantification [46]. Specifically, Roza and Gross used the term of resolution to define the level of detail needed from M&S: *"The degree of detail used to represent aspects of the real world or a specified standard or referent by a model of simulation"* [15]. Roza claimed in [45] that fidelity criteria should emerge from the relation between Conceptual Model and Simulation

System, as depicted in Figure 2.4. Meyer described detail as the manner according to which the dimensionality of a model is described with respect to the captured physical entity [35]. All of the above led research to assess the required fidelity for the tools involved, in respect to the required level of detail. In other words, detail was partly associated to determining the real-world representation and therefore to the particularities of the appropriate abstraction of reality that would be required.

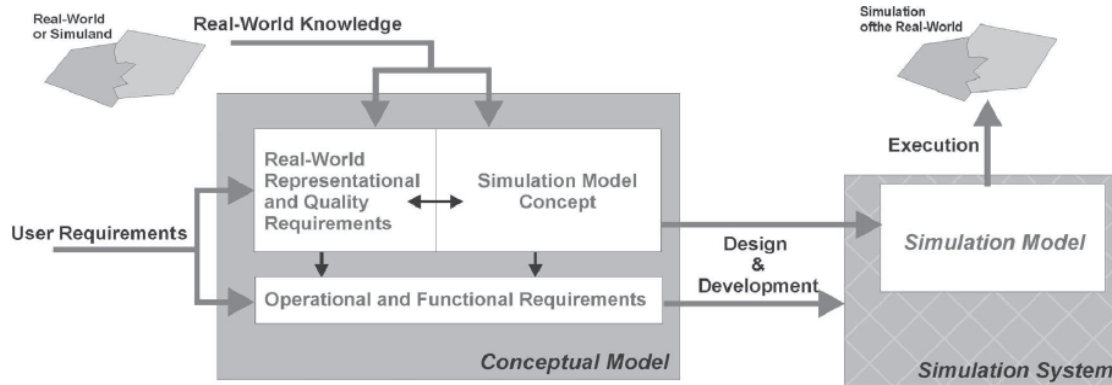


**Figure 2.4:** Real-World, Conceptual Model & Simulation Model Relations [45].

The required level of fidelity for a particular model or simulation should primarily be associated to the intention of use as well as to the nature of the processes implemented in the models [44]. Consequently, the level of depiction of the real-world that would be justified necessary, should be measured in respect to the predetermined specifications of the processes integrated in the examined tools. Specifically, Roza indicated that the level of fidelity was primarily examined for flight simulators in order to mitigate high operational costs, without nevertheless underachieving in providing appropriate training to future pilots [45]. The above example illustrates the manner in which the required fidelity of the examined tools should be evaluated, in an effort to efficiently determine the configuration of support structure for a particular offshore wind turbine, at an early design stage.

As a result a generic framework of parameters should be established in respect to the predetermined goals that should be achieved through the use of the tools, as well as the very nature and respective particularities of the design process of offshore wind structures. That framework should include all parameters that are essential to the offshore wind structure's design, and that should constitute of the benchmark for all evaluated tools. Specifically, the level of detail in relation to design parameters should be associated with the particular design driver that would be selected before the implementation of the proposed methodology. In the framework of this thesis, the design driver consisted of the determination of fatigue damage of offshore wind structures.

Naturally, the framework of parameters would derive from the rigorous assessment of fatigue damage determination, in respect to the particularities of the early design stage of the use case. Roza suggested a similar approach [45] in flight simulators, where the Real-World Referent and Simulation System would be compared on the parameters that would aggregate to overall detail, as depicted in Figure 2.5. Consequently, the framework would consist of N parameters that were justified essential in the aforementioned process. These N parameters

would shape the referent framework according to which all tools that were involved in the process of fatigue damage determination would be evaluated. In order to conclude to that framework, the process of fatigue assessment was thoroughly examined after the suggestion of the use case and its respective particularities in Chapter 5.

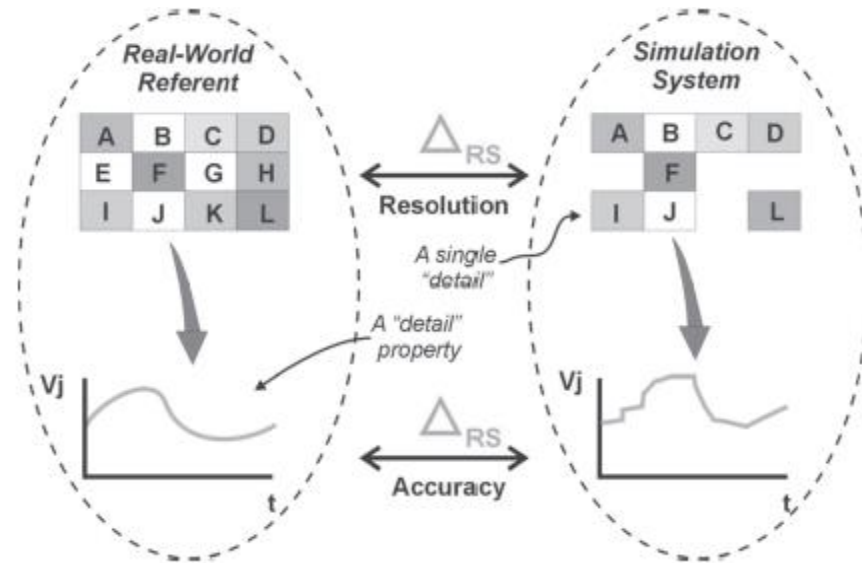


**Figure 2.5:** Detail, Resolution and Accuracy Illustration in respect to parameters A – L of the Real-World Referent and Simulation System [45].

The process of fidelity quantification however was solely conducted through the establishment of a framework of criteria and their respective metrics, which would eventually result to the desired fidelity metric [15], [44], [45]. As a result, detail was no exception to the rule and should be quantified through a particular process that would identify it as a criterion. On completion of the process, the metric for detail would constitute along with the other criteria the basis on which fidelity quantification would be established.

Additionally, detail was acknowledged as a criterion throughout the relevant literature review. Since a particular fidelity framework has not yet been established, and due to the vague and overlapping in multiple cases concepts of fidelity and respective fidelity criteria, the need to integrate the level of required detail to the fidelity criterion should be examined. For instance, it was mainly used in the suggested frameworks to determine fidelity for flight simulators [15]. Roza [45] and Gross [14] suggested that fidelity and accuracy should be separate concepts, as fidelity consisted of a measure of detail while accuracy was mostly defined as a measure of correctness of detail. These definitions prove nevertheless that its magnitude should be quantifiable and absolutely separated from the likeness of accuracy. In any case, the process of quantification required a finite mathematical framework for any determined variables.

The metric would basically result from the deviation of each parameter included in the tools from the established referent framework of parameters. In order to achieve that, all relative parameters in the tools should be examined, since they would not frequently appear in the same form, or even magnitude, as in the referent framework. In addition, the absence of referent parameters or the inclusion of additional variables that are not enlisted in the

framework should be mathematically expressed. Apart from the above claims however, the internal relations between the parameters that would constitute the framework, as well as their relative impact to the design driver, should be addressed.

These concepts were indicated in relevant literature. Ponnussamy et. al. [44] suggested that they would determine the particularities of the appropriate abstraction in fidelity of M&S and proposed that they would appropriately apply to the complexity of dynamic systems. In addition, Roza contradicted limited detail in her PhD thesis [45] and suggested that extensive assessment is more than required to formulate the relevant framework. It was decided that extended sensitivity analyses should be conducted in order to assess the relative impact of parameters to the design driver, with the additional assessment of the relative impact of the independent variable.

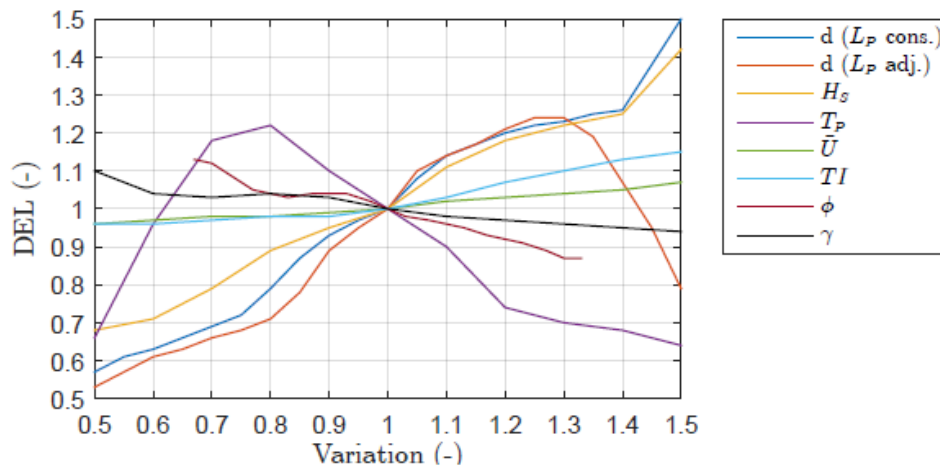


**Figure 2.6:** Sensitivity analyses of varying site conditions in respect to Damage Equivalent Load (DEL) [36].

The iterative sensitivity analyses that would be conducted in order to assess the relative alteration of model output due to parameter permutations, is included in relevant literature and in certain cases is associated to an additional criterion. Roza [45] defined sensitivity as *“the effects of imperfections and uncertainties of external stimulus (input variables) and internal simulation system parameters (data values) or structure on the accuracy of the simulated real-world system behavior and functions i.e. output”* and included it among the eight descriptive concepts or criteria that constitute the unified fidelity framework. In addition, sensitivity was described as twofold, in terms of output changes that are due to all input alterations as well as to tool changes to extreme input variables and combinations, respectively. The former approach is associated with the interaction between tool parameters while the latter is connected to *“identifying those aspects that have the most significant effect on the measured simulation execution outcome accuracy”* [45]. In addition, sensitivity was defined by SISO as *“the ability of a component, model or stimulation to respond to a low level stimulus”* [15] and in the same report the additional concept of the sensitivity error was defined as the manner in which a model error is magnified by a potential error in either internal or external parameters. In particular, Michalopoulos [36] performed sensitivity analysis of certain parameters to inspect their impact on DEL, in order to further

evaluate his proposed simplified fatigue assessment methodology, as shown in Figure 2.6. Judging from the above, the generic sensitivity concept is fairly applicable to the complexity of systems such as offshore wind structures and therefore sensitivity was partially integrated in the detail expression.

The concept of the sensitivity criterion is connected to detail and thus is considered under the detail criterion within the framework of this thesis. All required assessment is thus associated to the relative impact of referent parameters on the design driver, as indicated from extensive sensitivity analyses. As a result, detail could not be separated from the sensitivity analyses, in which the level of input alteration would result to significant diversion of the model’s output. Given the common nature and framework of the required to further quantification mathematical processes, the aggregation of both fidelity and sensitivity to one finite criterion is logically justified. Overall, the abstract character of all fidelity related concepts with overlapping and contradicting definitions coupled with the absence of a unified fidelity framework encouraged innovation and rational decisions in the determination of the fidelity criteria and their respective metrics. In that respect, this very criterion comprised of a fairly significant part of the fidelity expression, judging by the relevant literature. Concepts such as detail [15] [42] [45], sensitivity [15] [45], resolution [15] [45], interaction and precision of abstraction [15] [44] [45] [46] are all partly incorporated in this particular criterion. Figure 2.7 illustrates the above claims.

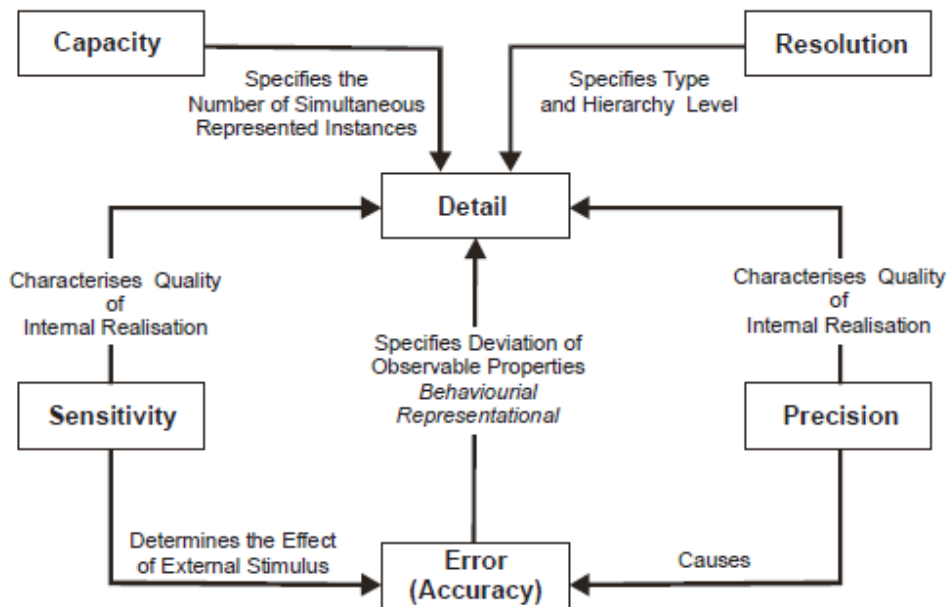


**Figure 2.7:** Interaction of Detail as illustrated in the report published from SISO in the Implementation Study Group for The Fidelity Definition and Metrics (FDM –ISG) [46].

Consequently, a particular mathematical framework should be established according to which detail would be quantified. The patterns are meticulously illustrated below in generic expressions, and later specified to the particularities of the use case, as suggested in Chapter 5. The framework was further evaluated in Chapter 6 in which it was applied to a case study.

As a result, for a set of N parameters of a particular model:

$$N = \{p_1, p_2, \dots, p_N\} \quad 2.5$$

The detail of the model would be defined as:

$$M_D = \frac{1}{N_r} (r_1 + r_2 + \dots + r_N) \quad 2.6$$

where  $N_r$  the number of parameters  $p_{r1}, p_{r2}, \dots, p_{rN}$  of the referent framework and  $r_1, r_2, \dots, r_N$  the referent factors that would emerge from the conducted sensitivity analyses. In case a parameter  $p_i$  is not involved in the examined tools but is included among the referent framework, the respective referent factor  $r_i$  would be accounted as 0 to the defined sum. In case  $p_i$  comprises of an additional parameter to the ones included among the referent framework, it would also be accounted as 0 to the defined sum. In case the parameter is included in both tool input and referent framework, the respective sensitivity analysis would result to its eventual value. For the latter, the referent factors were defined in the following equation 2.7:

$$r_N = \frac{1}{\sum_{i=1}^{s_1} \frac{p_{N_i}}{p_{r_{s_1}}} \sum_{j=1}^{s_2} \frac{iv_j}{iv_{s_2}}} \left[ \begin{aligned} & \frac{p_{N_1}}{p_{r_{s_1}}} \frac{\Delta dd_{s_1}^1}{\Delta dd_{\max}^1} \left( \frac{iv_{1,1}}{iv_{1,s_2}} \frac{\Delta dd_{1,s_2}^{1,1}}{\Delta dd_{\max}^{1,1}} + \frac{iv_{1,2}}{iv_{1,s_2}} \frac{\Delta dd_{1,s_2}^{1,2}}{\Delta dd_{\max}^{1,2}} + \dots + \frac{iv_{1,s_2-1}}{iv_{1,s_2}} \frac{\Delta dd_{1,s_2}^{1,s_2-1}}{\Delta dd_{\max}^{1,s_2-1}} \right) + \\ & \frac{p_{N_2}}{p_{r_{s_1}}} \frac{\Delta dd_{s_1}^2}{\Delta dd_{\max}^2} \left( \frac{iv_{2,1}}{iv_{2,s_2}} \frac{\Delta dd_{2,s_2}^{2,1}}{\Delta dd_{\max}^{2,1}} + \frac{iv_{2,2}}{iv_{2,s_2}} \frac{\Delta dd_{2,s_2}^{2,2}}{\Delta dd_{\max}^{2,2}} + \dots + \frac{iv_{2,s_2}}{iv_{2,s_2}} \frac{\Delta dd_{2,s_2}^{2,s_2-1}}{\Delta dd_{\max}^{2,s_2-1}} \right) + \dots + \\ & \frac{p_{N_{s_1-1}}}{p_{r_{s_1}}} \frac{\Delta dd_{s_1}^{s_1-1}}{\Delta dd_{\max}^{s_1-1}} \left( \frac{iv_{s_1-1,1}}{iv_{s_1-1,s_2}} \frac{\Delta dd_{s_1,s_2}^{s_1-1,1}}{\Delta dd_{\max}^{s_1-1,1}} + \frac{iv_{s_1-1,2}}{iv_{s_1-1,s_2}} \frac{\Delta dd_{s_1,s_2}^{s_1-1,2}}{\Delta dd_{\max}^{s_1-1,2}} + \dots + \frac{iv_{s_1-1,s_2}}{iv_{s_1-1,s_2}} \frac{\Delta dd_{s_1,s_2}^{s_1-1,s_2}}{\Delta dd_{\max}^{s_1-1,s_2}} \right) \end{aligned} \right]$$

$$\Delta dd_b^a = |dd_a - dd_b| \quad 2.8$$

$$\Delta dd_{\max}^b = |dd_{\max}^b - dd_{\min}^b| \quad 2.9$$

where  $S_1, S_2$  are the sets of simulations during sensitivity analyses of the specific parameter as well as of the independent variable, respectively. In addition,  $p_{N1}, p_{N2}, \dots, p_{Ns}$  are the values of the parameter in each simulation 1, 2, ..., s, and  $dd_1, dd_2, \dots, dd_s$  are the values of the design driver in each respective simulation.  $iv_1, iv_2, \dots, iv_{s2}$  are the values of the independent variable during the set of simulations  $S_2$  and  $p_{rs2}$  is the value of the referent parameter in that set. Moreover,  $\Delta dd_{\max}$  corresponds to the maximum difference throughout the tools for the

respective step and set of simulations.  $S_1$  and  $S_2$  are illustrated in the respective flow charts of Figure 2.8, in order to aid the reader to comprehend the stages of sensitivity analyses.

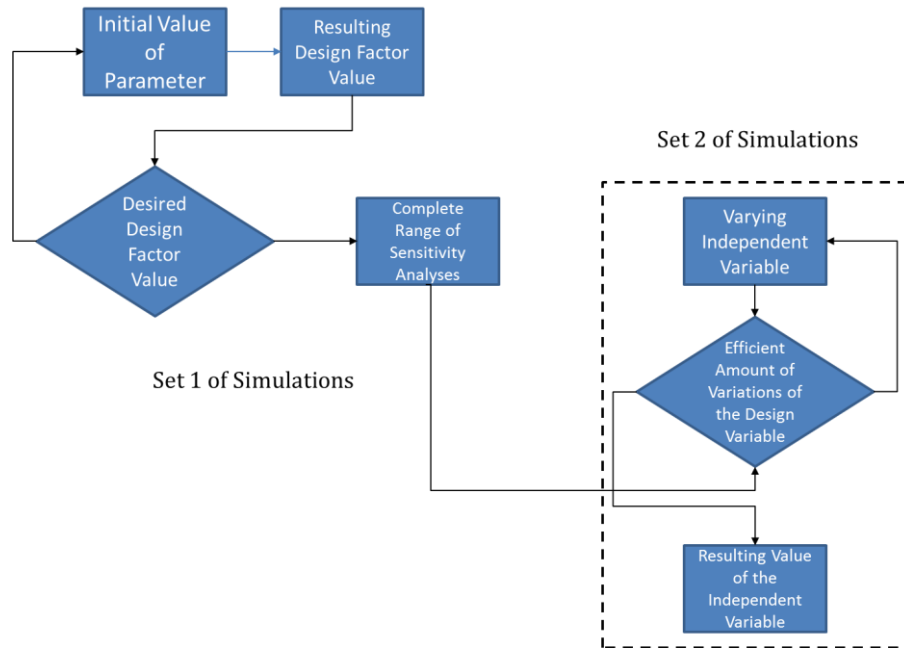


**Figure 2.8:** The proposed algorithms in order to acquire the respective score of a tool for the proposed detail criterion.

The fact that the two sets of simulations correspond at separate stopping points has to be mentioned, as simulations in  $S_1$  pause when an efficient range within the sensitivity analysis has been covered, while the number of the second set of simulations is dependent on whether an efficient amount of typical values of the dependent variable has been examined. Nevertheless, simulations should be conducted under the same conditions for every respective parameter, therefore the same amount of simulations in the second set would apply at every value of the first set. Overall, the number of simulations is proportional to the size of the examined values in the respective sensitivity analyses.

Expressions 2.6 and 2.7 were realized in a manner to appropriately assess the level of fidelity of each tool, based on the required level of detail that was justified prerequisite to suitably depict reality. The detailed assessment of the correct abstraction of reality would result to the referent framework of parameters and eventually pave the way to detail quantification, as shown in Chapter 5. Moreover, the metric is dimensionless, as the following proposed metrics, in an effort to appropriately compile the overall fidelity metric. The metric was defined as such that the respective values of detail would range from 0 to 1.

Unity is the greatest value the metric can acquire and results to the highest required detail. The term “*required*” is of significant importance, as higher level of detail would be redundant in multiple cases i.e. at an early design stage. As a result, in case a parameter is not included in the referent set of equation 2.5, it would be assigned as 0. The above practice is due to the time-consuming sensitivity analyses which frequently a user would be unable to perform. Varying forms of the same parameter in a tool’s input, the value of which could be altered in more than one ways would greatly hinder the user in the conduction of any kind of sensitivity

analysis, the outcome of which would even be doubtful. Consequently, in the context of the current thesis, the required level of detail was determined from the use case and resulted to the selected abstraction of reality for any conducted simulations. Overall, the above choice was also encouraged by the fact that increased detail after a certain point would result to the consumption of greater amounts of resources, which consisted one of the main reasons for establishing the fidelity framework in the first place [15].

### 2.3 Tool Ranking through MCDA

In order to appropriately result from the defined criteria to the eventual fidelity metric and reach to the ranking of the examined tools, further Multi-Criteria Decision Analysis (MCDA) was conducted. The impact of each criterion on fidelity should be examined and thus the eventual fidelity scoring illustrated different levels of dependence on each criterion. Detailed assessment of the criteria and careful examination of all alternatives is rigorously shown later in this section. The process is additionally applied in the 6<sup>th</sup> chapter, where it is further evaluated in a case study.

MCDA was primarily included in sets of general class of Operations Research models that addressed complex issues featuring among others *“high uncertainty, conflicting objectives, different forms of data and information”*, as well as *“multi interests and perspectives”* [30]. The associated methodologies involved conflict among criteria and choice of alternatives. These methodologies are further divided to two categories, the Multi-objective decision-making and Multi-attribute decision-making. Their main difference lies at the evaluated number of alternatives, with the former possessing a potentially infinite number. In addition, *“the alternatives are not predetermined as in Multi-attribute decision-making, but instead a set of objective functions are optimized subject to a set of constraints”* [30].

Multi-criteria decision-making methods or else MCDA selection have been analyzed by Tsoutsos et al. in [52], where four main reasons were displayed. First and foremost, detailed investigation and integration of both interests and objectives of multiple parties are allowed, since the inputs of both quantitative as well as qualitative data are taken under consideration through criteria and weighting factors. In addition, the quantifiable criteria as well as the simplicity of output format enable direct comparison and render the methodology user-friendly. Therefore output information is practical to communicate to all parties involved. Moreover, alternatives are assessed through the inclusion of multiple versions of the method that was developed in the framework of a specific use case of particular context. Overall, multiple concepts are included and expressed accordingly, in order to result to an objective comparison.

A set of particular drawbacks of the methodology should however be discussed. The direct comparison between the results is restricted, partly because of varying assumptions in the different tools under examination. Discrepancies may emerge due to information processing between different methods, with the corresponding weighting factors being misinterpreted [30]. Conclusively, emerging weighting factors could prove to be subjective, mainly due to the adopted approach of the analyst conducting the methodology [52].

Resulting from the conduction of MCDA, the tool has been assessed in two levels: the managerial level and the engineering level. The former mainly includes the definition of targets the tool should fulfill as well as the selection of the final optimal alternatives [30]. Within the framework of the engineering level all potential alternatives are defined and as a result their consequent multi-criteria ranking is conducted. The managerial level however involves decision-makers that may both accept or reject the proposed solution by the engineering level. They themselves act upon a set of five steps that are below listed [30]:

- Definition of the problem, generation of alternatives & establishment of criteria
- Assignment of weighting factors
- Construction of the evaluation matrix
- Selection of the appropriate method
- Ranking of the alternatives

There are multiple types of MCDA used, depending on the particularities of each use case as well as the desired end result. Among those types are the Analytical Hierarchy Process (AHP), the Weighted Sum and Weighted Product methods, (WSM) & (WPM), respectively, the Preference Ranking Organization Method for Enrichment Evaluation or in short PROMETHEE, and its respective types I & II, as well as certain types such as the one suggested by Butler J. et al. in [3]. Within the framework of this thesis the AHP and a Monte Carlo Method were selected. The reason behind the choice of the AHP was its popularity [30] while the second MCDA method was used due to its objectivity, which is analyzed later in the section.

### **Analytical Hierarchy Process (AHP)**

The Analytical Hierarchy Process (AHP) consists of a decision-making process, originally developed by Saaty in the 1970s [47]. Its main objective lies at the identification of the preferred alternative, as well as the consequent ranking when all criteria are taken under consideration simultaneously. Its application involves *“breaking down an unstructured problem into component parts”* [30]. Key to that is the establishment of hierarchical structures which result to consequent orders, according to which the predetermined goals are set at the top, criteria that influence the decision are placed at an intermediate hierarchy level, while the alternatives are situated at the bottom of the hypothetical hierarchy pyramid. To continue, the decision-maker maneuvers through a series of *“pair-wise comparison judgements”* [30], which are expressed in the form of assigned factors. These are eventually expressed in eigen-vectors, that determine the relevant priority among the values that are involved.

The AHP process is divided to four individual steps in order to thoroughly analyze any given problem and reach a certain resolution [30]. The sequence of steps is below displayed:

#### 1. Structure the decision model into a hierarchical model

The problem is decomposed into specific elements according to their common features and later form a multi-level hierarchical model, in which goals, criteria and alternatives are defined, as well as their relation is determined.

2. Acquisition of weighting factors for the existing criteria

A relative comparison is conducted between the elements situated at the same level of hierarchy and a particular element in the immediate upper level. The resulting judgmental matrix (A) includes factors of the form of  $\alpha_{ij}$  which state the quantified significance of a criterion  $i$  over a criterion  $j$ , with respect to the alternatives. According to Saaty [47], integer values from 1 to 9, or “the fundamental scale”, should be used under specific terms, as shown in the Table 2.1.

**Table 2.1:** The Fundamental Scale [47].

Intensity of importance of an absolute scale	Definition	Explanation
1	Equal importance	Two activities contribute equally to the objective
3	Moderate importance of one over another	Experience and judgment strongly favor one activity over another
5	Essential or strong importance	Experience and judgment strongly favor one activity over another
7	Very strong importance	An activity is strongly favored and its dominance demonstrated in practice
9	Extreme importance	The evidence favoring one activity over another of the highest possible order of affirmation
2, 4, 6, 8	Intermediate values between the two adjacent judgements	When compromise is needed
Reciprocals	If activity $i$ has one of the above numbers assigned to it when compared with activity $j$ , then $j$ has the reciprocal value when compared with $i$	
Rationals	Ratios arising from the scale	If consistency were to be forced by obtaining n numerical value to span the matrix

In addition, certain norms are followed when formulating the judgmental matrix:

- I. If  $a_{ij} = \alpha$  then  $a_{ji} = \frac{1}{\alpha}$ .
- II. If criteria  $i$  and  $j$  share more or less equal relative importance then:  
 $a_{ij} = a_{ji} = 1, a_{ii} = 1$
- III. If all relevant comparisons are absolutely consistent then:  
 $a_{ik} = a_{ij} = a_{jk} \forall i, j, k$

In order to acquire vector  $W$  that includes the initial weighting factors:

- IV. Each entry in column  $i$  is divided by the sum of entries in column  $j$ , which results to the acquisition of the normalized judgmental matrix  $A_{norm}$ , in which of course the sum of entries aggregate to unity, for all columns.
- V. The average of entries in row  $i$  of  $A_{norm}$  comprises of the  $W_i$  estimation.

In order to evaluate the consistency of the matrix, another procedure is suggested [30]:

- VI. Computation of  $AW^T$ , in which,  $W^T$ , the weighting vector's transpose matrix.
- VII. Calculation of the maximum Eigen value ( $\lambda_{\max}$ ) with the use of the following equation:

$$\frac{1}{n} \sum_{i=1}^n \frac{\text{ith entry in } AW^T}{\text{ith entry in } W^T} \quad 2.10$$

- VIII. Estimation of the Consistency Index (CI) through equation 2.11

$$CI = \frac{(\lambda_{\max}) - n}{n - 1} \quad 2.11$$

For a perfectly consistent decision-maker,  $CI=0$ .

- IX. Comparison of the CI indicator to the Random Index (RI) for the appropriate value of n, as shown in table 2.2:

**Table 2.2:** : RI for different values of n [30].

n	2	3	4	5	6	7	8	9	10	11	12
RI	0	0.58	0.90	1.12	1.24	1.32	1.41	1.45	1.49	1.51	1.48

If  $\frac{CI}{RI} < 0.10$  then the degree of consistency is satisfactory.

### 3. Estimation of the score of each alternative for each different criterion

In this step, comparison matrices for each criterion are established, in which each alternative is assigned a value according to its relative score. The values are again selected according to the fundamental scale and they represent the relative comparison between the scores of the criteria in each alternative.

### 4. Acquisition of the overall score of each alternative

The fourth and last step of this process includes the synthesis of the “objectives weights”, with the score of each alternative assigned on each criterion. The resulting overall score of each alternative leads to the “composite weight”, according to equation 2.12 [30]:

$$\text{Final Score of Alternative 1} = \sum_i (\text{Weighting Factor of Alternative 1 with respect to Criterion } i) \times (\text{Weighting Factor of Criterion } i \text{ with respect to goal}) \quad 2.12$$

## Monte Carlo Method

An alternate MCDA method suggested the utilization of Monte Carlo simulations in order to determine the final ranking of the tools. The weighting factors that were assigned to the criteria in the AHP by the decision-maker, judging by both the objectives as well as the relative comparison of the criteria, are instead examined in a range of varying values. In that respect, random weights are generated for each criterion, without any knowledge on the relative importance of each criterion to the eventual fidelity metric, in contrast to the AHP. In

the latter, the hierarchical scheme assessed the relative impact of each criterion to aggregate fidelity, and thus resulted to the consequent assignment of weighting factors to the respective fidelity criteria, as indicated by the fundamental scale (Table 2.1). In the Monte Carlo Method, multiple Monte Carlo simulations are conducted and the results are examined in the whole spectrum of those simulations. In the words of Butler J. et al. iterate Monte Carlo simulations “investigate the impact of varying the functional form of the multi-attribute aggregation” [3]. The mathematical framework proposed in [3] established the set of the following rules:

- All weighting factors  $w_i$  should be situated between 0 and 1.
- For  $n$  attributes:

$$\sum_{i=1}^n w_i = 1 \quad 2.13$$

An additional utility function was used in order to rank the alternatives, in which each criterion is multiplied by the respective weighting factor, as shown in equation 2.14:

$$U_j = \sum_{i=1}^n w_i u_i \quad 2.14$$

where  $U_j$  the single attribute utility function over the  $j^{th}$  alternative,  $w_i$  the weighting factor for the  $i^{th}$  criterion and  $u_i$  the score of the  $i^{th}$  criterion.

One of the examples in which the particular method was applied should provide insight on the overall process. In the context of this method, Butler J. et. al. used among others a case study concerning the site selection for a coal power plant [3]. In its application, there were initially five potential sites, hence five alternatives, and the choice of criteria involved Cost, Air Quality and Site Biology. All possible combinations were initially assessed rather than series of one-dimensional sensitivity analyses to a particular weight [3]. Figure 2.9 depicts a graph of the initial analysis, in which Sites 1 and 2 seem the most dominant. It is worth mentioning that Site Biology for any  $(x, y)$  pair is equal to  $1 - x - y$ .

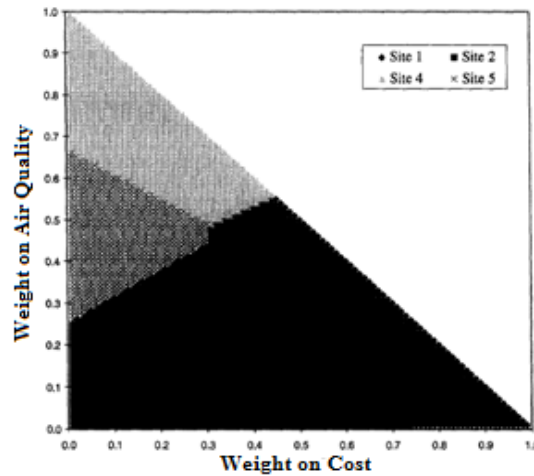


**Figure 2.9:** Most preferred alternatives at all possible weight combinations for a coal power plant site selection through the suggested method, for a set of three attributes: Cost, Air Quality and Site Biology [3].

### 3. Use case

A user has to select among a significant number of existing tools in order to perform stability checks in complex offshore wind systems. In that respect, the user should establish a set of goals that should be fulfilled in the simulation of those checks, at a certain design stage. Both intention of use as well as the particularities of those tools constitute the two main aspects of their relative comparison. The fact that a short number of certified TD tools however are mainly used in those checks should be addressed. Considering their long times of simulation, they frequently contribute to over-dimensioning of the support structure, due to inability of extensive application of different environmental conditions within the same OWF [36]. In contrast, potential tools of similar performance and greater speed of simulation are set aside, and valuable resources such as time and capital, are overconsumed.

#### 3.1 Particularities of the Use Case

The type of offshore wind structure examined in the current thesis was selected in respect to the offshore wind industry trend and short-term future targets. As a result, the examined type of offshore wind turbine should have a nominal power above the installed average, with a consequent greater size than the offshore wind turbines installed in the functioning OWFs. Additionally, the type of selected support structure should consist of a monopile, with the natural addition of a suitable transition piece, as most existing installed offshore wind structures. Moreover, the design should be determined to be installed in greater depth than the conventional installation depths in functioning OWFs, such as the Middelgrunden, a part of which is depicted in Figure 3.1, since offshore wind energy sector is oriented towards greater wind turbines, installed at greater depths with consequent greater energy yields.



**Figure 3.1:** Part of Middelgrunden offshore wind farm, situated in Danish part of the North Sea. All turbines have a nominal power of 2MW and a total nameplate capacity of 40MW [1].

As introduced in Chapter 1, the goal of this thesis was oriented towards the determination of fatigue damage for monopile-based offshore wind turbines, at an early design stage. In respect to the required checks, the design driver of the structure is considered fatigue damage. The magnitude of fatigue damage indicates whether the structure will fail during its nominal lifetime of 20 years [57]. In case the value of fatigue damage is less than 1, then the structure is justified safe for its lifetime and when greater than 1, the structure is unsafe and it is probable that it will fail at a certain point during its lifetime. However, if its value is less than unity, that suggests that the structure is over-dimensioned, hence more resistant against fatigue. Consequently, larger amounts of materials are used with costlier processes, which render the structure more expensive than it should be. As a result, it would only be logical to primarily assess whether the structure is safe, hence damage is less than 1, and then alternate dimensions or elevations of the structure in order to reach as close to unity as possible, in order to render it cost-efficient. Furthermore, the primary goal set by the offshore wind industry consists of lowering the cost per kWh, and the procedure would be aligned with the sector's directive [26] [28].

At this point the role of other stability checks of the structure should be mentioned such as (first) natural frequency checks, Ultimate Limit States, local and global buckling and lateral stability checks. It is possible that if a design is under tailoring to become more slender, the structure would be more susceptible to loading and potentially fail a number of that checks. Typically, constant trade-offs are assessed in order to both guarantee for the stability of the structure according to a number of the aforementioned design drivers, as well as to reduce initial capital. Within the framework of this thesis fatigue damage is the primary design driver of the structure but the issue of additional stability checks is addressed as well – Figure 3.2.

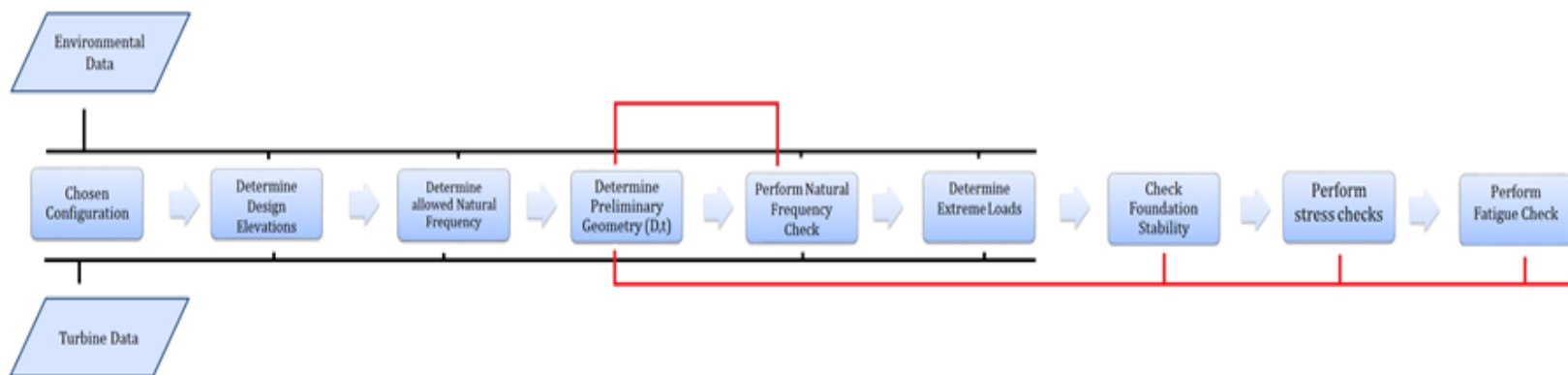


**Figure 3.2:** Flow Chart of the Design Process of an Offshore Wind Support Structure (monopile). Black lines illustrate the dependence of environmental and turbine data to the respective stages of the procedure while red lines indicate potential loops due to the imminent checks that would change the initial design [28]

## 3.2 Tools

### 3.2.1 Time & Frequency Domains

Fatigue assessment can potentially be performed in a number of tools in order to determine fatigue damage. The choice of tool is highly significant since accuracy and speed of simulation have been identified as the most important criteria [15] [30] [45] in tailoring the design and guaranteeing for its safety. Naturally, each tool possesses different characteristics, hence serves better specific purposes. Tools should be compared in simulation of the same design and therefore the selection of one tool over another should be justified. In the current thesis, three tools that perform fatigue assessment are used in order to determine the fatigue damage of a monopile-based offshore wind turbine. The first tool performs fatigue assessment in the FD, as presented by van der Tempel [48], the second tool consists of a simplified fatigue assessment in the FD [36] and the third type is associated to the conventional fatigue assessment in the TD [22]. Figure 3.3 illustrates both TD and FD signals.

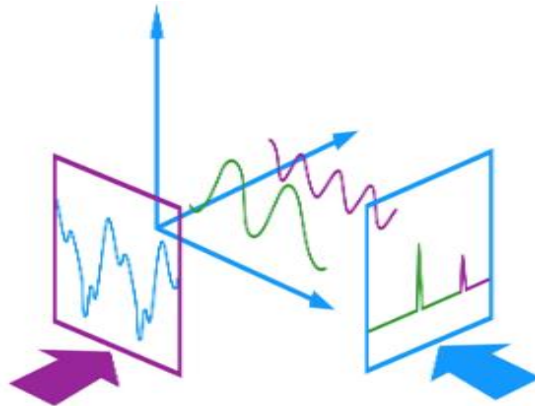


**Figure 3.3:** Illustration of signals in time(left) and frequency(right) domains.

In offshore engineering fatigue assessment is conducted in the FD, because waves can be effectively linearized [48]. In this kind of assessment the high speed of simulation comprises of a significant advantage in comparison to the respective tools operating in TD. In addition, the provision of all intermediate to the process results, as well as the “*clarity of presentation of the final outcome*” [48] comprise of the primary advantages of fatigue damage determination in the FD. In addition, users could be active in both TD and FD for calculation of various magnitudes. Time series are converted to Power Spectral Densities (PSDs) through Fast Fourier Transformations (FFTs) and reversely with the use of Inverse Fast Fourier Transformation (IFFTs). To specify, the Fast Fourier Transformation (FFT) was used in both FD tools, in the process of fatigue assessment. As a result, a brief description of the particular transformation as well as specific details that were dominant in the process should be highlighted [40] [50]. As a result, the most common output of the FFT algorithm is the Power Spectral Density (PSD), when plotted as a function of frequency [48].

In addition, a time signal can be recreated by a spectrum with the assumption of a random distribution of the phase angle. Consequently, harmonic waves emerge from the PSD at each

frequency through Inverse Fast Fourier Transformation (IFFT). The resulting time series from the frequency domain hold the same spectral parameters but are in no shape or form exact copies of the original series of the time domain the spectrum resulted from [48]. The conversion of signals from TD to FD and vice versa is illustrated in Figure 3.4.

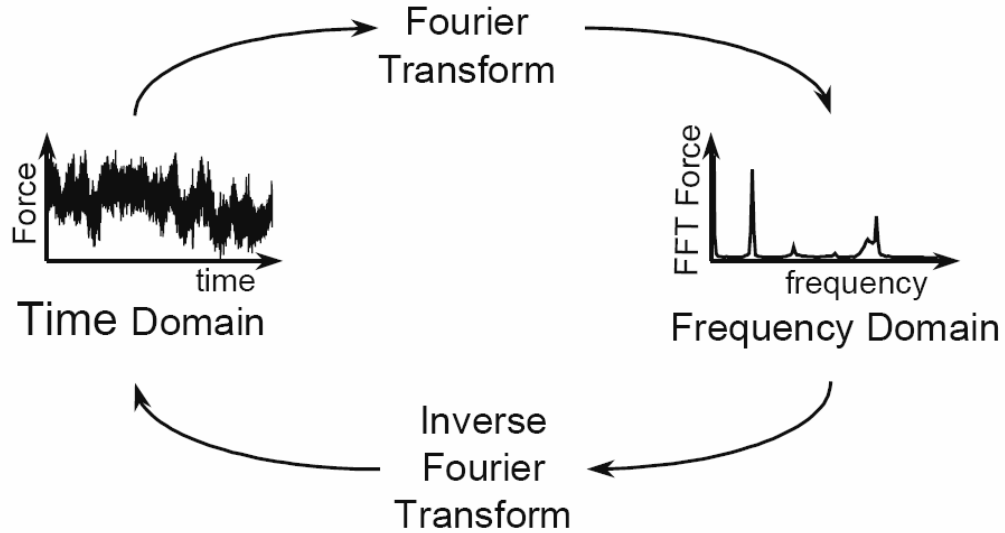


**Figure 3.4** : Conversion from both TD to FD via FFT as well as from FD to TD through IFFT, respectively [48].

### 3.2.2 Fatigue Assessment in the Frequency domain - Tool 1

The particular type of fatigue assessment was proposed by Jan van der Tempel in his PhD dissertation. It comprises of a FD type of assessment with a particular set of specifications. Series of quality controls are performed in order to evaluate and modify the resulting signal, such as the Nyquist frequency, that prevents the aliasing effect or windowing techniques such as Hanning's windows, in order to apply overlapping sub-records to regular sine wave records [48]. Diffraction of submerged members is also assessed through the MacCamy-Fuchs correction [5]. The system's transfer function (TRF) is determined in such a way to provide a direct connection between input and output amplitude for all frequency ranges. Through the TRFs, turbine calculations are uncoupled from the behavior of the support structure and the Kaimal spectrum [17] is used for the description of the wind spectrum. Consequently, equation 3.1 was used in order to determine the transfer function from wind speed to tower top load:

$$TRF = \sqrt{\frac{S_{F_{top}}(f)}{S_V(f)}} \quad 3.1$$

where  $S_{F_{top}}$  and  $S_V$  the tower top load and wind spectrum, respectively. The phenomenon of aerodynamic damping has to be calculated in order to successfully uncouple tower top from support structure and an engineering estimation is used in this case. Since TRF is computed,

the total bending stress spectrum can be calculated and is integrated to wave excitation. The spectra of stress response are used to calculate fatigue damage with the use of Dirlik method [36], which is the equivalent of Rain Flow Counting (RFC) of the time domain.

The above process was modelled in MATLAB by Ortega A. [62], and provided a tool through which fatigue assessment in the FD is performed. The tool was developed based on Jan van der Tempel's PhD dissertation [48], where all aforementioned theory was applied in the MATLAB environment. Overall, times of both simulation and operation are anticipated shorter than in the respective tools performing fatigue assessment in the TD, and the yielded outputs are pre-justified accurate in literature [36] [48]. The current tool will be mentioned as Tool 1 in the chapters to come, for the sake of brevity.

### 3.2.3 Simplified Fatigue Assessment in the Frequency Domain – Tool 2

This simplified type of fatigue assessment in the FD was based on the suggested approach of Arany et al. [1] and proposed by Michalopoulos V [36]. Instead of the TRF in section 3.2.2, a dynamic amplification factor (DAF) is implemented. Through DAF, the quasi-static response to the excitation that is analytically calculated is translated to fore-aft moment's PSD. These PSDs are converted to stress PSDs and with the use of Dirlik method fatigue damage is calculated [36]. The below scheme in Figure 3.5 illustrates the particular method.

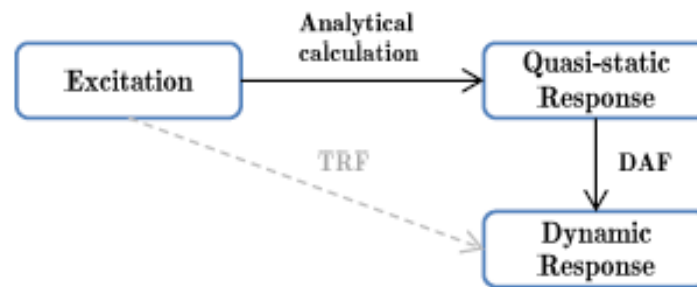


**Figure 3.5** : The by-pass of the TRF as proposed in [36].

The anticipated levels of complexity of this simplified method are even lower than in the van der Tempel's method, and simulations should be simpler. As a matter of fact, the methodology developed by Michalopoulos V. [36], through which the particular type of simplified fatigue assessment was also integrated in a MATLAB tool in the framework of his MSc Thesis [36]. Relevant simulation results have indicated that levels of accuracy should be considered high [36], similar to those of GH Bladed. In the framework of this MSc thesis, this model will be referred as Tool 2.

### 3.2.4 Fatigue Assessment in the Time Domain – Tool 3

This type of fatigue assessment is considered to yield the most accurate results since all non-linearities are taken under consideration [48]. Knowledge of the values of all required parameters enables analytical computation for both aerodynamic and hydrodynamic loading.

The respective stresses are calculated with the use of RFC for a predetermined number of cycles and fatigue damage is accurately computed.

The most common tool to perform fatigue assessment in the TD is GH Bladed, a complex tool, in which operation and simulation consume significantly greater amounts of time than in Tools 1 and 2. All things considered, the accuracy of the results and access to any kind of simulation for all of the offshore structure's systems, have established GH Bladed as the most popular software in the offshore wind industry, with a consequent number of certifications. However due to the unavailability of a sustainable license for a consistent period of time, the use of NREL's FAST v8 was decided instead, which also conducts fatigue assessment in the TD. Accuracy is utterly comparable, when indeed the current use case is supposed at an early design stage. FAST v8 is addressed as Tool 3 in the remainder of the thesis. The aggregation of the associated to FAST processors is depicted in Figure 3.6.

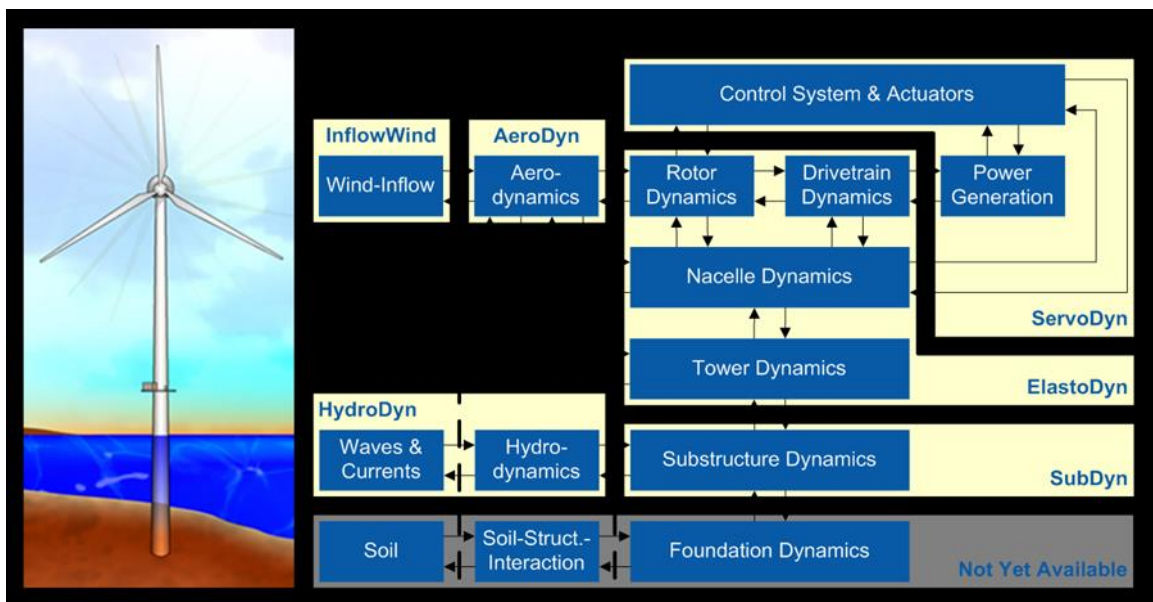


**Figure 3.6:** FAST v8 control volumes (BeamDyn, IceFloe and IceDyn are not shown) [54].

## 4. Fatigue Specification

In this chapter, detailed information that is relevant to the process of fatigue damage determination for offshore wind structures is displayed. All fundamental to the process of fatigue assessment theory paves the way to the proposed methodology fitting of Chapter 5. In that respect, all steps in fatigue damage determination are analyzed in significant detail, in order to identify all relevant parameters. Readers familiar with fatigue assessment of offshore wind turbines can continue reading in Chapter 5.

### 4.1 Fatigue Assessment

As aforementioned, fatigue damage is considered to be the design driver within the boundaries of this thesis. As a result, extended information should be displayed concerning all relative data and basic theories that build up to that particular magnitude. To specify, basically wind, wave and soil are examined, as shown in Figure 4.1, and further analyzed in order to formulate competent expressions for aerodynamic and hydrodynamic loading. Moreover, the concept of fatigue along with the suitable S-N curves are presented and eventually result to the targeting Damage Equivalent Load (DEL) and eventual fatigue damage.

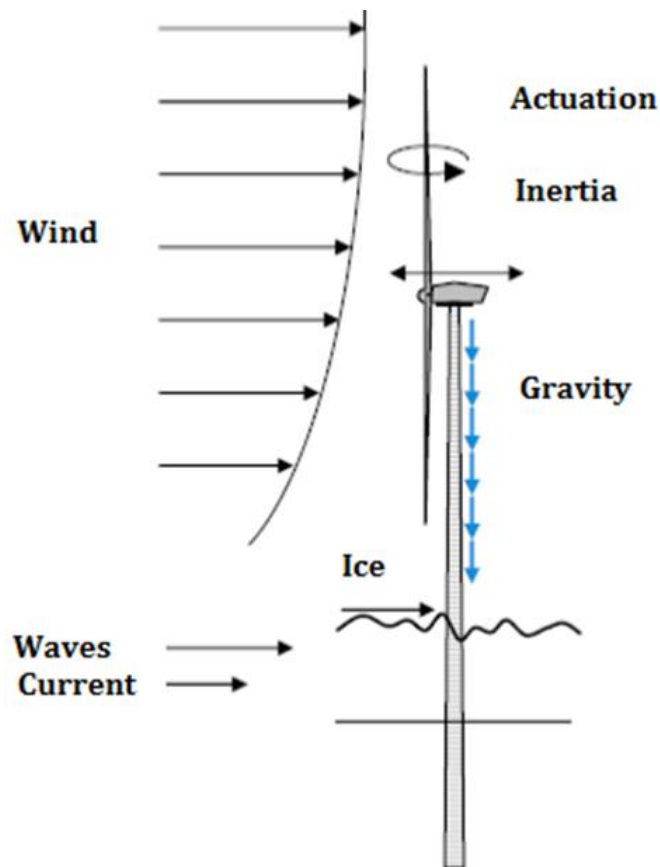


**Figure 4.1:** Load sources for a monopile - based offshore wind turbine [27].

## 4.2 Aerodynamic Loading

The term of aerodynamic loading is used in order to efficiently express the loading exerted by the wind on an offshore wind structure, in which case a series of parameters should be taken under consideration. Wind-related loading mainly results from three basic concepts: wind speed, wind turbulence and wind shear.

Wind speed at a certain height  $z$  above the ground is defined as:

$$U(z, t) = \bar{U}(z) + u(z, t) \quad 4.1$$

where  $U$  the instantaneous wind speed at time  $t$ ,  $\bar{U}$  the mean wind speed over a specific time period and  $u$  turbulent wind speed around mean speed  $\bar{U}$ .

Turbulence intensity is defined:

$$TI_i = \frac{\sigma_i}{\bar{U}} \quad 4.2$$

where  $\sigma_i$  is the standard deviation and  $\bar{U}$  is the respective wind speed. Three types of turbulence intensity have been defined in order to best describe the magnitude in 3-dimensional space. As a result, longitudinal, lateral and vertical turbulence intensities were established and are abbreviated by  $TI_x$ ,  $TI_y$  and  $TI_z$ . There are multiple turbulence models used in wind simulations but mainly the von Karman and Kaimal spectra are used.

$$S_{Karman}(f) = \frac{\sigma_i^2 4L_i / \bar{U}}{[1 + 70.8(fL_i / \bar{U})^2]^{5/6}} \quad 4.3$$

$$S_{Kaimal}(f) = \frac{\sigma_i^2 4L_i / \bar{U}}{1 + 6(fL_i / \bar{U})]^{5/3}} \quad 4.4$$

where  $f$  is the frequency,  $\sigma_i$  is the velocity component standard deviation,  $i$  the index referring to the velocity component direction (i.e. 1=longitudinal, 2=lateral, 3=vertical) and  $L_i$  the velocity component integral scale parameter [17].

Wind shear is defined in [17] as '*the variation of wind speed across a plane perpendicular to the wind direction*'. The variation is put down to the friction phenomena that occur on the surface of the terrain and greatly determine both power extraction as well as aerodynamic loading of the structure. Specifically, two models mainly determine that variation and result in alternative wind and consequently power and loading estimations. Both logarithmic and power laws are shown in equations 4.5, 4.6.

$$U(z) = U(z_r) \frac{\ln(z/z_0)}{\ln(z_r/z_0)} \quad 4.5$$

$$U(z) = U(z_r) \left(\frac{z}{z_r}\right)^\alpha \quad 4.6$$

where  $z_r$  is the reference height above ground used for fitting the profile,  $z_0$  is the roughness length and  $\alpha$  is the wind shear or power law exponent [17].

The determination of the resulting loads exerted on the structure should follow the established wind profile. The combination of the momentum theory with the blade-element theory results to the Blade Element Momentum (BEM) theory, which constitutes the basis for the computation of thrust on the rotor, as shown in equation 4.7:

$$T_R = C_{T_R} \frac{1}{2} \rho_{air} \pi \frac{D_R^2}{4} \bar{U}^2 \quad 4.7$$

where  $T$  is thrust,  $C_{T_R}$  the thrust coefficient of the rotor,  $\rho_{air}$  the air density and  $D_R$  the diameter of the rotor [36]. Since the current thesis is focused in fatigue assessment rather than power production in offshore wind systems, detailed analysis of power extraction from the wind and the aerodynamic phenomena at the blades of the rotor were not further developed in this chapter.

Additionally, another significant part of aerodynamic loading is the wind-induced load exerted across the length of the turbine's tower, or else known as tower drag. Tower drag is heavily dependent on wind shear and is computed with the use of equation 4.8:

$$f_T = C_{D_T} \frac{1}{2} \rho_{air} D_T \bar{U}^2 \quad 4.8$$

where  $f_T$  is the tower drag,  $C_{D_T}$  the tower drag coefficient and  $D_T$  the diameter of the tower.

### 4.3 Hydrodynamic Loading

Apart from aerodynamic loading, waves exert loads of greater amplitude to offshore structures and significantly determine their design, which is determined in order to sustain them and normally function throughout their designated lifetime. The framework of this thesis is associated with fatigue assessment in which currents are of minor significance [48]. As a result, the impact of solely wind and consequent wave states on the structure is examined. Consequently, in order to appropriately assess hydrodynamic loading, wave states and the variety of their existing expressions are rigorously examined.

Waves are efficiently described by the determination of three particular parameters: amplitude, frequency and direction. Wave amplitude is adequately expressed by the height of elevation in respect to still water level whereas the time intervals interceding between the passing of equal elevations from a reference point determine unique wave periods and therefore their respective frequencies. The latter is mainly defined by two terms in the respective literature, zero-crossing or peak period. In addition, wave direction implies the direction of wave propagation. At this point, the relationship between wind and wave

directions is crucial as their relevance determines the total load exertion on the structure, depending on their co-directionality, misdirectionality and in any case what these directions particularly [18].

A number of wave theories have been used in order to appropriately characterize the anticipated behavior in simulations. The two most general models comprise of the deterministic and stochastic models, which naturally are constituted of numerous and more exclusive models. The deterministic and periodic model integrate linear and non-linear theory according to which there is one dominant wave frequency in the former, while in the latter higher harmonics constitute the wave, respectively. In the framework of this thesis, given both the requirements of the estimated use case as well as the involved tools, two particular theories are further analyzed in order to familiarize the reader to the following processes. In that regard, these two theories are no other than the Airy theory in respect to the deterministic approach and the JONSWAP spectrum in relation to the stochastic model. The first theory is mostly applicable to deep water depths with consequent waves of minor wave amplitude [54] as in the second theory a wave spectrum is developed based on the Pierson-Moskowitz (PM) spectrum, which was modified “for a developing sea state in a fetch limited situation” [18].

According to the linear Airy theory the expression of orbital velocity is defined as:

$$u_w(x, z, t) = H_s \pi f \frac{\cosh(k(z+d))}{\sinh(kd)} \cos(kx - 2\pi ft) \quad 4.9$$

where  $u_w(x, z, t)$  the water particle velocity,  $H_s$  the significant wave height,  $k$  the wave number and  $d$  the water depth. However the Airy theory is applicable from seabed to still water level, and as a result additional measures are taken for the rest of the required calculations [19]. In that regard, Wheeler stretching is frequently applied [56].

The JONSWAP spectrum is included along the PM spectrum in the stochastic models, within which individual wave particles potentially differ in all amplitude, frequency and direction. As aforementioned, it comprises of a fetch-limited spectrum and as a result peaks at higher spectral densities than the PM respective spectrum. They are both illustrated in Figure 4.2 for a typical North Sea Storm State.

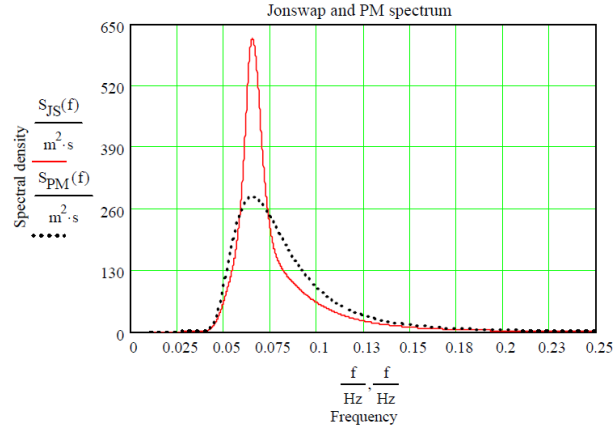


**Figure 4.2:** JONSWAP (red line) and PM (black line) spectrums for North Sea storm state [18].

The JONSWAP spectrum ( $S_{JS}$ ) is defined as:

$$S_{JS}(f) = \frac{a_{JS} g^2}{(2\pi)^4 f^5} \exp\left(-\frac{5}{4} \left(\frac{f}{f_p}\right)^4\right) \gamma^{\alpha_{JS}} \quad 4.10$$

where  $\gamma^{\alpha_{JS}}$  the peak enhancement factor,  $\gamma_p$  the peak-shape parameter and  $\alpha_{JS}$ :

$$a_{JS} = \exp\left[\frac{(f - f_p)^2}{2\sigma_{ss}^2 f_p^2}\right] \quad 4.11$$

$$\begin{aligned} \sigma_{ss} &= 0.07, f \leq f_p \\ \sigma_{ss} &= 0.09, f > f_p \end{aligned} \quad 4.12$$

where  $\sigma_{ss}$  the sea surface elevation standard deviation and  $f_p$  the wave spectral peak frequency [18].

The Morrison equation is used in order to describe the wave load exerted on the structure. The type of support structure is directly linked to the type of expression used in order to calculate anticipated wave loads. The monopile supported structures simulated in the framework of this thesis qualify and thus are included in the slender structures category [7]. As a result, the incident wave field is not modified at an extent at which Morrison's equation do not apply, hence equation 4.13 is used.

$$dF = \frac{\rho_w}{2} C_{Dp} D_p u |u| + \rho_w C_{Mp} \frac{\pi}{4} D_p^2 \dot{u} \quad 4.13$$

where  $dF$  is the hydrodynamic force,  $\rho_w$  the density of sea water,  $D_p$  the monopile's diameter,  $C_{Dp}$  the drag coefficient of the pile,  $C_{Mp}$  its inertia coefficient,  $u$  the water particle's velocity and  $\dot{u}$  its acceleration [8].

## 4.4 Soil

The integrity of an offshore wind structure is only guaranteed when respective loads are efficiently transferred to the soil under the structure. The soil greatly interacts with the support structure, and checks that involve natural frequency and damping determination are directly dependent to its properties. In addition soil consists of several layers of a variety of materials such as sand, clay and silt. In addition, the two aforementioned materials which consist most of the soil areas of the North Sea present certain fundamental properties that determine structural calculations. Throughout the North Sea, where most of the current OWFs are currently operating, the most common layers consist of sand and clay. However, accurate soil data are more than challenging to acquire for an average area, since there are enormous variations even within the same wind farm. These properties are expressed through established magnitudes, the most significant of which are below displayed.

$\gamma$ : The effective or submerged unit weight of soil and is defined as the ratio of the total submerged weight of soil to the total volume of soil [36] [kN/m<sup>3</sup>].

$\varphi$ : This abbreviation stands for the external friction angle between a soil medium and a material, as in the case of a monopile [degrees]. It is defined for sand but not for clay.

$c_u$ : It is defined as undrained shear strength and expresses the amount of shear stress soil can withhold [N/m<sup>2</sup>]. It is defined for clay but not for sand [8].

## 4.5 Additional Variable Loading

Apart from the aforementioned environmental loading, the offshore wind structure is subject to another kind of loading of significant magnitude. The Rotor-Nacelle-Assembly (RNA) comprises of heavy equipment and heavy components that are in state of constant motion. As a result, additional cyclic loads are induced and derive harmonic loading to the structure.

Given the state of the offshore wind turbine, these loads are both diversified and attributed to varying causes. For all types of conventional wind turbines, aerodynamic imbalance and mass imbalance are governed by the rotational frequency 1P of the rotor. For a 3-bladed wind turbine, tower shadow constitutes of the main driver of the 3P cyclic load and therefore is associated to the rotational 3P frequency. Apart from the main origins of the 3P cyclic loading, additional variable loading is attributed to wind-shear as well as yaw misalignment. In the context of this thesis, given the focal point of the assessment at an early design stage, mass imbalance and tower shadow result to 1P and 3P cyclic loading, respectively [36]. Consequently, these loads are taken under consideration in the fatigue damage determination along with the rest aforementioned environmental loads.

## 4.6 Fatigue

Fatigue failure is associated to a particular effect observed at certain types of structures. When internal stress is varying, even if never above average or yield stress, as shown in figure 4.3, at some point failure occurs, which type is defined as fatigue failure. This particular effect occurs when the cracks inside the material, due to its imperfections grow and eventually cause material failure. This occurs due to the fact that not only stress in the material is evenly distributed, but is also concentrated at the edges of the cracks. The stress at those edges is

greater than the average stress in the material, since local stress concentration is exceeding both yield and ultimate stress in load cycles, resulting to significant and eventually terminal growth at the cracks. Specifically in cyclic loading, in which there are continuous loading variations, every time there is an extreme there could be an incremented growth at the crack. Therefore, fatigue failure is associated to the imperfections in the material that increase in size because of the stress concentration at the edges of the cracks. Eventually cracks are developed to an extent that the residual strength in the material is not enough to prevent failure, as shown in Figure 4.3, even if average stress is globally below the yield stress of the material [57].

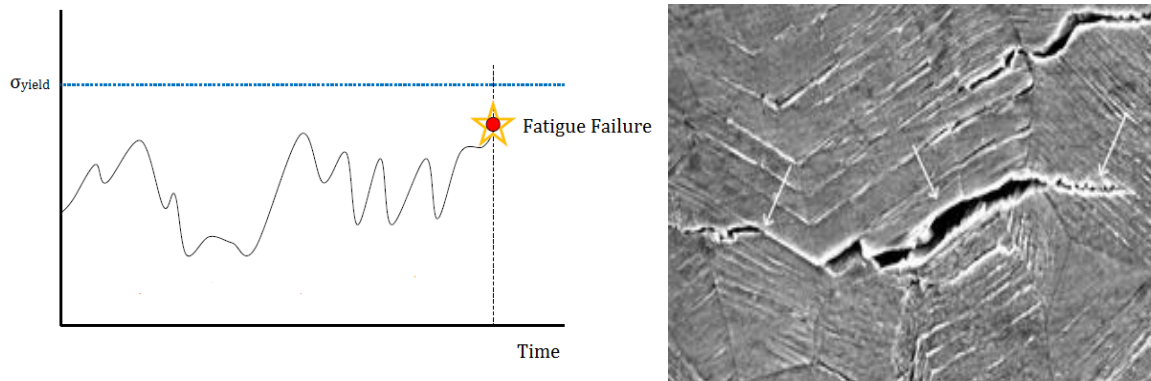


**Figure 4.3** : Stress plotted versus time with the inclusion of yield stress and point of failure (left). Imperfections that are developed due to high stress concentrations and lead to failure (right) [57].

#### 4.7 Rain Flow Counting & Dirlik Method

Fatigue damage calculations are associated to both RFC and Dirlik methods, in the TD and the FD, respectively. The bending moments that result from all aforementioned steps are converted to bending stresses and additionally computed by applying either RFC or Dirlik method, depending on the type of domain the assessment is conducted. Both methods should be presented in further detail, due to the significance of fatigue damage in the selected use case as well as because both methods are used in all three tools.

##### Rain Flow Counting (RFC)

In order to appropriately assess stress cycles in broad band time series, a particular counting method has been introduced, defined as Rain Flow Counting (RFC). Due to both variable amplitude and varying cycles of the examined stresses, RFC has provided an adequate break down of stress history into individual cycles that aggregates to a stress range distribution [55].

A set of rules determine the process of RFC, according to which the desired stress range is acquired. The main principle in RFC focuses in the account of reversals through hysteresis loops in relation to the material's stress/strain correlation. Concordantly, each time a

hysteresis loop is closed, a cycle is counted through RFC. The following set of principles typify a conventional application of the RFC process [55]:

- RFC commences at each peak and trough.
- In case of a trough, the flow stops when the opposite trough is more negative than the initial.
- In case of a peak, the flow stops when the opposite peak is more positive than the initial.
- If the flow intercepts with an existing one of an earlier path, the present path is stopped.

The below displayed Figure 4.4 aids the reader to comprehend the generic process of a RFC of a process  $X(t)$ .

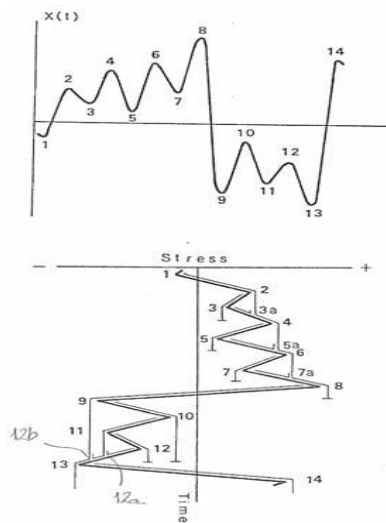


**Figure 4.4:** The emerging half cycles of trough and peak generated stress ranges aggregate to a total count of full cycles 2-3-3a,4-5-5a, 6-7-7a, 9-10-12b and 11-12-12a and a total count of half cycles 1-8, 8-13and 13-14, respectively [55].

### Dirlik Method

The Dirlik method comprises of the RFC correspondence to the FD. It is an empirical method that emerged from the application of broad-band signals to both TD and FD, and their relative comparison [48]. The specific method that was used in both Tool 1 and Tool 2 is rigorously described in [6] with the additional specifications situated in [38] [39] and [51].

### 4.8 S-N curve

S-N or Wöhler curves consist of two-dimensional curves in which constant cyclic stress amplitude  $S$  which is applied to a specimen is plotted versus the number of loading cycles  $N$ , up to the moment of its failure or the creation of a crack of predefined size [53]. These curves were developed in order to establish empirical means of quantification of the fatigue process, and design structures in ways to prevent fatigue failure. The simplified version of the curve, in which the term accounting for the thickness ratio is constant and equal to 1, is expressed in equation 4.14:

$$\log_{10}(N) = \log_{10}(\alpha) - m \log_{10}(\Delta\sigma) \quad 4.14$$

where  $\Delta\sigma$  is the stress range,  $N$  the number of stress cycles until failure which occurs at  $\Delta\sigma$ ,  $\log_{10}(\alpha)$  the intercept of  $\log_{10}N$  axis and  $m$  the negative slope of the curve which is constant at this simplified version [36].

This simplified version of the curve is not directly applicable to multiple cases since it does not include all load cycles. Less significant load cycles which are not accountable for the primary creation of a crack, while they contribute to growth extension of an already existing crack are not taken under consideration. A limit below which no failure would occur under constant amplitude loading was defined as fatigue strength  $\Delta\sigma_A$  ( $dS_A$  in Figure 4.5), the intersection of which with the original S-N curve occurs in  $N_D$  cycles as shown in the same figure. Beyond  $N_D$  cycles the curve resulting from experimental data of however disputable accuracy is shown as the 'Original Miner curve'. The modifications that have been established included a series of corrections. The conservative approach suggested by Corten-Dolan indicated the extension of the right part of the curve, with the same slope however, in an effort to include lesser cyclic loads. In addition, Haibach suggested that the slope at the lower right part of the curve should be considered:

$$m_{right} = 2m_{left} - 1 \quad 4.15$$

where  $m_{left}$  the slope at the left part of the figure while  $m_{right}$  the negative slope in the lower right.

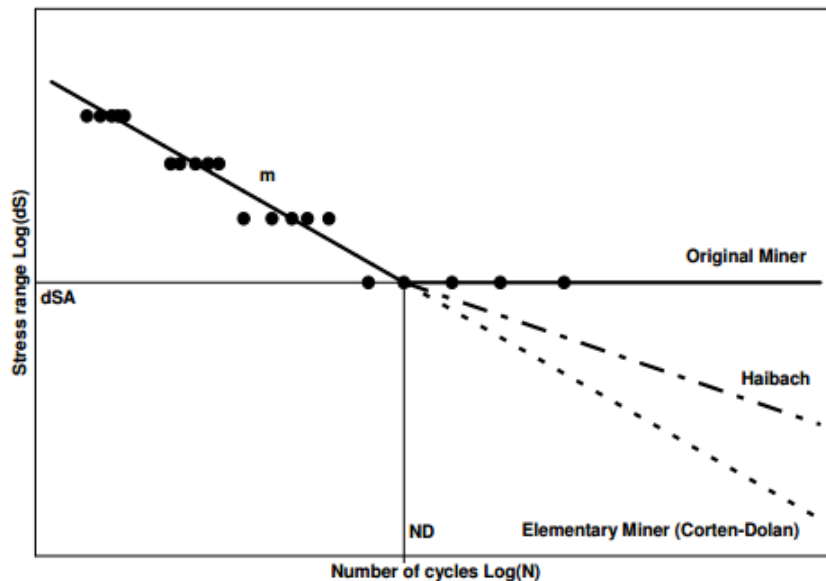


Figure 4.5: Various suggestions on S-N slopes [53].

All things considered, due to the accuracy of the 'Original Miner curve' and the conservatism of the Elementary Miner, Haibach's suggestion is more popular in fatigue assessment. In addition, all of the above are valid primarily for metals which constitute the monopile rather than composites, which are irrelevant to fatigue assessment in the framework of this thesis.

## 4.9 Fatigue Damage

Miner's sum is defined as "the summation of individual fatigue damage ratios caused by each stress cycle or stress range block according to Palmgren-Miner rule" [9]. Palmgren-Miner rule suggests that total fatigue damage is computed by the summation of damage caused by each individual load cycle linearly, therefore enhancing its near universal use - probabilistic approach. As a result, when Miner's sum reaches unity fatigue failure is expected. The exact expression is shown in equation 4.16:

$$D = \sum_{i=1}^k \frac{n_i}{N_i} = \frac{n_1}{N_1} + \frac{n_2}{N_2} + \dots \quad 4.16$$

where  $n_i$  are the cycles of a particular signal  $i$ ,  $N_i$  the cycles to failure and  $D$  is the fatigue damage [53].

## 4.10 Damage Equivalent Load

The concept of damage equivalent load (DEL) eases the comparison of two or more fatigue load spectrums and is relatively simple to perform. In addition, multiple loads due to respective stress signals are rounded to that damage equivalent load of constant amplitude which is representative of the load. Hence, fatigue damage equivalent load consists of the load that for a chosen number of cycles  $N_{eq}$  would result to the same damage as all actual loads combined [53]. The definition is given in equation 4.17:

$$DEL = N_{eq}^{1/m} \left( \sum_{i=1}^n n_i \Delta F_i^m \right)^{1/m} \quad 4.17$$

where  $N_{eq}$  the equivalent cycles,  $\Delta F_i$  the fatigue load cases,  $n_i$  the cycles of each load case and  $m$  the inverse slope of the respective S-N curve [53].

## 5. Generic Application of the Fidelity Framework

The specification of the fidelity criteria to the use case and the nature of the process of fatigue damage determination should be addressed. In an attempt to suitably conform fidelity criteria to this very use case, and later apply the suggested methodology to the case study of Chapter 6, the establishment of the referent framework of parameters, as described in Chapter 1, was determined necessary. Especially for the detail criterion and all relevant fidelity theory, the determination of the referent level of detail, according to which the comparison between the in disposal tools would be conducted, was justified compulsory.

The framework of fidelity criteria suggested in Chapter 2 was expressed in a generic manner. All selected criteria were assigned respective metrics that did not limit their boundaries of application and were quantified accordingly. In addition, the referent level of detail that would be determined to establish the benchmark for tool comparison, was identified through fatigue-related parameters and their internal relations.

Nevertheless, the determination of the use case and the introduction of the specifics of the three in disposal tools required adequate fitting to the criteria. The determination of fatigue damage as the design driver of the structure imposed the type of parameters that should be considered in fidelity expression. In relation to the detail criterion, the parameters that would constitute the detail metric are associated with the process of fatigue damage determination and were derived from the aggregation of intermediate steps of fatigue assessment, as described in Chapter 4. Additionally, all accuracy, ST and OT should be integrated to the tools in order to acquire the scores that would lead to fidelity quantification and eventual tool comparison. As a result, tool environments should be meticulously analyzed in order to implement the criteria accordingly.

### 5.1 Referent Framework of Parameters

The establishment of a framework of parameters is justified indispensable to the determination of the detail criterion (eq. 2.6, 2.7). The use case indicated that the structure should be considered at an early design stage, with fatigue damage being the design driver. The parameters that would be included in the referent framework were justified prerequisite to fatigue assessment. The depiction of reality that would determine the level of detail required to fatigue damage determination was thus expressed through the particular framework. Hence, the referent framework of parameters required thorough examination of all stages of the overall process that eventually resulted to fatigue damage determination, as analyzed in Chapter 4.

In order to determine the referent framework and include all required parameters, the division of all parameters to subcategories would contribute to the acquisition of the desired end result. Environmental loading should be naturally separated to wind and wave related parameters, in respect to aerodynamic and hydrodynamic loading, respectively. Moreover, soil-related parameters that are justified decisive to damage equivalent load [36] were included in the soil-related set of respective parameters. Additionally, the installed wind turbine's specifications that influence load exertion and therefore fatigue damage should be included in a separate subcategory. Furthermore, series of design elevations and various masses should also constitute an additional subcategory, since they impact fatigue damage.

To continue, the attributes of pile and transition piece impact fatigue damage were included in the Designer’s Framework. Overall, the division of the main framework in five subcategories (Tables 5.1 – 5.5) contributed to the inclusion of all parameters that were justified prerequisite, as well as mitigated overlapping between categories and possible repetition of parameters in the referent framework.

The indication of fatigue damage is dependent on the environmental loading of the structure, hence the wind load. Wind results into the aerodynamic load exerted on the offshore structure, and therefore certain relative magnitudes consist of basic parameters to the suggested subcategory. To specify, the aforementioned wind speed and turbulence in multiple directions are highly involved in the determination of aerodynamic loading, and therefore included in the framework. Moreover, the variables in the wind spectrum equations are justified significant to the load, as shown in equations 4.3 & 4.4, and result to the inclusion of  $\sigma_i$ , the velocity component standard deviation (i the index referring to the velocity component direction (i.e. 1=longitudinal, 2=lateral, 3=vertical)) and  $L_i$ , the velocity component integral scale parameter of the respective Kaimal spectrum [17].

Apart from the above, the thrust normal to the rotation plane as well as the tower’s drag force that is determined from the wind shear, impact aerodynamic loading, especially the former. Additionally, judging by the logarithmic law in equation 4.5, sea surface roughness should be included to the set of existing parameters. Similar magnitudes such as air density  $\rho_{air}$  or integral length scale  $L_v$  that are indicated by design codes [8] [17], were also included in the same framework. In addition, drag coefficients such as  $C_{DT}$  and  $C_{TR}$  and respective rotor and tower diameters that are subject to equations 4.7 and 4.8 were included among the aforementioned parameters. All above parameters that were justified indispensable to fatigue damage determination are displayed in Table 5.1.

It is worth mentioning however that in the both MATLAB tools and in FAST v8 the input of environmental conditions was associated to alternate parameters. In both MATLAB tools the environmental conditions are simulated through lumped load cases of a particular wind speed and turbulence intensity. In FAST v8 through TurbSim, particular time series were produced, which required an input of average wind speed and longitudinal deviations. This should not be misinterpreted as parameter exclusion, since the respective parameters were still derived in the tools and were taken under consideration, even if the user did not include them among the input. Table 5.1 enlists the parameters that were related to wind-load:

**Table 5.1:** Parameters related to Aerodynamic Loading.

Aerodynamic Load-related Framework	
Mean wind speed	$\bar{U}$
Longitudinal Turbulence Intensity	TI
Rotor’s Thrust Coefficient	$C_{TR}$
Rotor Diameter	$D_R$
Tower’s Drag Coefficient	$C_{DT}$
Tower Diameter	$D_T$
Surface Roughness	$Z_0$
Air Density	$\rho_{air}$

Hydrodynamic loading comprises of additional environmental loading and thus determined a significant part of the parameters of the overall referent framework. In particular, since waves are characterized by their respective height and period, their magnitude is highly important to load configuration, hence included in the proposed framework. Sea depth and tidal range were also included as they determine the magnitude of waves. Water particle's velocity and acceleration were calculated by equation 4.9 [36]. All above parameters should be naturally considered in fatigue assessment.

Wave spectral density was taken into account in hydrodynamic loading as well. The JONSWAP spectrum best describes the wave spectra that are present in the location of North sea, as instructed in multiple credited design codes [8] [18]. The respective wave spectra which are defined by the JONSWAP equation (eq. 4.10), resulted to the inclusion of the peak enhancement factor  $\gamma$ , and peak wave periods  $T_p$ , among the hydrodynamic load-related Framework.

In addition, both coefficients and dimensions of the pile of the structure that are associated with the Morison equation 4.13 were included in the same framework. As in the case of aerodynamic loading, the associated to hydrodynamic loading parameters, that were justified essential to fatigue damage determination are enlisted in Table 5.2.

**Table 5.2:** Parameters related to hydrodynamic loading.

Hydrodynamic Load-related Framework	
Significant wave height	$H_s$
Wave peak period	$T_p$
Pile diameter	$D_p$
Enhancement Factor	$\gamma$
Submerged structure's drag coefficient	$C_{Dsp}$
Submerged structure's inertia coefficient	$C_{Msp}$
Diffraction Moment Coefficient	$C_{DM}$
Water depth	$d$
Tidal range	TR
Probability of occurrence of lumped state	$P_{occ}$
Water Density	$\rho_w$
Acceleration of Gravity	$g$

Soil properties and the respective scour created at sea depth are highly significant to fatigue assessment [36]. The lateral stiffness of the structure is associated with the soil properties [28]. Soil properties such as the effective unit weight of soil  $\gamma$ , the external friction angle  $\varphi$  and the undrained shear strength  $C_u$  [8] are directly linked to that stiffness determination. Scour also partially determines the stiffness since holes appear around the pile of the structure at seabed level, thus reducing soil properties.

**Table 5.3:** Parameters related to soil configuration.

Soil-related Framework	
Effective unit weight	$\gamma_s$
External friction angle	$\Phi$
Undrained shear strength	$C_u$
Scour length	$L_s$

Additionally, the selection of wind turbine is crucial to fatigue assessment. Dimensions such as tower top diameter determine the respective stresses and exerted loads. In addition parameters such as rotor diameter, thrust coefficients and RNA mass, significantly contribute to load determination as shown in Chapter 4. Moreover, other design parameters such as the diameter of the yaw bearing which determines the tower top diameter and design elevations such as hub height, that determine the upper limit of wind shear, should evidently be included in the overall referent framework. All design parameters and elevations contributing to fatigue damage determination are displayed in Table 5.4.

**Table 5.4:** Parameters set by turbine manufacturers

Wind Turbine-related Framework	
Operational Wind Speeds	$U_{\text{cut-in}}, U_R, U_{\text{cut-out}}$
Operational Rotor Speeds	$\Omega_1, \Omega_2$
RNA mass	$M_{\text{RNA}}$
Rotor Overhang	$b$
Yaw Bearing Diameter	$D_Y$
Tower mass imbalance	$m_I$
Tower top diameter	$D_{\text{Tt}}$
Center of mass position	$X_{\text{CM}}$

Certain dimensions, such as the rotor diameter, were not listed in Table 5.4 because they were already included in Table 5.1. The parameters should be only included once, in order to mitigate error in later computations in the detail criterion configuration.

The variety of elevations determined by the designers of the structure such as pile diameter and respective wall thickness as well as structural choices such as the selection of a particular kind of steel with its own intrinsic properties, were all included in the fifth subcategory. In addition, directives indicate the slope or knee in the S-N diagram or the particularities of the definition of a load case which should be selected for simulations in order to grant certification to the structure [9]. In brief, the parameters in Table 5.5 represent significant designers' choices to the structure. All respective dimensions and elevations greatly contribute not only to the determination of fatigue damage of the structure, but also in other stability checks that are conducted throughout the various design stages. Lastly, it is worth mentioning that the spacing of the OWF that determines the wake of the respective wind turbine, and comprises of a design option in all three in examination tools, was excluded from the framework. That is due to the stipulated use case, since it is associated with the examination of a single wind turbine at an installation site and at an early design stage.

**Table 5.5:** Structural & design parameters.

Structural & Design-related Framework	
Tower top wall thickness	$t_{Tt}$
Tower base diameter	$D_{Tb}$
Tower base wall thickness	$D_{Tt}$
Interface elevation	$z_l$
Grout Length	$L_g$
Grout thickness	$t_g$
Transition piece diameter	$D_{TP}$
Transition piece thickness	$t_{TP}$
Transition piece base elevation	$z_{TPb}$
Pile wall thickness	$t_p$
Penetration depth	$L_p$
Young's Elasticity Modulus	$E$
Steel density	$\rho_s$
Material factor	$\gamma_f$
Stress concentration factor	SCF
S-N steel Curve	$S, N$

The aggregation of the above displayed frameworks in Tables 5.1 – 5.5 constituted the referent framework of parameters for fatigue assessment. This framework ordains the anticipated level of detail from the tools for the current use case. In addition, the referent parameters included in the definition of detail in Chapter 2 were selected from the particular framework, and were submitted to further sensitivity analyses.

## 5.2 Implementation of Criteria

The proposed methodology in Chapter 2 was expressed in a generic manner and as a result needed further specification to fatigue assessment. According to section's 5.1 referent framework of parameters, the requested level of detail was ordained for the use case of Chapter 3, through the choice of the parameters in the respective framework. In addition, all fidelity criteria should apply to the case study of Chapter 6. Towards that end, the intention of use which partially determined the fidelity quantification process [44] determined the specification of the criteria to the tools of Chapter 3.

Accuracy was conformed to the specifications of Chapter's 3 use case by specifying the design driver to fatigue damage. The referent fatigue damage would be set marginal to unity, since the tower's and pile's wall thicknesses that would result to unity should be rounded to millimeter accuracy, due to manufacturer's limitations. Considering the theoretical grounds of the very magnitude of fatigue damage as well as the absence in data, referent accuracy was identified to the theoretically most accurate tool in disposal, GH Bladed [48].

Time of simulation was measured throughout the total of simulations. In order to render the measurements comparable, ST should be measured with the same means of measurement in all three tools. The form of the criterion suggests that shorter times of simulation result to higher values of the respective metric, which ranges from 0 to 1. Overall, this criterion along with operational time were the most straight forward in both expression and measurement.

The type of ST measurement could be selected from a variety of methods. Floating Point Operations (FLOPs) is considered any mathematical operation that involves floating point numbers that contains decimal points [37]. They are more complex than binary numbers, hence FLOPs take longer to execute. As a result, applications prevent wide-spread usage of FLOPs in order to shorten ST. Additionally, MATLAB timed all simulations and provided another potential expression of the same magnitude that could be used under 'Run & Time', where the total time plot is presented for each part of the code [37]. Furthermore, in the MATLAB environment, the 'tic' and 'toc' functions measured the elapsed time in each run. The 'tic' function triggered a stopwatch to measure speed in performance while 'toc' read the elapsed time from the timer that started by 'tic' [31]. The last manner was selected, and as a result the "tic" & "toc" functions were applied in the MATLAB environment.

The metric of operational time was defined in the same manner as time of simulation. Shorter operational times resulted to greater metric values, just as in ST, with unity being the greatest possible value of the metric. In addition, time of operation should be measured with the use of a conventional digital timer, which would be applicable to all tools. The timer was initiated in the commencement of tool usage and paused after the acquisition of the eventual fatigue damage. Operational time was then computed by subtracting time of simulation from the measured amount of time. In order to provide a thorough analysis, the whole of simulations should be conducted under an entirely different input each time. It is worth mentioning that the user should change the exact same number of parameters before each simulation, in an attempt to render timing fully comparable.

The criterion of detail was proposed in a generic fashion and should be conformed to the referent framework of parameters. All 5 subcategories (Tables 5.1 – 5.5) that constitute the overall referent framework comprise of the 'data base' of the criterion. As a result, the respective parameters form the set of referent parameters in the proposed metric of equation 2.6. Additionally, the design driver (*dd*) of equations 2.7, 2.8 and 2.9 is fatigue damage and along with the aforementioned in this paragraph specifications, suitably fitted the criterion to the specifications of Chapter's 3 use case.

In relation to the sensitivity analysis conducted for each parameter, the following conditions were applied. Each parameter was assessed at a range of ratio ( $p_N/p_r$ ) that amounted from 0.25 – 2, with a 0.25 step. Moreover, the values for each of the referent parameters in the denominators of all ratios emerged from the simulation of the structure in GH Bladed that resulted to unity output for fatigue damage. As a result, a set of 8 points for each parameter led to an approximation, given the total number of parameters and their relative impact on fatigue damage. To specify, the number of simulations  $S_1$  for each tool resulted from the product of the values that constituted the range for each parameter's sensitivity analysis as shown in equation 5.1. The set of simulations of  $S_2$  was associated with the number of values for the independent variable, which according to the defined use case is the pile's wall thickness. It is worth mentioning that the values of the wall thicknesses were limited to typical pile wall thicknesses, as ordained by manufacturers in the respective industry. Overall, the aggregation of simulations within the sensitivity analysis of  $S_1$  and independent variable range  $S_2$  resulted to a total number of  $N$  simulations as shown in equation 5.1.

$$N_{simulations} = N_{tools} \times N_{referent\ parameters} \times N_{S_1} \times N_{S_2} \quad 5.1$$

## 6. Case Study

In order to evaluate the proposed methodology of Chapter 2, a case study is examined. The location of the offshore wind structure is aligned with the current ambitions of the offshore wind energy sector, which are associated with relatively large wind turbines of significant power production which are installed to deeper waters. The above fact renders the case study realistic and conformed to the industry trend. Overall, the fidelity framework is applied and the three tools of the use case are ranked for the particular case study.

### 6.1 Selection of Location

The site location is situated west of Horns Rev 1 OWF, and south of the rest of the Horns Rev OWFs. The coordinates of the exact location of the site are 55.45N and 7.4E for the latitude and longitude, respectively. The site is located at a distance of 75 km from the port of Esbjerg in Denmark, at which point the sea depth is measured at approximately 25m. As indicated in Chapter's 6 introductory paragraph, this location is selected due to the fact that installation at deeper waters with higher wind speeds is one of the basic targets of the offshore wind industry. There is no current wind farm installed at that specific location, but a significant number of OWFs are situated at a relatively short distance i.e. Horns Rev 1 and Horns Rev 2. The exact location is depicted with the red X on the map of Figure 6.1.



Figure 6.1: Site location indicated by the red X sign [60].

### 6.2 Environmental Data

The availability of environmental data is crucial to load assessment for offshore wind structures. Data relative to wind, wave and soil all determine local loading and therefore are collected. In addition, the input requirements of the tools concerning local environmental conditions greatly differ from the initial form of the available data. Pre-processing that is prerequisite in all fatigue assessment tools was demanded in order to properly and

accurately transform all relevant data, in order to extract required information. All primary data provided for this particular site are shown in Appendix A.

In particular wind and wave data were given in 2-D scatter diagrams, as is frequently the case in offshore locations, and a 3-D scatter diagram should be formulated in order to reach the desired environmental states. This 3-D scatter diagram resulted by combining the 2-D diagrams, by focusing in the appropriate assessment of probability of occurrence, as shown in Appendix A. The respective number of states resulted from the probability of occurrence of particular wave heights with zero-crossing periods for varying wind speeds and targeted the inclusion of all probable cases. This diagram was fundamental to fatigue assessment as it determined the environmental input for the total of the predetermined tools. The resulting states are shown in Table 6.1:

**Table 6.1:** Final environmental states as resulted from data processing.

States	$U_{avg}$ [m/s]	TI [-]	$H_s$ [m]	$T_p$ [s]	Occurrence [%]
1	2.644	0.344	0.75	5.5	7.478
2	3.966	0.259	1.25	6.5	7.214
3	5.288	0.217	1.75	6	5.209
4	6.610	0.192	0.25	8	10.141
5	6.610	0.192	0.75	7	9.381
6	9.254	0.163	1.25	5.5	7.188
7	10.576	0.154	3.5	7	4.004
8	13.220	0.141	0.75	5.5	10.332
9	14.543	0.136	2.25	5.5	8.635
10	15.864	0.132	2.75	6	8.635
11	17.187	0.129	0.75	5	9.789
12	17.187	0.129	1.75	5.5	10.333
13	26.441	0.115	6.5	8	1.657

Wind, wave and soil data were processed in order to acquire the suitable input for the tools of the use case. As a result, the following steps were implemented, in order to process that data and reach to the information that is displayed in Table 6.1.

- Wind Data

Wind data were to undergo alterations from the form they were provided in the 2-D diagrams as they were measured in 3-h time intervals and at 10m. Hence, they had to be translated to 10 minute values and expressed at hub height. Hub height was set at 90m because of turbine selection. The 3-h wind speeds were converted to 10-minute values with the use of equation 6.1:

$$U_{10} \approx \frac{U_{3h}}{1 - 0.047 \ln \frac{T}{10}} \quad 6.1$$

where T is the period of 3 hours expressed in minutes [8]. In addition, the values were then converted to hub height, with the use of the logarithmic law with the use of equation 4.5, with

a typical roughness length of 0.0002m [8]. In addition, longitudinal Turbulence Intensity (TI) for each lumped case was acquired through the Normal Turbulence Model (NTM) [17]. Moreover, in the wind data that were managed to be retrieved, a relative wind speed distribution was included, the histogram of which is depicted in Figure 6.2:

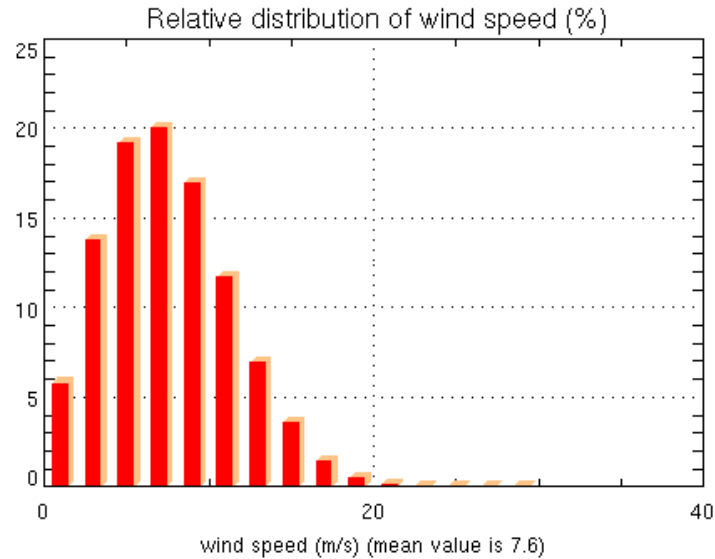


**Figure 6.2:** Relative wind distribution for the particular location [61].

The average wind speed which is set at 7.6 m/s, refers to an altitude 10m above sea level. In case the resulting value is further translated to hub height (90m) with the use of the logarithmic law, the resulting average wind speed is calculated at approximately 10.6m/s.

- Wave Data

Wave data determine hydrodynamic loads which are crucial to fatigue assessment. All significant wave height  $H_s$ , wave peak period  $T_p$  and probability of occurrence  $P_{occ}$  resulted from the 2-D and 3-D scatter diagrams that were provided for the particular installation site. To specify, these included the probability of occurrence of a particular wave height with a zero-crossing period for a significant range of wind speeds. These consisted the basis of the 3-D scatter diagram that is displayed in Appendix A and resulted to the FLS scheme that is depicted in Table 6.1. In addition, wave direction which is critical to fatigue assessment, as wind and wave misalignment should result to alternate loading on the structure. All aforementioned environmental data were included in Appendix A.

- Soil Data

As mentioned in Chapter 4, the task of gathering accurate soil information for a particular offshore location is more than challenging. Table 6.2 enlisting values for soil properties that correspond to the particular B1 type, as depicted in Figure 6.2, at a consequent sea depth of 25m and is below displayed. An additional soil map was among other relevant data gathered for the particular location, which depicts the variety of soil configuration in the wider area and is displayed in Figure 6.3.

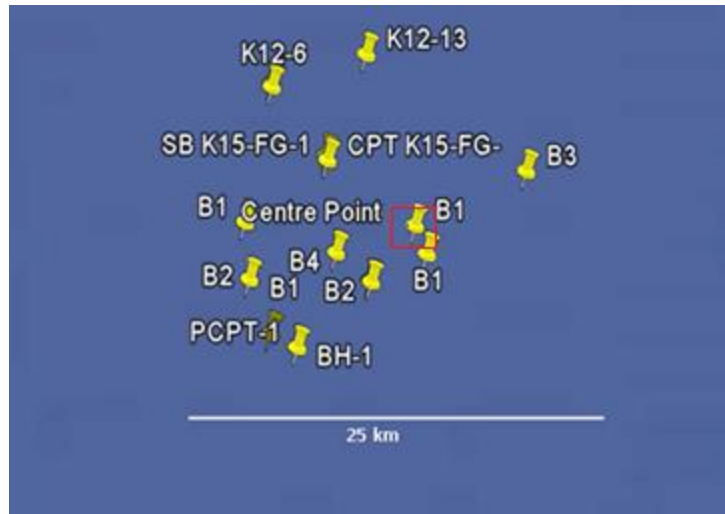


**Figure 6.3:** Several locations among the installation site with their respective soil profiles. The red frame marks the specific location of the installation site.

**Table 6.2:** Soil properties in depth [m] below mudline.

Layer	d[m]	$\gamma$ [kN/m <sup>3</sup> ]	$\phi$ [degrees]	Cu[kPa]
1	0- 9.2	9.5	35	-
2	9.2-10.2	9.5	0	100
3	10.2-14.7	9.5	33	-
4	14.7-36.0	10	35	-
5	36.0-39.3	10	33	-
6	39.3-43.4	9.5	0	200
7	43.4-50.0	9.5	30	-
8	50.0-62.0	10	33	-
9	62.0-67.7	10	35	-
10	67.7-69.7	9.5	0	200
11	69.7-73.5	10	33	-
12	73.5-82.2	10	25	-

### 6.3 Wind Turbine Selection

In order to correspond to the current needs of the industry and align with its respective goals, a wind turbine of relatively high power and thus greater dimensions than the majority of the existing operating offshore wind turbines should be examined. In particular, the NREL 5MW reference wind turbine for offshore system development was selected [22]. The basic turbine specifications are identified in table 6.3:

**Table 6.3:** Basic properties of 5MW NREL offshore wind turbine [22].

Turbine Parameter	Value [unit]
Rated Power $P_R$	5 [MW]
Rotor Diameter $D_R$	126 [m]
Hub Height $h$	90 [m]
Operational Wind Speeds in $U_{cut-in}, U_R, U_{cut-out}$	3, 11.4, 25 [m/s]
Operational Rotor Speeds in $\Omega_1, \Omega_2$	6.9, 12.13 [RPM]
Mass of RNA $m_{RNA}$	350,000 [Kg]
Radial Position of Mass Imbalance $R_{1P}$	42 [m]

The rated wind speed of the wind turbine, which is set by the manufacturer at 11.4m/s, should be similar to the average wind speed at hub height of the selected location in order to increase efficient power production and structural stability over its lifetime. The above consist of integral requirements to the turbine selection process.

## 6.4 Support Structure Configuration

Since the design driver of the use case is fatigue damage, the support structure configuration should be designed accordingly. Conventionally, certain design checks among which is the examination of natural frequency of the structure should be taken into consideration in the determination of the initial design. Overall, particular checks had to be performed in order to adequately assess the design of the structure.

The first eigenfrequency of the structure should be within certain margins in order to avoid resonance and consequent devastating effects on the structure. These excitation frequencies are determined by the rotational frequencies of the wind turbine, which in case of our 3-bladed rotor are 1P , 3P, 6P etc. [29]. The main excitation frequencies are the 1P and 3P, and the natural frequency of the structure should primarily avoid their ranges. The 1P and 3P frequency ranges determine 3 different kinds of regions and respectively structures, the soft-soft, the soft-stiff and the stiff-stiff region, as shown in Figure 6.4. Since the wave energy spectrum is present in the soft-soft region, the natural frequency of the structure should avoid it due to consequent large deflections. The stiff-stiff region requires stiffer and as a result larger and therefore more expensive structures. Overall, the most appropriate regions for the first eigenfrequency of the structure are situated at a safe margin from 1P and 3P spectrums, at the soft-stiff region, as indicated in the Figure 6.4.

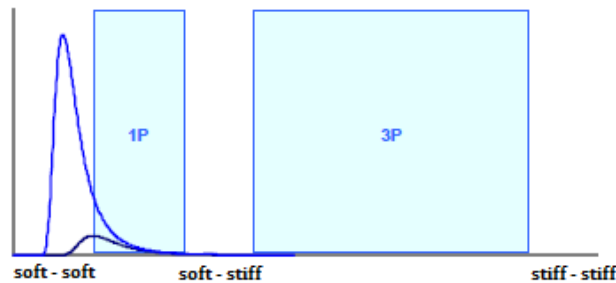


**Figure 6.4:** Qualitative diagram of frequency regions. The curves in blue color correspond to wave spectrums. 1P and 3P regions are displayed with their upper and lower limits [29].

Definitions of the natural frequency for cylinders, provide valuable insight to dimensioning the initial design. Simplified assessments on cylinders provide valuable information for the parameters that are involved in fatigue assessment. One in particular qualitatively indicates the dependence on basic parameters of the offshore wind structure, as shown in equations 6.2, 6.3, 6.4 [29]:

$$f \cong \sqrt{\frac{3.04}{4\pi^2} \frac{EI}{(M_{RNA} + 0.227\mu L_p)L_p^3}} \quad 6.2$$

$$I \cong \frac{1}{8} \pi D_p^3 t_p \quad 6.3$$

$$\mu = \rho_s \pi D_p t_p L_p \quad 6.4$$

where  $f$  is the first natural frequency,  $EI$  pile's bending stiffness,  $M_{RNA}$  is the mass of the rotor-nacelle assembly,  $L_p$ ,  $D_p$ ,  $t_p$  height, diameter and thickness of the pile, respectively,  $\mu_p$  tower mass per meter of the pile,  $\rho_s$  steel density.

The fact that the tower's top mass is significantly larger than in the conventional wind turbines, amounting to 350,000 Kg, and hub height is set significantly higher than in most existing offshore wind turbines, as shown in Table 6.3, indicate that the first eigenfrequency should be anticipated low – equation 6.2.

In terms of fatigue assessment, the respective S-N curve of Figure A.2 was implemented according to standards [9] and is included in Appendix A. In addition, fatigue damage is measured at mudline for the offshore wind structure. As defined by the use case, the structure should be safe but not over-dimensioned, which is translated to fatigue damage values marginal to unity, since over-dimensioning of offshore wind structures is frequently the case in existing OWFs [36]. As a result, the following dimensions of Table 6.4 were considered for the support structure of NREL's 5MW offshore wind turbine that was selected. The design is illustrated in Figure 6.5.

**Table 6.4:** Dimensions & Elevations of pile and transition piece.

Parameter	Value [unit]
Tower Top Diameter $D_{Tt}$	4 [m]
Tower Top Thickness $T_{Tt}$	0.04 [m]
Tower Base Diameter $D_{Tb}$	5 [m]
Tower Base Thickness $D_{Tb}$	0.05 [m]
Tower Length $L_T$	69 [m]
Transition Piece Diameter $D_{TP}$	5.3 [m]
Transition Piece thickness $t_{TP}$	0.055 [m]
Transition Piece Base Elevation $Z_{TPb}$	16 [m]
Grout Length $L_G$	9 [m]
Monopile Diameter $D_p$	5 [m]
Monopile Thickness $t_p$	0.045 [m]
Penetration Depth $Z_{Pd}$	-30 [m]
Platform Elevation $Z_{Pl}$	43 [m]

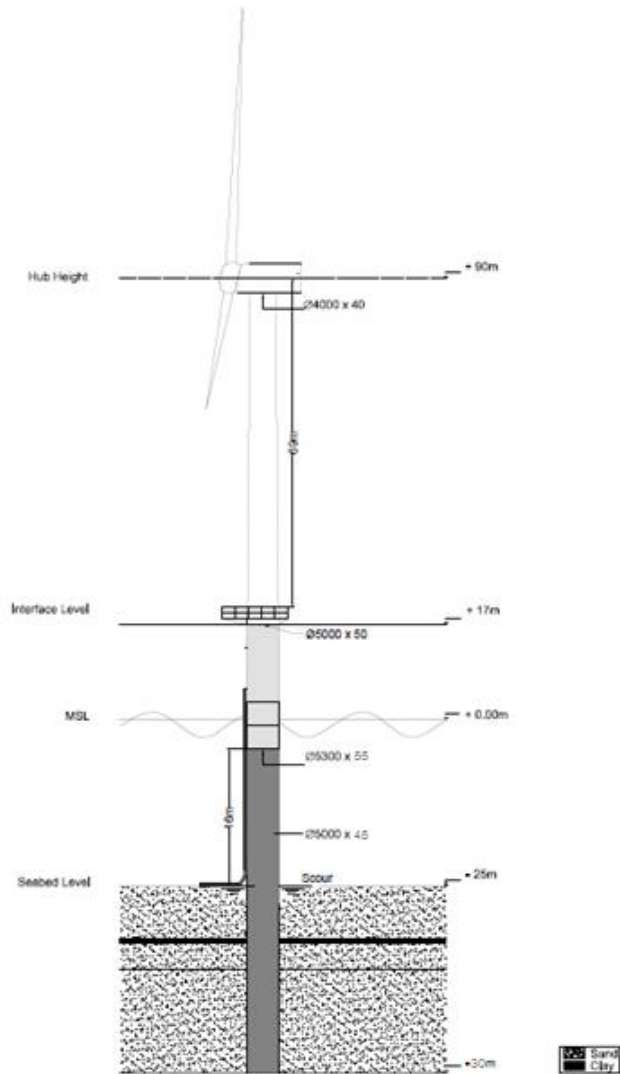


**Figure 6.5:** Design of the offshore wind structure within the case study.

The first natural frequency of the particular structure amounted at 0.064Hz. This output value is situated out of the 1P rotational frequency region, and at a safe margin as well. Nevertheless, it is situated in the soft-soft region, which emerges a variety of issues. At first, a range of wave spectrums are located below the first rotational frequency, the frequencies of which would probably coincide with the first eigenfrequency of the structure. However their maxima of all significant and extreme waves for the current location would be amplified at frequencies in the region of 0.08 - 0.1Hz in the North Sea [18]. The above fact does not constitute any kind of guarantee that the structure would not significantly oscillate to any excitations, but indicates that devastating effects on the structure would probably be avoided.

The nature of the structure should be further justified to a number of other criteria and subject to more stability checks. The dimensions of the design render the structure slender for the particular site, in comparison to structures situated at the soft-stiff region for the

particular turbine, rendering it more cost-efficient. ULSs should be particularly examined because the structure is lighter and thus increasingly susceptible to the exerted loads. The most suitable tools to measure all data required for the design are GH Bladed or FAST v8 since the other tools do not yield the required output, as well as the former globally certified and thus more reliable [48]. Nevertheless, fatigue damage has been identified as the design driver in the framework of this thesis and no additional checks were implemented within its boundaries. Overall, the dynamically challenging design provides a suitable test for the detection of differences between the in disposal tools.

## 6.5 Scoring of Criteria

### 6.5.1 Accuracy

The fidelity framework that was suggested in Chapter 2 was applied to this case study in order to evaluate the proposed methodology. The metrics of the aforementioned criteria of all accuracy, time of simulation, operational time and detail resulted from the measurements that were taken during sets of simulations of the same structure. In addition, scoring of the resulting metrics were further analyzed through the application of MCDA for each respective tool, in order to acquire the ranking of the tools.

Scoring of the accuracy criterion resulted from the difference between fatigue damage output of the tools and the referent value of fatigue damage. As conducted for all criteria, a set of 10 simulations for the same structure rendered values for the particular magnitude, as it is considered the design driver within the current thesis. In section 2.2.1 the generic metric for the criterion was defined and then later fitted to the use case of Chapter 3 in section 5.2.

As a result, the values of fatigue damage throughout the simulations consist of input data for equations 2.1 & 2.2. As aforementioned in section 5.2, the metric for accuracy for FAST v8 was assigned values that resulted from the simulation of the same structure in GH Bladed, due to inability of RFC post-processor to FAST v8. The values of the metric for accuracy are depicted in Table 6.5 for each tool.

**Table 6.5:** Values of the proposed Accuracy metric for Tools 1,2 and 3 for the case study.

Accuracy Metric [-]	Tool 1	Tool 2	Tool 3
	0.103	0.731	1

The level of accuracy in Tool 1 is almost 10 times less than in Tool 3, and more than 7 times lower than the respective magnitude in Tool 2. To specify, fatigue damage was calculated almost double in Tool 1 than in Tool 3, with average fatigue damage amounting at 1.857, in contrast to 0.979 in Tool 3. In Tool 2 the simulation of the structure resulted to a fatigue damage of 1.243, which is at a relatively short margin from the 0.979 value. Once again, Tool 2 yielded comparable results to Tool 3, which should predispose for a high position in the eventual ranking. It is worth mentioning that comparison between Tools 1 and 2 would yield the same results due to the definition of the metric of equation 2.2, given in section 2.2.1.

## 6.5.2 Time of Simulation

### Tools 1 and 2

In terms of simulational time, a set of simulations was conducted in order to acquire an average time of simulation throughout the examined tools. 10 simulations were implemented in both Tools 1 and 2 and under the same conditions. To specify, the same input was applied in the whole of simulations in Tools 1 and 2, with the consequent acquisition of required output of fatigue damage. All respective amounts of time are shown in Appendix C. From those tables, all required average values of STs were calculated and applied to the proposed ST's metrics. All minimum and maximum averages of simulational time were calculated throughout the whole of simulations for all three models and input in equation 2.3. Table 6.6 shows the consequent extracted values of the proposed ST metric.

**Table 6.6:** Values of ST proposed metric for Tools 1 and 2 for the case study.

Time of Simulation Metric [-]	Tool 1	Tool 2
	0.105	0.777

The main reason behind the significant difference in the ST metric between the two tools is attributed to the simultaneous simulation of all environmental states in Tool 2. Tool 1 could simulate one state in each simulation, while Tool 2 simulated all states at the same time. Given the number of 13 states of the case study, as depicted in Table 6.1, it is apparent why there is a significant difference between them. Even if simulation time was significantly lower for each state in Tool 1, as shown in the respective tables of Appendix C, the number of states strongly favored Tool 2 over Tool 1 in terms of overall speed of simulation.

### Tools 1,2 and 3

Both FAST v8 & GH Bladed are operating in the TD and as a result should require significantly greater amounts of time in order to simulate the same structure. As depicted in Tables C.3 and C.4 of Appendix C, simulational time is one order of magnitude greater than the respective times of simulation in Tools 1 and 2 that operate in the FD. Consequently, a set of only two simulations is still comparable to a set of 10 simulations, in terms of ST, due to their substantial difference. As a result, the metric of ST in that case is illustrated in the following Table 6.7 for all three tools.

**Table 6.7:** Values of ST proposed metric for all 3 tools for the case study.

Time of Simulation Metric [-]	Tool 1	Tool 2	Tool 3
	0.998	0.999	0.068

As shown in Table 6.7, Tool 3 is by far the least favorable in terms of ST, while Tools 1 and 2 are comparable due to their relatively greater speed of simulation in comparison to Tool 3. Mainly, the generation of time series for environmental loading that amounts from 5 to 7 minutes on average for each environmental state significantly hinders fast simulations in TD. In addition, the inclusion of all non-linearities in Tool 3 [21] which however lead to greater degrees of accuracy and detail in the tool, increase time of simulation. In contrast to TD operating tools, the assessment in the FD of both Tools 1 & 2 only required seconds, as shown

in Tables C.1 & C.2 of Appendix C. It is worth mentioning that in the comparison between Tools 1 and 2 the results were that different because the  $ST_{max}$  term of equation 2.3 was 20.928s, while in the comparison of all three tools the same term amounted 5654s.

### 6.5.3 Operational Time

#### Tools 1 and 2

OT consists of an additional significant fidelity criterion as proposed in the suggested methodology in Chapter 2. The amount of time a user consumes in operating a tool, apart from the ST could prove decisive in the imminent comparison between the tools. As aforementioned in section 2.2.3, even if simulation is conducted faster in one tool in comparison to another, there is no essential benefit in case time of operation is significantly higher in the former.

The same structure was simulated and for the same amount of simulations between Tools 1 and 2. The “tic” and “toc” functions were used in order to measure the ST during simulations in MATLAB. The respective amounts of OT are rigorously illustrated in Appendix D and for both Tools 1 and 2. The OT metrics of equation 2.4 are below displayed in Table 6.8.

**Table 6.8:** Values of the OT Metric for Tools 1 and 2 in their comparison for the case study.

Operational Time Metric [-]	Tool 1	Tool 2
	0.249	0.746

In the same manner as in terms of ST, the significant difference between the two scores lies in the simulation procedure. Once again, each state is simulated individually in Tool 1, while in Tool 2, all the environmental states of Table 6.1 are simulated simultaneously. In that the user is prompted for each load case separately to input data while in Tool 3 all 13 load cases are entered at once. That results in significantly lesser amounts of OT in Tool 2, as shown in the respective tables of Appendix D.

#### Tools 1, 2 and 3

As for the aforementioned criteria, measurements were taken during the same set of 10 conducted simulations for Tools 1, 2 and 3. As presented in the tables of Appendix D, the difference is justified substantial between the respective OT of Tool 3 and the directly comparable OTs of Tools 1 and 2. With the manner of measurement being described in section 5.2, the respective results are rigorously shown in Tables D.1 – D.5 of Appendix D.

These measurements formulate the input of equation 2.4 and result to the quantification of the respective fidelity metric. All minimum and maximum averages of OT are calculated throughout the whole of simulations for all three models and are implemented to that equation. The relevant results are enlisted in Table 6.9.

**Table 6.9:** Values of the OT Metric for all 3 tools in their comparison for the case study.

Operational Time Metric [-]	Tool 1	Tool 2	Tool 3
	0.936	0.978	0.026

As in the ST metric, Tool 3 is the least favorable in terms of OT, while Tools 1 and 2 are comparable, with Tool 2 amounting the greater value. That is due to increased operational time and at complex environment in the TD tools. In FAST v8 the user would spend significantly greater amounts of time in comparison to the FD tools. The input and output files of FAST v8, are ordained in such a way that alteration at a single parameter would result to a domino of alterations in the majority of all scripted input files to the tool. In addition, the shape of output required extensive post – processing, as FAST v8 does not output fatigue damage or DELs, and additional MATLAB models were integrated. Overall, they required extensive pre-processing operational time, in order to appropriately input all required parameters, especially the ones associated to environmental loading. Post-processing time was necessary, as fatigue damage related parameters would be calculated for each state, and then processed in order to acquire the desired magnitude of fatigue damage. As a result, the metric expressed the grand difference in OTs between FD and TD tools.

#### **6.5.4 Detail**

In order to suitably express the metrics in all three tools, the same set of simulations should be applicable in all tools. Unfortunately, that set of simulations could not be carried out in the TD, in which FAST v8 and GH Bladed operate. The inability to acquire licensed usage of GH Bladed for offshore wind structures for a sustained amount of time hindered the implementation of iterative and time-consuming sensitivity analyses that were required, in order to fully realize the proposed detail metric. In addition, FAST v8 [21] did not feature fatigue analysis and additional post-processors that were adopted in order to perform fatigue damage determination in TD yielded doubtful results. The sensitivity analyses that were required for the scores of the detail criterion could not be obtained. Therefore, a full comparison according to the fidelity framework was only performed for Tool 1 and Tool 2.

In order to apply a comparison between all 3 tools that were included in the case study, approximations were justified prerequisite for the implementation of the detail criterion. Sensitivity analyses that were compulsory in the comparison of all three tools were by-passed and instead an alternate approach was adopted, as analyzed in section 6.5.4. As a result, two separate types of comparison follow, in order to evaluate the proposed fidelity framework of Chapter 2.

Detail was defined in section 2.2.4, in which equations 2.5-2.9 would yield the respective metric values. The input to those equations would emerge from the parameters that are associated with the process of determination of fatigue damage in each tool, in respect to the referent framework of parameters for fatigue, as suggested in section 5.1. In addition, separate sensitivity analyses would be conducted, where feasible, in order to apply the full definition of detail metric to the particularities of the case study.

#### **Tools 1 and 2**

Sets of the same simulations for the proposed structure of the case study of section 6.4 were carried out in both tools. Iterative sensitivity analyses were conducted in order to appropriately define all terms of the proposed detail metric. Certain parameters that were associated to fixed values such as air or water density were excluded from the sensitivity analyses. In addition, structural parameters relevant to the wind turbine were also excluded

from the sensitivity analyses, in respect to Table 5.4, since they consisted of the same type of input in both tools. Numerous parameters applied in the same category, and in particular cases, any alterations at input would halt simulations. All above considered, a set of 13 parameters were included in the sensitivity analyses, as displayed in equation 6.5 and shown in the respective tables of Appendix B.

$$Detail = f(U, TI, H_s, T_p, TR, d, L_p, \varphi, \gamma, L_s, z_p, L_g, z_{TP}) \quad 6.5$$

As stipulated in the detail metric of section 2.2.4 and further fitted to the specifics of the use case in section 5.2, two sets of simulations  $S_1$  and  $S_2$  were required in order to fully quantify the referent factors of equation 2.7 and therefore the detail metric of equation 2.6. The results of the sensitivity analyses conducted for the set  $S_1$  of simulations, are depicted in Figure 2.8, with varying fatigue damage output for each tool. The fatigue damage output according to alteration of input in each tool, for each of the 13 parameters, is also depicted in Figures 6.6 & 6.7. In addition, within the set  $S_2$  of simulations, five different wall thicknesses were simulated in each step of the sensitivity analyses of set  $S_1$  of simulations. All results are situated in Tables B.1 and B.2 in Appendix B. It is worth mentioning that the independent variable for the set  $S_2$  of simulations was kept constant during set  $S_1$  of simulations.

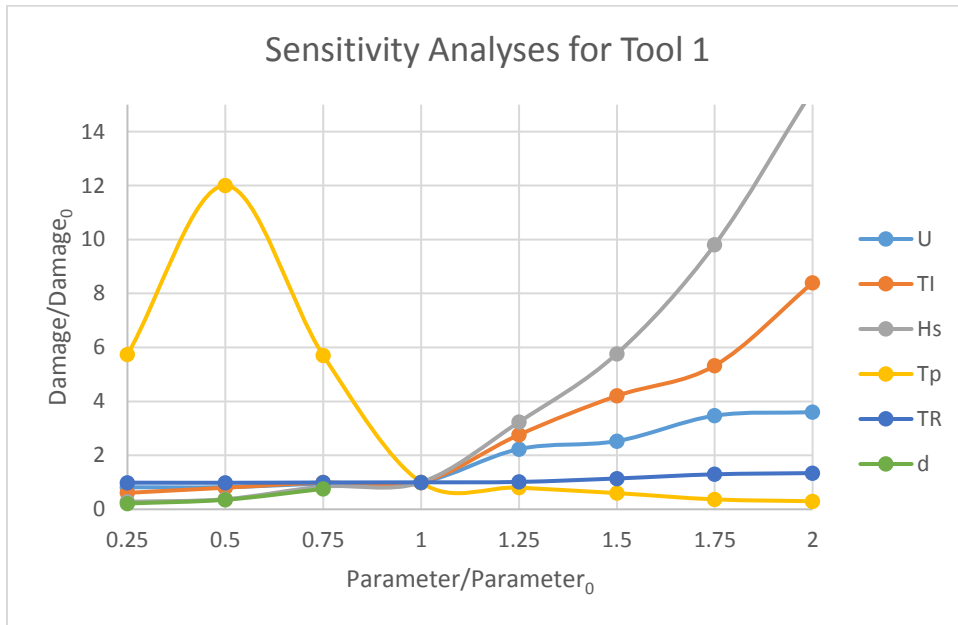


**Figure 6.6:** Results of Sensitivity Analyses for the 6 parameters that are included in the respective memorandum in Tool 1.

Parameters such as  $L_p$ ,  $\varphi$ ,  $\gamma$ ,  $L_s$ ,  $Z_p$ ,  $L_g$  and  $Z_{TP}$  could not be included in the sensitivity analysis of Tool 1. All  $L_s$ ,  $L_p$ ,  $Z_p$  and  $Z_{TP}$  were excluded because they were not included in the input of the tool and resulted from other elevations and dimensions. Therefore, they could not be altered in the framework of the sensitivity analyses of  $S_1$ . In respect to soil parameters  $\varphi$  and

$\gamma$ , soil could be simulated only for a sole layer, in contrast to Tool 2, where all layers of the case study could be simulated, as shown in Table 6.2. In addition, no scour was taken into account during simulations, which naturally resulted to the exclusion of  $L_g$  from the sensitivity analyses. Moreover, in relation to sea depth ( $d$ ), the tool could only simulate until the installation site depth of 25m, and only at the end of later modifications conducted by Aythel Ortega [62], since it originally simulated up to 20m.

A number of valuable observations could be implemented from the sensitivity analyses of  $S_1$  and are illustrated in Figure 6.6. Wind-related parameters such as wind speed ( $U$ ) and longitudinal turbulence intensity ( $TI$ ) exert significant influence on fatigue damage from sensitivity ratios of 1.25 – 2. Loading is greatly intensified with increased wind speeds, especially the aerodynamic loading on the rotor, which is the most significant. In fatigue damage determination, turbulence intensity is even of higher importance than wind speed, as it constantly alters aerodynamic loading and consequently leads to greater stress variation, and therefore greater damage. In addition, wave-related parameters such as significant wave height ( $H_s$ ) and wave peak period ( $T_p$ ) had separate kinds of impact on fatigue damage. Increasing significant wave height, especially from ratios of 1 – 2, resulted to steeper increase of fatigue damage, which is naturally explained from the fact that water particle velocity of the Morrison equation is proportional to significant wave height (eq. 4.13). However the increase in fatigue damage is steeper than anticipated, leading to significantly greater figures from ratios 1.25 - 2. Given the fact that the linear wave theory contributes to an underestimation of equivalent fatigue loads by 5 – 10%, the above results seem contradicting [34]. In addition, peak wave period has an immense escalation at the 0.5 ratio, that can only be attributed to resonance. The structure is excited near its natural frequency with the consequent amplitude dynamically challenging the structure. In general, from 0.5 to 2 ratios, increasing  $T_p$  leads to decreasing fatigue damage, apart from the 1.1 – 1.25 ratios, which is justified from the JONSWAP spectrum (equations 4.10 – 4.12). Tidal range seems to have insignificant impact on fatigue damage, which is slightly enhanced from ratios 1.5 -2. To conclude, fatigue damage seems to be significantly decreased at lower ratios of sea depth, in respect to ratios closer to unity, an observation that was anticipated. Lower lever-arm leads to lower moments and thus decreased loading and fatigue damage of the structure. Overall, hydrodynamic loading exerts higher influence on fatigue damage than aerodynamic loading, as anticipated in offshore wind structures.

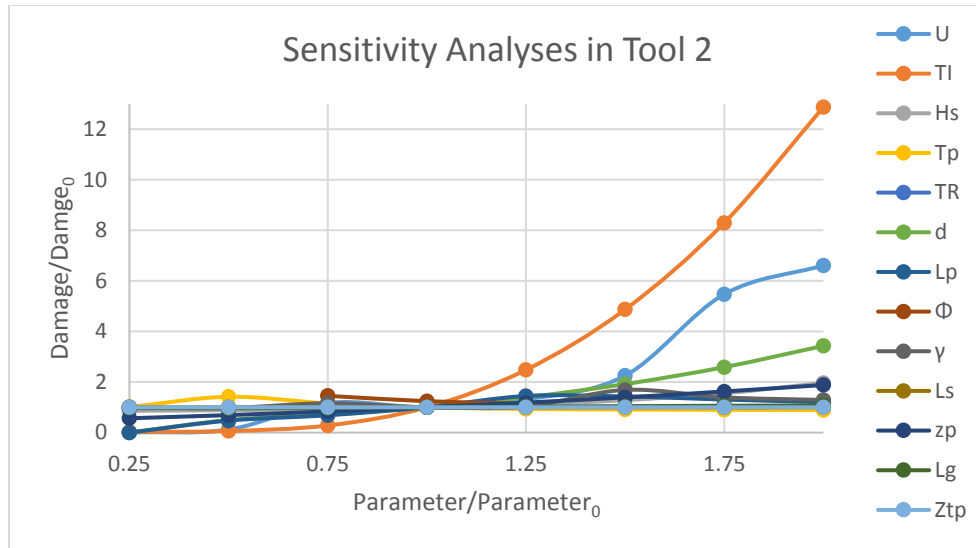


**Figure 6.7:** Results of Sensitivity Analyses for the 13 parameters that are included in the respective memorandum in Tool 2.

In Tool 2, all 13 parameters were included in the sensitivity analyses of  $S_1$ , as shown in Appendix B, and additional remarks should be made regarding their impact on fatigue damage. Wind-related parameters exerted greater influence to fatigue damage determination than in Tool 1. To that end, that is partly justified by the omission of tower drag in the method leading to fatigue damage determination that was implemented in Tool 1, in contrast to Tool 2 in which it was included in the respective fatigue assessment process. In addition,  $H_s$  is naturally proportional to fatigue damage for the previously aforementioned reasons. However it exerted significantly lesser influence on fatigue damage at increased ratios. In the area of 1.5 – 2 ratios, the difference is obvious with fatigue damage ratios ranging from 6 to 15 in Tool 1, and from 1.2 to 2, in Tool 2.

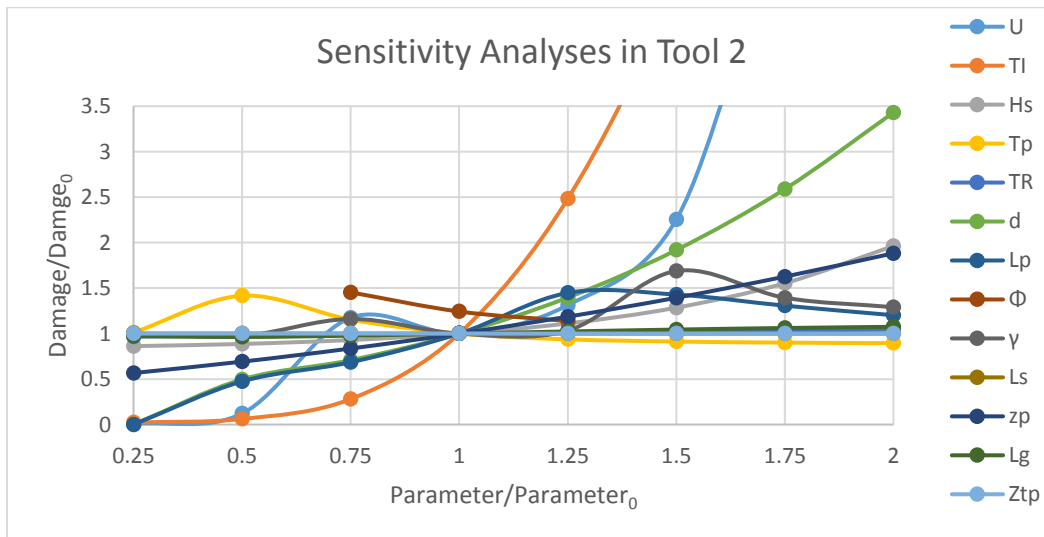


**Figure 6.8:** Enlarged version of Figure 6.7 in the ratios of 0 – 3.5, for fatigue damage ratios.

In addition,  $TR$  and  $d$  illustrate the same behavior as in Tool 1. For the latter, increase in sea depth could be simulated to the full ratio scale. The respective results were logical, due to increased lever-arm and possibly higher flexibility towards the structure's excitation frequencies. In relation to soil parameters, increased  $\varphi$  contributed to higher structure stiffness, and therefore lower fatigue damage. On the other hand, the  $\gamma$  variation yielded unexpected results, as increase should be associated to fatigue damage decrease. However there are two local maxima at ratios 0.75 and 1.5, that indicate unexpected impact on the design driver. In addition, all elevation change in  $L_s$ ,  $L_g$  and  $z_p$  with adjustable relevant elevations exerted minor influence on fatigue damage of the offshore structure. Lastly, increase in transition piece elevation  $z_{TP}$ , with adjustable depth, naturally increased loading due to higher lever-arm, and therefore led to increased fatigue damage ratios, as shown in figure 6.8.

In addition, a set of simulations  $S_2$  were implemented, in order to assess the behavior of fatigue damage to pile's wall thickness alterations. The application of the results emerging from those later sensitivity analyses to equation 2.7 and the further application of the referent factors to equation 2.6 resulted to the detail metric for both tools. The results of the sensitivity analyses with variable pile thickness are shown in Appendix B. The relative results for the detail criterion are illustrated in Table 6.10:

**Table 6.10:** Detail Metric values for Tools 1 and 2, in their comparison for the case study.

Detail Metric [-]	Tool 1	Tool 2
	0.358	0.872

The above results imply that detail in Tool 2 is more than double than in Tool 1. This difference in magnitude is associated to reasons that relate both to the structure of the tools, as well as the definition of the metric. Increased values of the wind-related parameters within the framework of the sensitivity analysis resulted to significantly greater values of fatigue damage and therefore to higher figures of the respective terms in the proposed referent factors. It is worth mentioning that the omission of 6/13 parameters in the sensitivity analyses in Tool 1 is the main reason that the value of the metric is less than half of the respective value in Tool 2. The relevant referent factors in the detail metric have been omitted from the metric and therefore the eventual overall value would significantly drop. To continue, larger fatigue damage values for increased sensitivity ratios of the wave-related parameters however in Tool 1 than in Tool 2, have attributed greater values to the respective terms of the metric. Nevertheless, Tool 2 has outscored detail in the remaining referent factors, hence the significant difference that is displayed in Table 6.10.

### Tools 1,2 and 3

In the comparison of all three types of fatigue assessment, the set of parameters that were included in each tool, in respect to the referent framework, would fully express the metric. Detail for Tool 3 would amount to unity, as would accuracy (section 5.2), and the relative comparison between the parameters included in Tools 1 and 2 and the referent parameters of the respective framework of section 5.1 would render the value for the detail metric. Consequently, detail would be quantified for all three tools and an in between them comparison could be possible.

The full referent factor expression, as described in equation 2.7, required iterative sensitivity analyses for both sets of simulations  $S_1$  and  $S_2$ , as analyzed in section 2.2.4. However, given the aforementioned conditions in the introduction of the particular section, an alternate approach should be implemented. As a result, expression 2.7 is not taken under consideration and the sole factor of the metric comprises of the referent parameter. In other words, in case a parameter is included in the process of fatigue damage determination in a tool, it is then assigned with the value of the referent parameter throughout the tools. In any other scenario, if the parameter is omitted from the respective process in a tool, the particular parameter in the detail metric expression 2.6 is assigned zero value. As a result, the values for the specific detail metric for each tool are enlisted in Table 6.11.

**Table 6.11:** Detail Metric values for Tools 1, 2 and 3, in their comparison for the case study.

Detail Metric [-]	Tool 1	Tool 2	Tool 3
	0.423	0.808	1

The results of Tool 1 and Tool 2 are comparable to those of their in between them comparison. Tool 3 was assigned unity, since unity has been assigned in each of the involving referent factors of equation 2.6. In addition, Tool 1 received a low score due to the inability of input alteration, in contrast to Tool 2, in which apart from 2 parameters, the rest could have been subject to sensitivity analysis. Tool 2 received a high score, similar to the absolute score of unity of Tool 3. As aforementioned in section 2.2.4, apart from a fidelity criterion, detail has been considered as a metric of the simulated reality. That high score consisted of an indicator that the level of detail needed for the specific case study was provided by the specific tool, even in comparison to a TD tool.

## 6.6 Tool Ranking

### 6.6.1 AHP

MCDA was later applied to the scores of the criteria that were acquired during the simulations of the case study. Both AHP and the Monte Carlo Method as proposed by Butler J were applied [3]. The AHP constitutes one of the most popular MCDA methods, as described in section 2.3 [30]. It additionally consists of a partially subjective method, as the decision-maker exerts influence on the overall ranking process. The AHP was fully applied in both comparison of Tools 1 and 2, as well as in the comparison of all 3 Tools. Apart from the AHP, the Monte Carlo Method proposed by Butler J. [3] was applied, in which the influence of the decision maker in the process is minor, thus enhancing both objectivity and credibility of the method.

The method was applied including all respective steps, as proposed in section 2.3. The first step comprised of the structure of the decision model into a hierarchical model. That hierarchical model should consist of three separate levels. The main objective is situated on the top of the hierarchy, while all criteria are situated in the intermediate level. Additionally, the alternatives are situated at the bottom of the hierarchical structure. All determination of goals, criteria and alternatives should be determined in this particular step. In the assessment of the case study, the criteria have been defined among Detail, Accuracy, ST & OT, as earlier

proposed from the fidelity framework of Chapter 2. In addition, the examined alternatives are identified in the use of the three tools, with consequent application of different types of fatigue assessment.

The second step of the AHP included the acquisition of weighting factors for the existing criteria. Following the determination of criteria of the first step, and their relative significance in the hierarchical model, additional values were assigned to the different criteria, primarily according to the fundamental scale of Table 2.1. The use case was determined at an early design stage, in which speed of simulation and speed in operation are directly associated to the objective. Under the same set of conditions, detail and accuracy are also considered of significant importance, and their respective interrelation with ST and OT should be further assessed. All above considered, the following values were initially selected in the initial judgmental matrix  $A_j$ , or else known as pairwise comparison matrix, as depicted below.

$$A_j = \begin{bmatrix} 1 & 1 & 3 & 3 \\ 1 & 1 & 3 & 3 \\ \frac{1}{3} & \frac{1}{3} & 1 & 1 \\ \frac{1}{3} & \frac{1}{3} & 1 & 1 \end{bmatrix} \quad 6.6$$

The 4x4 dimension of the matrix is due to the 4 criteria of the proposed fidelity framework. In general, a component  $a_{ij}$  expresses the significance of criterion  $i$  over criterion  $j$  in respect to the objectives. In the particular matrix, the terms from first to last stand for Time of Simulation, Operational Time, Detail and Accuracy. As implied, ST and OT have been assigned higher significance in relation to detail and accuracy, the magnitude of which was quantified according to the fundamental scale of Table 2.1. In terms of the assigned value, 3 implies that criterion  $i$  is marginally more significant than criterion  $j$  and therefore is associated to the main objective of the use case at a higher degree. The increased significance of both time criteria over detail and accuracy is rationalized due to the early design stage of the structure, in which cost-efficient simulations are increasingly favored [48]. Long STs and OTs have been associated to TD simulations in comparison to FD tools, which yielded similar results in significantly shorter simulations, just as Tools 1 and 2. In other words, ST & OT are at a shorter distance from the objectives of the hierarchical model for the particular use case than detail and accuracy. It is worth mentioning that a higher factor of the fundamental scale could be assigned in order to prioritize time from accuracy and detail. However, the particular value was decided in order to mitigate the exertion of influence of the decision-maker on the particular process and consequently on the final ranking of the tools. Furthermore, the rest of the matrix components emerge from the rules that were suggested in section 2.3 and thus are implemented to its completion.

The following step includes the extraction of the normalized judgmental matrix  $A_{jnorm}$ , which results from the division of each component by the sum of its respective column of the matrix.

$$A_{jnorm} = \begin{bmatrix} \frac{3}{8} & \frac{3}{8} & \frac{3}{8} & \frac{3}{8} \\ \frac{3}{8} & \frac{3}{8} & \frac{3}{8} & \frac{3}{8} \\ \frac{1}{8} & \frac{1}{8} & \frac{1}{8} & \frac{1}{8} \\ \frac{1}{8} & \frac{1}{8} & \frac{1}{8} & \frac{1}{8} \end{bmatrix} \quad 6.7$$

The average of each row leads to the weighting factors that constitute the vector  $W_1$  :

$$W_1 = [0.375 \quad 0.375 \quad 0.125 \quad 0.125] \quad 6.8$$

The above pairwise comparison matrix  $A_j$  is proven consistent with the use of equations 2.10 and 2.11, as indicated in [30]. The next step of the process included assessment of the alternatives, in which case was identified in two separate types of comparison:

1. 2 Alternatives (Tool 1, Tool 2)
2. 3 Alternatives (Tool 1, Tool 2, Tool 3)

### 1.Tools 1 and 2

The same set of simulations in Tools 1 and 2 that operated in the FD resulted to the following criteria scoring, as indicated in Table 6.12.

**Table 6.12:** Values of all criteria for both Tools 1 and 2 in their comparison for the case study.

Alternative	Simulational Time [-]	Operational Time [-]	Accuracy [-]	Detail [-]
Tool 1	0.105	0.249	0.103	0.358
Tool 2	0.777	0.746	0.731	0.872

The above values determined the quantified criteria which would consist the basis of the following comparison matrices. These matrices were dimensioned 2x2, given the alternatives, and amounted to 4 in total, in respect to the 4 criteria of the fidelity framework. Each element  $a_{ij}$  signifies the predominance of Tool  $i$  over Tool  $j$ , in respect to the criterion of the matrix. As a result, after considering the scores of each tool and the fundamental scale, the resulting matrices are established:

$$ST_1 = \begin{bmatrix} 1 & \frac{1}{5} \\ 5 & 1 \end{bmatrix} \quad 6.9$$

$$OT_1 = \begin{bmatrix} 1 & \frac{1}{3} \\ 3 & 1 \end{bmatrix} \quad 6.10$$

$$A_1 = \begin{bmatrix} 1 & \frac{1}{5} \\ 5 & 1 \end{bmatrix} \quad 6.11$$

$$D_1 = \begin{bmatrix} 1 & \frac{1}{3} \\ 3 & 1 \end{bmatrix} \quad 6.12$$

The selection of values for the components of the respective matrices was conducted in an attempt to best quantify their relation in respect to each criterion. In regard to the fundamental scale (Table 2.1), all values were again selected in order to mitigate the subjectivity of the decision-maker. The values for ST were selected in such a manner due to the significant difference in value of the ST metric between Tools 1 and 2, with the latter being more than 7 times greater. In addition, the OT metric in Tool 2 was approximately three times greater than in Tool 1, which resulted to the assignment of the particular values that are shown in equation 6.10. In terms of accuracy, the accuracy metric score in Tool 2 was significantly greater, at a degree of justifying the choice of values 1 and 5 for the particular criterion.

As in the judgmental matrix ( $A_j$ ), the weight vectors are obtained in the same way for the comparison matrices 6.9 – 6.12. As a result:

$$c_{11} = [0.167 \quad 0.833] \quad 6.13$$

$$c_{21} = [0.25 \quad 0.75] \quad 6.14$$

$$c_{31} = [0.167 \quad 0.833] \quad 6.15$$

$$c_{41} = [0.25 \quad 0.75] \quad 6.16$$

The overall score of each alternative emerges from the use of equation 2.12, from which the final tool scoring is acquired, as shown in Table 6.13. The equation includes both judgmental matrix weight vector 6.8, as well as the above listed weight vectors 6.13 - 6.16. To specify, the product of the respective weights results to the eventual scoring of the compared tools.

**Table 6.13:** Rankings and scores for each alternative between Tools 1 and 2.

Ranking	Alternative	Score
1	Tool 2	0.792
2	Tool 1	0.208

As a result, Tool 2 is ranked higher than Tool 1 and therefore its use over Tool 1 is justified through the AHP for the particular case study.

## 2.Tools 1, 2 and 3

The fidelity criteria metrics were calculated in all 3 tools in order to perform their overall comparison. Their scores for each criterion are depicted in Table 6.14.

**Table 6.14:** Values of all criteria for all Tools 1, 2 and 3 in their comparison for the case study.

Alternative	Simulational Time [-]	Operational Time [-]	Accuracy [-]	Detail [-]
Tool 1	0.998	0.936	0.103	0.423
Tool 2	0.999	0.978	0.731	0.808
Tool 3	0.068	0.026	1	1

As in the comparison between Tools 1 and 2, the values in Table 6.14 display the quantified criteria upon which the respective comparison matrices will be developed. Due to the comparison of all tools, 3 alternatives resulted to 3x3 dimensioned matrices. They amounted at 4 in total, in respect to the fidelity framework criteria. The resulting matrices are below displayed:

$$ST_2 = \begin{bmatrix} 1 & 1 & 9 \\ 1 & 1 & 9 \\ \frac{1}{9} & \frac{1}{9} & 1 \end{bmatrix} \quad 6.17$$

$$OT_2 = \begin{bmatrix} 1 & 1 & 9 \\ 1 & 1 & 9 \\ \frac{1}{9} & \frac{1}{9} & 1 \end{bmatrix} \quad 6.18$$

$$A_2 = \begin{bmatrix} 1 & \frac{1}{5} & \frac{1}{9} \\ 5 & 1 & \frac{5}{9} \\ 9 & \frac{9}{5} & 1 \end{bmatrix} \quad 6.19$$

$$D_2 = \begin{bmatrix} 1 & \frac{1}{3} & \frac{1}{5} \\ 3 & 1 & \frac{3}{5} \\ 5 & \frac{5}{3} & 1 \end{bmatrix} \quad 6.20$$

The values in matrices 6.17– 6.20 were assigned according to the metrics of Table 6.14, in the same manner that matrices 6.19 – 6.12 were selected, within the comparison of Tools 1 and 2. The following weighting vectors of these comparison matrices are below displayed:

$$c_{12} = [0.474 \quad 0.474 \quad 0.052] \quad 6.21$$

$$c_{22} = [0.474 \quad 0.474 \quad 0.052] \quad 6.22$$

$$c_{32} = [0.067 \quad 0.333 \quad 0.600] \quad 6.23$$

$$c_{42} = [0.111 \quad 0.333 \quad 0.556] \quad 6.24$$

The overall score of each of the three alternatives resulted from the use of equation 2.12, and includes both judgmental matrix weight vector (eq. 6.8), as well as the above listed weighting vectors (eq. 6.21 - 6.24). To specify, the product of the respective weighting vectors determined the eventual scoring of the compared tools.

**Table 6.15:** Rankings and Scores of Tools 1, 2 and 3 resulting from the AHP.

Ranking	Alternative	Score
1	Tool 2	0.438
2	Tool 1	0.378
3	Tool 3	0.184

The relative scoring in Table 6.16 indicates that the use of Tool 2 should be preferred over the use of Tools 1 and 3, in respect to the simulated case study. In addition, Tool 1 should be preferred over Tool 3, even with the respective scores of Accuracy and Detail being significantly lower than in Tool 3. That is due to both ST and OT metrics, which are significantly greater in Tool 1 than in Tool 3.

### 6.6.2 Monte Carlo Method

The Monte Carlo Method was applied to the case study, as described in section 2.3. The generation of random weights for the criteria in the conduction of iterative Monte Carlo simulations were implemented in order to acquire the ranking of the tools within the particular MCDA method, as proposed by Butler J. et al. [3]. The absence of any hierarchical scheme among the criteria of the fidelity framework as well as the assignment of random weighting factors differentiated the method from the aforementioned in the previous section AHP. The consequent absence of the decision-maker in the assignment of weights enhanced

the method with increased objectivity in comparison to the previously applied AHP. Overall, in the application of the Monte Carlo Method the user could examine the sensitivity of the provided rankings.

A series of simulations were conducted in order to result to tool ranking in the implemented tool comparisons. In relation to the comparison between Tools 1 and 2, the Monte Carlo Method was not applied, since the scores of the criteria did not require the additional application of MCDA. Tool 2 outsourced Tool 1 in every criterion, so the application of the particular method was not required. The AHP was applied in the same comparison in order to initially evaluate the applicability of the method and additionally familiarize the reader to the mathematical frameworks that would be applied in the comparison of all Tools 1,2 and 3. In respect to the latter comparison, a series of 10,000 simulations were performed in the tool created by S. Sanchez Perez-Moreno [42]. The results are shown in Figure 6.9.

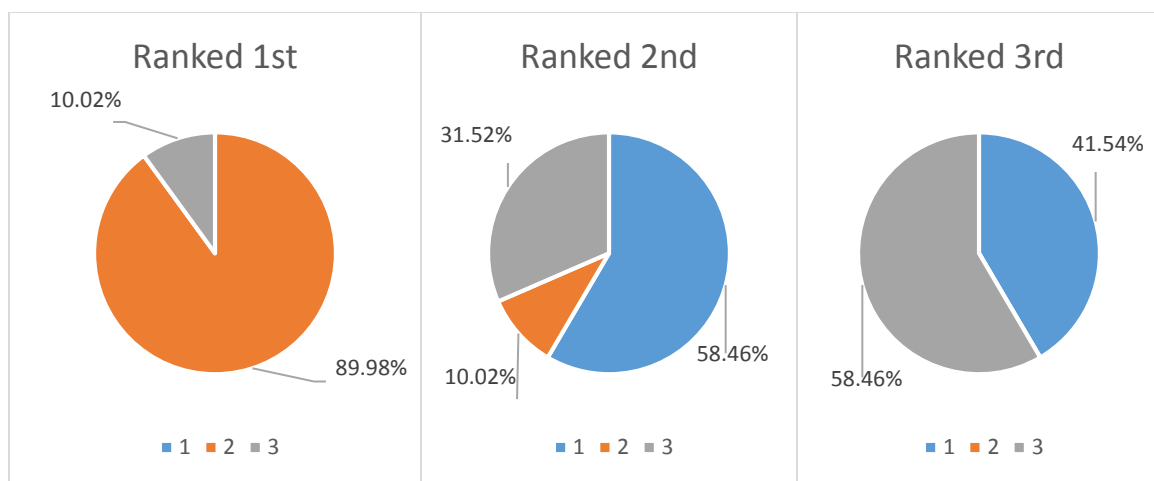


**Figure 6.9:** The pie charts display the percentages of simulations in which each of the tools was ranked 1<sup>st</sup>, 2<sup>nd</sup> and 3<sup>rd</sup> throughout the performed simulations. In that respect, Tool 1 was never ranked 1<sup>st</sup> as Tool 2 was never ranked 3<sup>rd</sup> throughout the whole of simulations. Colors of 1, 2 and 3 of the memorandums correspond to Tool 1, Tool 2 and Tool 3, respectively.

The results of the Monte Carlo Method led to a number of observations. Throughout the whole of simulations, Tool 2 was ranked 1<sup>st</sup> in almost 90% of simulations while Tool 3 topped the rankings in 10% of the 10,000 simulations. The results are similar to the ones of the AHP in terms of the 1<sup>st</sup> place among the tools, which additionally rendered Tool 2 first in the rankings. The fact that Tool 2 was never ranked 3<sup>rd</sup> among the simulations was anticipated since it outsourced Tool 1 in every criterion. In addition, as shown in Figure 6.9, Tool 2 came 2<sup>nd</sup> in only 10% of the simulations, while Tools 1 and 3 were ranked in second place in 58.5% and 31.5% of simulations, respectively. In terms of the bottom position in the tool rankings, Tool 1 came last in 41.5% of the conducted simulations while Tool 3 was ranked 3<sup>rd</sup> in 58.46% in the same set of runs. Overall, the Monte Carlo Method suggested that the use of Tool 2 should be preferred over the use of Tools 1 and 3, which was in agreement to the AHP output.

## 6.7 Discussion

The proposed fidelity framework, comprising of all detail, accuracy, time of simulation and operational time, was applied to two separate types of comparison within the case study. The results were in accordance in both types, justifying the use of Tool 2 over the use of the other two tools and for both MCDA methods. Thus the particular simplified type of fatigue assessment in the FD, as described in section 3.2.3, has been evaluated preferable over the types integrated in Tools 1 and 3, as described in sections 3.2.2 and 3.2.4, at the early design stage of the use case.

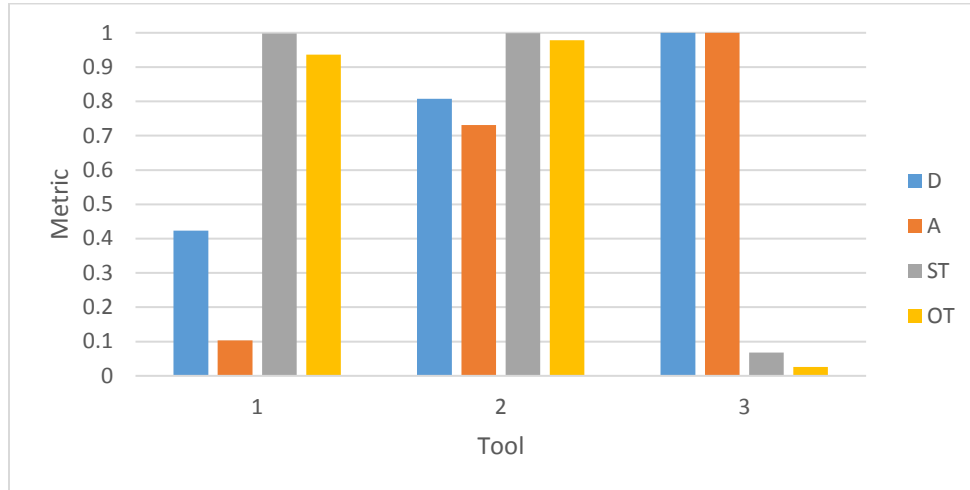


**Figure 6.10:** Illustration of all metric scores for each tool where D, A, ST & OT stand for Detail, Accuracy, Time of Simulation and Operational Time, respectively.

The particular choice of criteria to constitute the full fidelity framework has provided a multifaceted approach. None of the tools had the higher score in all four criteria, as illustrated in Figure 6.10, a fact that intensifies the necessity of using multiple criteria in the fidelity framework. In terms of detail and accuracy, the TD tool yielded the highest score, as anticipated. In contrast, in respect to ST and OT metrics, Tool 2 was justified preferable over all three, while Tool 3 was ranked last. In addition, the popular among relevant fidelity literature trade-off between speed vs accuracy [15] [30] [45] was assessed in both definition of criteria as well as in the MCDA. In the latter, the assignment of factor 3 according to the fundamental scale of Table 2.1 was used in order to marginally favor ST and OT over accuracy & detail, given the early design stage of the suggested use case of Chapter 3.

The inclusion of detail among the criteria of the fidelity framework has been associated to additional fidelity concepts. Simuland, as described in section 2.1, has been defined in an attempt to quantify the appropriate level of reality, given the particular conditions of the use case. In other words, the level of required fidelity of simulation should be referent to that particular depiction of reality, rather than reality itself. Towards that end, the level of detail of Tool 2 was similar to that of Tool 3, the difference between which was anticipated significantly greater [21]. That observation was due to the manner of definition of the detail metric, which comprised of a function of a particular set of parameters, as shown in equation 6.5. In addition, the  $S_2$  set of simulations was established in order to assess the influence of varying pile wall thickness to the ongoing sensitivity analyses of  $S_1$ . In diagram of figure 6.10,

fatigue damage is plotted versus the 5 different pile wall thicknesses which were used in the second set of the sensitivity analyses.

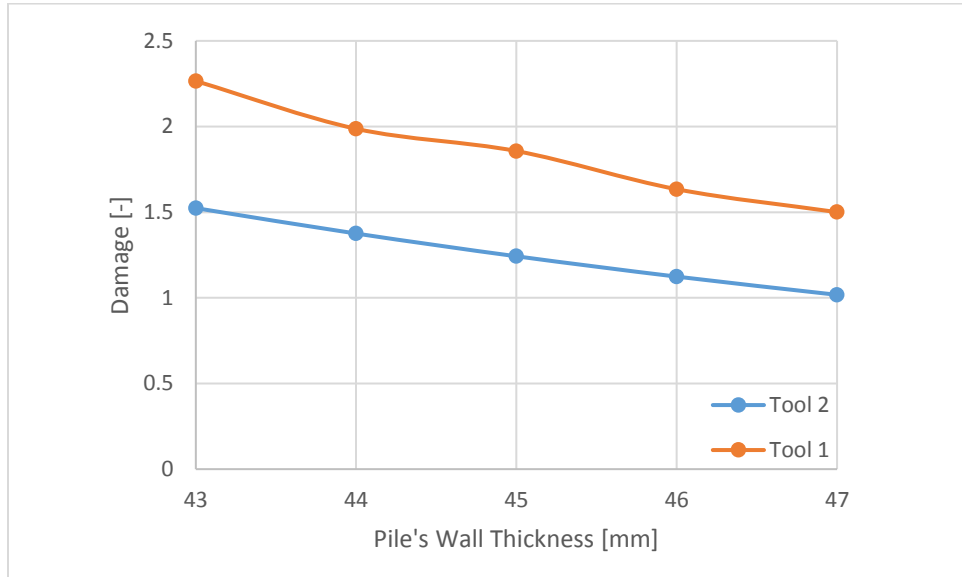


**Figure 6.11:** Damage plotted versus pile's wall thickness in Tools 1 and 2.

As shown in the graph of Figure 6.11, decrease in damage in Tool 2 as a result of the increase in pile's wall thickness seems to be at a constant rate. In Tool 1, there is a rather decreased rate from the second to the third value of pile's wall thickness, but in general, the rate seems to be similar. The results for all five wall thicknesses in every stage of the sensitivity are shown in Tables B.1 and B.2, in Appendix B. The impact of the relative wall thickness assessment on the detail criterion was minor, since the respective rates in the two FD tools were similar. Nevertheless, the full sensitivity analyses should be performed in Tool 3 as well, in order to acquire the relative comparison of all tools that were included in the use case. However the unresolved issues that were described in section 6.5.4 hindered the application of complete sensitivity analyses.

In addition, operational time was included among fidelity criteria in an effort to partially quantify the human factor, as aforementioned in section 2.2.3. Long pre-processing and post-processing times are usually attributed to tool environments that are not user-friendly, as well as to the inability of integration of post-processors, respectively. These usually lead to input errors and foul reading of output, which hinder the process of fatigue damage determination in the tools. The long pre-processing times consumed in Tool 3 as well as the inability of simultaneous simulation of all lumped cases in Tools 1 and 3 rendered Tool 2 preferable. The respective scores in the OT metric, in both sets of comparison, substantiated the above statement. In the first comparison conducted between the two FD tools, Tool 2 scored 0.746 while Tool 1 scored 0.249, as shown in Figure 6.12. Additionally, in the second comparison, Tool 2 yielded a score of 0.978 which is more than an order of magnitude greater than the 0.026 score of Tool 3, as illustrated in Figure 6.12.

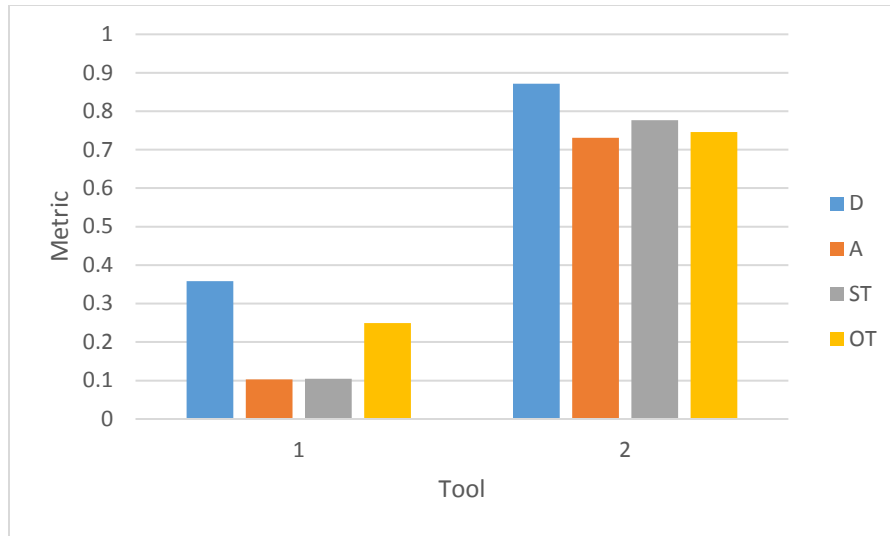


**Figure 6.12:** Illustration of all metrics’ scores for both Tools 1 and 2 where D, A, ST & OT stand for Detail, Accuracy, Time of Simulation and Operational Time, respectively.

The choice of operational time among the criteria has also been both innovative as well as decisive to the final tool ranking. In order to verify the above claim, an additional comparison with the implementation of the AHP type of MCDA was included in Appendix E, and its results substantiated the particular point. In case operational time was omitted from the comparison of all three tools, Tool 2 would still be first in the rankings, but Tool 3 would come second, leaving Tool 1 at the bottom of the respective list, as listed in Table 6.16. Nevertheless the omission of one time criterion from the AHP resulted to the dominance of accuracy and detail over the decreased time criteria. In that manner, they were inevitably assigned higher weights.

**Table 6.16:** Rankings and scores of all 3 tools in case of omission of OT from the fidelity framework within the case study.

Ranking	Alternative	Score
1	Tool 2	0.403
2	Tool 3	0.315
3	Tool 1	0.282

In terms of accuracy, simulations in Tool 2 yielded significantly more accurate results in comparison to Tool 1. The application of a DAF to the quasi-static response of the structure seemed to result in more accurate fore-aft moments PSDs, in comparison to the application of the TRF, as described in [48]. The relevant results of accuracy in both figures 6.10 & 6.12 substantiate the particular claim, in which damage of Tool 2 is directly comparable to the same magnitude of Tool 3.

In order to assess the impact of the MCDA on the proposed fidelity framework, an alternative approach was adopted in which the MCDA application was omitted from the proposed methodology. Instead the criteria would be assigned with the same factors and the summation of their product would result to the fidelity metric. Further ranking of the tools

would solely emerge from the score of their average. In that regard no trade-offs would be assessed between the fidelity criteria and all would be assigned with the same factor. The application of this simplified approach in the comparison between Tools 1, 2 and 3 is conducted through equation 6.25.

$$M_{F,i} = 0.25ST_i + 0.25OT_i + 0.25A_i + 0.25D_i \quad 6.25$$

where  $M_{F,i}$  is the fidelity metric for the  $i^{th}$  alternative. Scores and rankings of Tools 1, 2 and 3 are enlisted in Table 6.17.

**Table 6.17:** Ranking and Scores for Tools 1,2 and 3 after omitting the MCDA.

Ranking	Alternative	Score
1	Tool 2	0.879
2	Tool 1	0.615
3	Tool 3	0.524

The results were similar to those of the two MCDA methods. One again Tool 2 was ranked first , while Tools 1 and 3 came second and third, respectively. The similarity in rankings enhances the objectivity of AHP and credibility of the Monte Carlo Method, since in the former the decision-maker impacts the determination of weights while in the latter random weights are generated through iterative Monte Carlo Simulations.

## 7. Conclusions & Recommendations

A multidisciplinary approach has been suggested in the proposed methodology of the current thesis. Fidelity-related concepts have been defined and quantified in the fidelity framework that was proposed in Chapter 2. The same framework was later fitted to fatigue assessment in order to be conformed to the selected use case of Chapter 3 and later applied in the case study of Chapter 6. The application of the fidelity framework in monopile-based offshore wind turbines has led to conclusions in relation to both credibility and applicability of the developed methodology. In an attempt to further improve that proposed framework, additional recommendations for future work are suggested.

### 7.1 Conclusions

The primary purpose of this thesis was identified in the justification for the selection of the type of fatigue assessment that should be applied to monopile-based offshore wind turbines. Tools 1, 2 and 3 that integrated fatigue assessment in the Frequency Domain (FD), simplified fatigue assessment in the FD and fatigue assessment in the Time Domain (TD), respectively, were examined and a relative comparison was conducted among them. In the offshore wind industry, the use of tools operating in the TD has been established for strength and fatigue checks, that are certified for their high levels of accuracy and detail. Nevertheless, long times of both simulation and operation, along with the additional cost of licensed operation have provided incentives in order to assess the use of other tools instead. Originating from the offshore oil and gas industry, the use of FD tools to perform stability checks at early design stages, has initiated the implementation of FD tools to conduct fatigue assessment of offshore wind turbines. In order to further investigate on their use, a fidelity framework was established within their comparison.

The concept of fidelity was adopted in an attempt to form a framework which would constitute the base of comparison between the tools. Fatigue assessment tools were subject to comparison, in order to examine the use of more cost-efficient tools without decreasing the required levels of accuracy and detail. Towards that end, a series of fidelity criteria were integrated in the proposed fidelity framework, the aggregation of which would result to their eventual levels of fidelity. The selection of all accuracy, time of simulation, operational time and detail was justified integral to substantiate the comparison between the tools, in contrast to alternative concepts such as precision or repeatability that were excluded from the suggested fidelity framework.

In terms of accuracy, the metric was defined in respect to the design driver, as stipulated in the use case. That being fatigue damage, the output of GH Bladed was considered as the referent value for all tools. The results between Tool 2 that operated in the FD, and Tool 3 that operated in the TD, were similar. In addition, similar applications of Tool 2 presented lesser differences in accuracy, especially in the comparison of Damage Equivalent Load (DEL) rather than fatigue damage, in the work of Michalopoulos V. [36]. However the results of Tool 1 in comparison to Tool 3 were discouraging, since the accuracy in fatigue damage was at a significant distance from the referent value. Overall, the choice of accuracy among the criteria provided a versatile approach in the comparison, as it favored Tool 3 over the FD tools, in contrast to the time metrics that resulted to the opposite effect.

Time of simulation (ST) as well as operational time (OT) exerted significant impact on tool comparison. The ST metric values for Tool 3 disadvantaged its use over the FD tools, as the simulations yielded results that were significantly lower in value than in Tools 1 and 2. The derivation of time series for all lumped cases in TD tools greatly contributed to long times of simulation, in contrast to the FD simulations, where simulations were conducted in greater speed. In addition, the complexity of input in TD tools and required post-processing of the results contributed to long operational times, that eventually bottomed Tool 3 in the overall comparison between the three tools. Within the definition of the criterion, the integration of the human factor in the OT metric was achieved, as both long pre-processing and post-processing were quantified in the respective metric.

Both definition and quantification of detail comprised of the most challenging tasks among the 4 criteria, given its heightened abstract nature. Detail would express the abstraction of reality that would be prerequisite to fatigue damage determination. In other words, it would ordain the boundaries of simulation in the tools, that would result to fatigue damage determination. The detail criterion that was assessed in this research comprised of a list of parameters that were deemed essential to fatigue damage determination. As a result, the sensitivity of fatigue damage to alterations in these parameters was examined in order to quantify the criterion. The sensitivity analyses included the assessment of all fatigue related parameters, in which pile's wall thickness was altered in the process. The sensitivities in the fatigue related parameters were justified decisive, as the respective terms exerted significant influence to the metric, while alterations in pile's wall thickness yielded underwhelming results. The latter was attributed to the fact that the respective tools responded to alteration of the pile's wall thickness in similar ways. The results could however be different, in case the full metric could have been applied in all three tools instead of the two FD tools. In addition the results were encouraging, as in two different types of comparison of the tools, the same tool topped the rankings.

Both Analytical Hierarchy Process (AHP) and Monte Carlo Method were applied to the criteria in order to reach to the eventual tool ranking. The implementation of the former Multi-criteria Decision Analysis (MCDA) method resulted to a tool ranking that was influenced at a certain degree by the subjectivity of the decision-maker. The AHP was used because it consists of the most-common MCDA method, as well as due to the hierarchical structure that it stipulates, which was partially implemented during the establishment of the detail criterion. The initial values assigned to the components of the judgmental matrix were extracted from the fundamental scale that was established within the AHP, a choice that had a relative impact on the ranking. However, the relevant values were selected in a manner that would marginally favor ST & OT over detail and accuracy, given the early design stage of the defined use case. In addition, the implementation of the Monte Carlo Method that involved the assignment of randomly generated weighting factors to the criteria during the conduction of iterative Monte Carlo simulations provided results similar to the AHP. The additional types of comparison of Appendix E, that were conducted with both the omission of OT, as well as with the fidelity metric resulting from the average of the criteria, again resulted in ranking Tool 2 over the other two tools. As a result, the consistency and credibility of the proposed fidelity framework was enhanced, since all aforementioned methods provided similar results.

Ultimately, Tool 2 was ranked first among the three examined tools for the selected case study. The level of detail of the specific tool was identified similar to that of Tool 3 which was assigned with the highest detail score among the tools. The application of a Dynamic Amplification Factor (DAF) to the quasi-static response of the structure seemed to result in more accurate fore-aft moments Power Spectral Densities (PSDs), in comparison to the application of the Transfer Functions (TRFs) that were implemented in Tool 1. In addition, the ability of simultaneous simulation of all lumped environmental cases resulted in shorter times of simulations in comparison to the other two tools. In terms of operational time, the user-friendly environment and provision of direct output of the desired fatigue damage value, granted the specific tool the highest score in the OT metric. Conclusively, the application of both types of MCDA as well as the alternative patterns included in Appendix E, all rendered Tool 2 preferable over Tools 1 and 3 for the selected case study.

## 7.2 Recommendations for Future Work

Based on the boundaries of the proposed methodology and the evaluation of its application in the case study of Chapter 6, additional recommendations are provided for relevant future work. These propositions would potentially improve the credibility of the suggested fidelity methodology and therefore increase its applicability in tool comparison. In that respect, the following suggestions should be considered:

- Full implementation of the fidelity framework in the TD tool. The unavailability of licensed operation for GH Bladed over a sustained period of time, as well as the inability to successfully integrate the Rain-Flow Counting (RFC) algorithm in FAST v8 post-processors, hindered sensitivity analyses in the TD tools. The proposed expression for detail and consequently the proposed fidelity methodology would then be re-evaluated.
- Increased number of referent parameters for the detail metric. The inability of extended sensitivity analysis due to tools' limitations constrained the number of parameters from the referent framework that were included in the detail metric.
- Integration of additional criteria to the fidelity framework. An increased amount of criteria would broaden the range of tool comparison and possibly provide more credible results. Specifically, precision and consistency could be included and defined according to the particularities of the suggested use case.
- Application of additional MCDA methods to the eventual ranking of the tools. The extra MCDA methods would potentially provide additional results and therefore additional insight on the overall comparison process. In case all methods resulted to the same ranking, then the reliability of the methodology would be enhanced.
- Application of the methodology in other tools. With suitable modifications depending on the use case, the proposed methodology could be applied in tools that perform other kinds of stability checks. However, the application in optimizers would particularly require inclusion of additional criteria in the proposed framework, such as repeatability or optimality, as suggested by S. Sanchez Perez-Moreno [42].

In conclusion, additional conditions would further enhance the credibility of the proposed methodology. Further sensitivity analyses of additional parameters that determine fatigue damage in offshore wind structures would increase the reliability of the relative tool comparison. The example that stands out is the exclusion of wind and wave misalignment from FLS estimations, due to inability of simulation in the available tools. Nevertheless, the user should not modify existing functions in the examined tools, as that would alter the results of the conducted comparison and render the overall procedure unreliable. Overall, the results emerging from the evaluation of the fidelity framework were justified encouraging. Bearing that in mind, the suggested improvements provide the directions towards which relevant future work could advance and potentially establish the proposed methodology among the candidates in tool comparison.

## Bibliography

- [1] Arany, L. et al. "Simplified critical mudline bending moment spectra of offshore wind turbine support structures." *Wind Energy* (2014).
- [2] Benjamin, P. et al. "Using ontologies for simulation modeling". *Proceedings of the winter simulation conference*. (2006).
- [3] Butler, J., Jia, J., Dyer, J. "Simulation techniques for the sensitivity analysis of multi-criteria decision models". *European Journal of Operational Research* 103 (1997): 531-546.
- [4] Carstens, H., Nielsen, H. B. et al. "Lowering Costs by Individual Design of Foundation Structures". *Ramboll*. (2007).
- [5] Chakraborti, S.K. "Hydrodynamics of Offshore Structures". *Computational Mechanics Publications Southampton*. (1987).
- [6] Dirlik, T. "Application of Computers in Fatigue Analysis". *The University of Warwick*. (1985).
- [7] DNV. "Design of Offshore Wind Turbine Structures". *Offshore Standards*. (2007).
- [8] DNV. "Environmental Conditions and Environmental Loads". *Offshore Standards*. (2010).
- [9] DNV. "Fatigue Design of Offshore Steel Structures". *Offshore Standards*. (2012).
- [10] Engelen, T., Oei, T., Rieffe, H., Dragt, J. "TURBU-I Computer Program for Turbulence Load Analysis of Horizontal Axis Wind Turbines". *ECN*. (1991).
- [11] Foster, L. "Fidelity in Modelling and Simulation". *Spring Simulation Interoperability Workshop*. (1997).
- [12] Giannakoglou, K. H., Anagnostopoulos, I., Bergeles, G. "Numerical Analysis for Engineers". *National Technical University of Athens*. (2003).
- [13] Girard, A. Pappas, G. J. "Approximation Metrics for Discrete and Continuous Systems". *IEEE Transactions on Automatic Control* 52 (2007): 782-798.
- [14] Gross, D. C. "A case study in fidelity differential measurements". *Spring Simulation Interoperability Workshop*. (1998).
- [15] Gross, D. C. Roza, M. et al. "Report from the Fidelity Implementation Study Group". *99 Spring Simulation Interoperability Workshop Paper 167*. (1999).
- [16] Hayman, G. J., M. Buhl, Jr. "MLife User's Guide for Version 1.00". *NREL Technical Report*. (2012).
- [17] IEC. "IEC 61400-1 Ed.3: Wind Turbines – Part 1: Design requirements". (2005).
- [18] IEC. "IEC 61400-3 Ed.3: Wind Turbines – Part 3: Design requirements for offshore wind turbines". (2007).

- [19] Institute of Electrical and Electronics Engineers. "Standard for Distributed Interactive Simulation – Fidelity Description Requirements". IEEE. (1995).
- [20] Jonkman J. M., Robertson A. N., Hayman G. J. "Hydrodyn User's Guide and Theory Manual". NREL. (2016).
- [21] Jonkman, J. "FAST v8.16.00a-bjj". National Renewable Energy Laboratory. (2016).
- [22] Jonkman, J. et al. "Definition of a 5-MW Reference Wind Turbine for Offshore System Development". National Renewable Energy Laboratory. (2009).
- [23] ] Kragh, A. K. Fleming, P. "FAST – HAWC2 Model Conversion MATLAB Toolbox – Manual". Risø DTU and NREL. (2011).
- [24] Levin, J. "Choice under Uncertainty". Stanford University. (2006).
- [25] Loper, L. M. "Modeling and Simulation in the Systems Engineering Life Cycle". Georgia Tech Research Institute. (2015).
- [26] Lourens, E. M. "Course Introduction". Offshore Wind Farm Design. Course Lecture. TU Delft. (2015).
- [27] Lourens, E. M. "Loads & Load Cases". Offshore Wind Support Structures. Course Lecture. Delft University of Technology. (2015).
- [28] Lourens, E. M. "Monopile Design – Part 1", Offshore Wind Farm Design. Course Lecture. TU Delft. (2015).
- [29] Lourens, E. "Monopile Design – Part II", Offshore Wind Support Structures. Course Lecture. TU Delft. (2015).
- [30] Mateo, J. R. S. C. "Multi-Criteria Analysis in the Renewable Energy Industry". Green Energy and Technology. (2012).
- [31] Mathworks, 2015 (accessed April 2016). [Online]. Available: <http://www.mathworks.com/matlabcentral/fileexchange/50608-counting-the-floating-point-operations--flops-/content/CountFLOP/FLOPS.m>
- [32] Matthies, H. G., et al. "Study of Offshore Wind Energy in the EC". Joule I (JOUR 0072). Verlag Natürliche Energie. Brekendorf. (1995).
- [33] McDonald, B. "A proposed process for defining required fidelity of simulations". Spring Simulation Interoperability Workshop. (1998).
- [34] van der Meulen, M. B. "Influence of Nonlinear Irregular Waves on the Fatigue Loads of an Offshore Wind Turbine". Delft University of Technology. (2012).
- [35] Meyer, R. J. "You say resolution, I say fidelity, You say accuracy, I say detail,.... Let's not call the whole thing off!" Spring Simulation Interoperability Workshop. (1998).

- [36] Michalopoulos, V. "Simplified fatigue assessment of offshore wind support structures accounting for variations in a farm". TU Delft. (2016).
- [37] Moler, C. "Numerical Computing with MATLAB". SIAM. (2004).
- [38] Mrsnik, M., Slavic, J., Boltezar, M. "Frequency-domain methods for a vibration-fatigue-life estimation - Application to real data". Faculty of Mechanical Engineering, University of Lubljana. (2016).
- [39] Newland, D. E. "An introduction to Random vibrations and spectral analysis". Longman Scientific & Technical. (1993).
- [40] Osgood, B. "The Fourier Transform and its Applications". Electrical Engineering Department of Stanford University.
- [41] Pace, D. K. "The Roles of Metrics in Simulation Verification and Validation". Spring Simulation Interoperability Workshop. (2003).
- [42] Sanchez Perez-Moreno, S. "Model Fidelity Selection for Multi-disciplinary Design Analysis and Optimization of Offshore Wind Farms". University of Delft. (2015).
- [43] Sanchez Perez Moreno, S. et al. "Model Fidelity Selection in the Multidisciplinary Design Analysis and Optimisation of Wind Energy Systems". Journal of Physics: Conference Series 753. (2016).
- [44] Ponnusamy, S. S. A., Thebault, P. "A Simulation Fidelity Assessment Framework". Institute of Electrical and Electronics Engineers. (2014).
- [45] Roza, Z. C. "Simulation fidelity theory and practice". PhD thesis, TU Delft. (2005).
- [46] Roza M., J. Voogd, H., J., van Gool, P. "Fidelity Requirements Specification: A Process Oriented View". "99 Fall Simulation Interoperability Workshop". Paper 032. (1999).
- [47] Saaty, T. "The analytical hierarchy process". McGraw-Hill. (1980).
- [48] van der Tempel, J. "Design of support structures for offshore wind turbines". TU Delft. (2006).
- [49] Tervonen, T. "Stochastic Multicriteria Acceptability Analysis". Faculty of Economics and Business, University of Groningen. (2010).
- [50] Thompson, W. J., MacDonald, J. R. "Discrete and integral Fourier transforms: Analytical examples". Department of Physics and Astronomy, University of North Carolina. (1993).
- [51] Tovo, R. "Cycle distribution and fatigue damage under broad-band random loading". Int. J. Fatigue, 24(11):1137-1147. (2002).
- [52] Tsoutsos, T. et al. "Sustainable energy planning by using multi-criteria analysis application in the island of Crete". Energy Policy 39 (2009): 1587-1600.

- [53] Veldkamp, H. F. "Chances in wind energy: a probabilistic approach to wind turbine fatigue design". TU Delft. (2006).
- [54] Vugts, J. "Handbook of Bottom Founded Offshore Structures – Volume 1". Delft University of Technology. (2002).
- [55] Waegter, J. "Stress range history and Rain Flow counting". (2009).
- [56] Wheeler, J. D. "Method for Calculating Forces Produced by Irregular Waves". Journal of Petroleum Technology 22.03 (1970): 359-367.
- [57] Zaaier, M.B. "Strength and Fatigue". Introduction to Wind Energy. Course Lecture. Delft University of Technology. (2014).
- [58] Zaaier, M. B. "Dynamics". Introduction to Wind Energy. Course Lecture. Delft University of Technology. (2014).
- [59] Ziegler, B. P. et al. "Theory of modelling and simulation". Academic Press. (2000).
- [60] 4coffshore, 2016 (accessed May, 2016). [Online]. Available: <http://www.4coffshore.com/>
- [61] Argos, 2016 (accessed May, 2016). [Online]. Available: <http://www.argos-system.org/using-argos/argos-platforms/>
- [62] TU Delft, 2016 (accessed May, 2016). [Online]. Available: <https://www.tudelft.nl/lr/organisatie/afdelingen/aerodynamics-wind-energy-flight-performance-and-propulsion/wind-energy/education/master-projects/current-master-projects>

# Appendix A – Environmental Data

**Table A.1:** The 3-D scatter diagram that was used in order to extract the initial lumped states.

ts	Tz	1.0-2.0	2.0-3.0	3.0-4.0	4.0-5.0	5.0-6.0	6.0-7.0	7.0-8.0	8.0-9.0	9.0-10.0	10.0-11.0	11.0-12.0	12.0-13.0	13.0-14.0		
>4.0	28.0-30.0							6.04E-05	2.01E-05							
	26.0-28.0							0								
	24.0-26.0						6.04E-05	8.05E-05	4.03E-05							
	22.0-24.0					2.01E-05	0.000161	0.000201	8.05E-05	0.000121						
	20.0-22.0						0.000423	0.000523	0.000181	8.05E-05	2.01E-05					
	18.0-20.0						0.001208	0.001651	0.000382	8.05E-05						
	16.0-18.0						0.00151	0.00308	0.000644		2.01E-05					
	14.0-16.0						0.000443	0.002456	0.000443							
	12.0-14.0						0.000443	0.002134	0.000262	2.01E-05						
	10.0-12.0							4.03E-05	2.01E-05							
22.0-24.0					2.01E-05	2.01E-05										
20.0-22.0					0.000121	0.000101										
3.5-4.0	18.0-20.0				8.05E-05	0.001006										
	16.0-18.0				2.01E-05	0.003885	0.000242									
	14.0-16.0					0.005857	0.001449	2.01E-05								
	12.0-14.0					0.002516	0.00153	0.000141								
	10.0-12.0					0.000342	0.000242									
	8.0-10.0					0.000101	4.03E-05									
6.0-8.0					0	2.01E-05										
3.0-3.5	22.0-24.0					2.01E-05										
	20.0-22.0				0.000121											
	18.0-20.0				0.000624	0.000101										
	16.0-18.0				0.002053	0.001228										
	12.0-14.0				0.000906	0.010145	0.000845									
	10.0-12.0				6.04E-05	0.004811	0.000423									
	8.0-10.0				2.01E-05	0.000765	2.01E-05									
	6.0-8.0					0.000121	2.01E-05									
2.5-3.0	22.0-24.0					2.01E-05										
	20.0-22.0					2.01E-05										
	18.0-20.0				4.03E-05	0.000242										
	16.0-18.0					0.002778	2.01E-05									
	12.0-14.0					0.016184	0.003462	2.01E-05								
	10.0-12.0					0.011842	0.006522	2.01E-05								
	8.0-10.0					0.00469	0.002234									
	6.0-8.0					0.000745	0.000926									
	4.0-6.0					0.000121	0.000181									
	2.0-4.0						4.03E-05									
2.0-2.5	20.0-22.0					2.01E-05										
	18.0-20.0					4.03E-05	2.01E-05									
	16.0-18.0					0.000604	0.000181									
	12.0-14.0					0.004409	0.012607	8.05E-05								
	10.0-12.0					0.001127	0.03285	0.000101								
	8.0-10.0					0.000141	0.022853	0.000403								
	6.0-8.0					2.01E-05	0.008635	0.000584								
	4.0-6.0						0.001993	0.000282								
	2.0-4.0						0.000664	4.03E-05								
	0.0-2.0						0.000181									
1.5-2.0	16.0-18.0					6.04E-05										
	12.0-14.0					0.015882	0.000503									
	10.0-12.0					0.032005	0.005153	2.01E-05								
	8.0-10.0					0.033145	0.016586	4.03E-05								
	6.0-8.0					0.013043	0.0187	0.000403	2.01E-05							
	4.0-6.0					0.002093	0.01093	0.000564	0							
	2.0-4.0					0.000403	0.00467	0.000201	2.01E-05							
	0.0-2.0					6.04E-05	0.000986	4.03E-05	2.01E-05							
1.0-1.5	16.0-18.0					2.01E-05										
	12.0-14.0				0.000684	0.001812										
	10.0-12.0				0.003563	0.022021	4.03E-05									
	8.0-10.0				0.005717	0.063265	0.000765									
	6.0-8.0					0.000523	0.064754	0.006802	8.05E-05	2.01E-05						
	4.0-6.0					0.028643	0.015318	0.000543								
	2.0-4.0					0.00944	0.012158	0.000564	4.03E-05	2.01E-05						
	0.0-2.0					0.002174	0.004408	0.000322	2.01E-05							
0.5-1.0	12.0-14.0					2.01E-05										
	10.0-12.0					0.000644	2.01E-05									
	8.0-10.0					0.016244	0.003684	2.01E-05								
	6.0-8.0					0.048752	0.03275	0.001188	2.01E-05	4.03E-05						
	4.0-6.0					0.02186	0.058192	0.011802	0.00151	0.000282	0.000101	2.01E-05	4.03E-05			
	2.0-4.0					0.001751	0.032045	0.01713	0.002536	0.000342	0.000201	6.04E-05	2.01E-05	4.03E-05	4.03E-05	0.000121
0.0-2.0					0.000242	0.010849	0.008052	0.001167	0.000181	0.000101	2.01E-05	0	4.03E-05	4.03E-05	0	
0.0-0.5	8.0-10.0					4.03E-05										
	6.0-8.0					0.002154	0.000735									
	4.0-6.0					0.000101	0.017915	0.011071	0.002637	0.000604	0.000302	0.000181	0.000101	4.03E-05		
	2.0-4.0					8.05E-05	0.01252	0.021182	0.006663	0.002033	0.001268	0.000403	0.000221	0.000141		
	0.0-2.0					2.01E-05	0.004247	0.010326	0.003764	0.001349	0.000765	0.000322	0.000181	4.03E-05		

**Table A.2:** The lumped environmental states, as resulted from Table A.1.

States	$V_{avg}$ (m/s)	TI	TI(%)	$H_s$ (m)	$T_p$ (s)	Occ. (%)
1	2.644	0.3441	34.4	0.75	5.5	7.4779
2	3.966	0.2594	25.9	1.25	6.5	7.2142
3	5.288	0.2171	21.7	1.75	6	5.2093
4	6.610	0.1917	19.2	0.25	8	10.1405
5	6.610	0.1917	19.2	0.75	7	9.3807
6	9.254	0.1626	16.3	1.25	5.5	7.1880
7	10.576	0.1535	15.4	3.5	7	4.0036
8	13.221	0.1408	14.1	0.75	5.5	10.3321
9	14.543	0.1362	13.6	2.25	5.5	8.6346
10	15.865	0.1324	13.2	2.75	6	8.6346
11	17.187	0.1291	12.9	0.75	5	9.7886
12	17.187	0.1291	12.9	1.75	5.5	10.3334
13	26.441	0.1154	11.5	6.5	8	1.6566

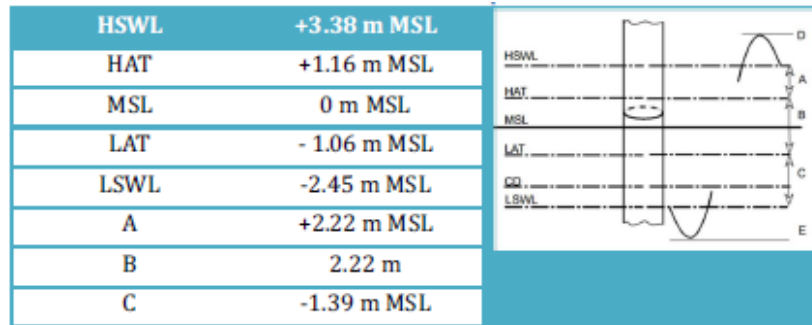


**Figure A.1:** Sea elevations in the installation site, in respect to MSL.

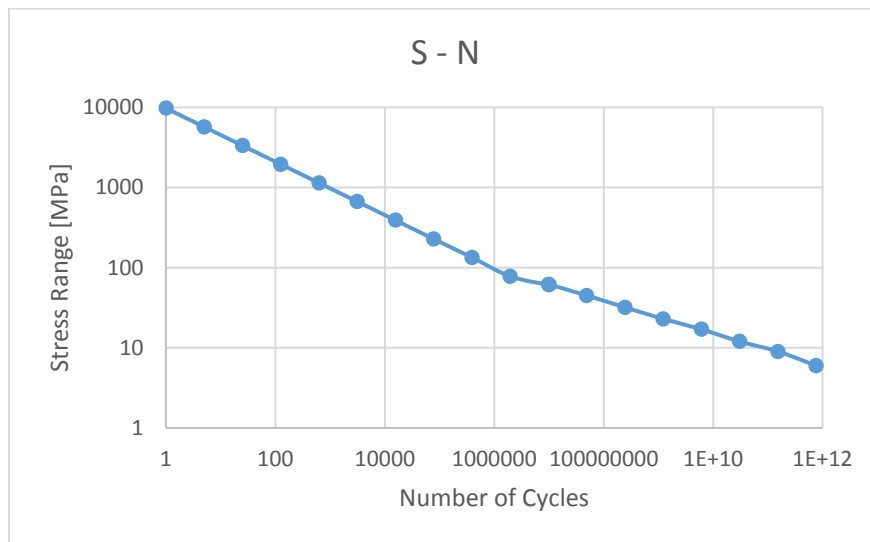


**Figure A.2:** The S-N curve used in fatigue assessment [9]

## Appendix B – Sensitivity Analyses Data

**Table(s) B.1:** Results of Sensitivity Analyses of simulations  $S_1$  &  $S_2$  in Tool 1.  $p/p_r$  expresses the ratio of 0.25 – 2 that was used for each parameter, as listed in the following 4 sub-tables.

$p/p_r$	0.25	0.25	0.25	0.25	0.25	0.5	0.5	0.5	0.5	0.5
t	$t_1$	$t_2$	$t_3$	$t_4$	$t_5$	$t_1$	$t_2$	$t_3$	$t_4$	$t_5$
U	1.8817	1.6981	1.5175	1.3612	1.2261	3.1335	2.8277	2.5270	2.2667	2.0418
TI	1.3942	1.2605	1.1335	1.0247	0.9374	3.0573	2.7640	2.4856	2.2470	2.0556
$H_s$	0.6359	0.5737	0.5178	0.4680	0.4236	0.8585	0.7746	0.6991	0.6318	0.5719
$T_p$	13.0731	11.7945	10.6545	9.6317	8.7154	1228.3633	1108.2300	1001.1111	905.0044	818.9089
TR	4.1085	3.7050	3.3457	3.0251	2.7368	4.1409	3.7343	3.3721	3.0490	2.7584
d	0.4076	0.4040	0.4008	0.3976	0.3944	0.6690	0.6631	0.6578	0.6525	0.6473

$p/p_r$	0.75	0.75	0.75	0.75	0.75	1.25	1.25	1.25	1.25	1.25
t	$t_1$	$t_2$	$t_3$	$t_4$	$t_5$	$t_1$	$t_2$	$t_3$	$t_4$	$t_5$
U	3.4272	3.0928	2.7639	2.4792	2.2332	5.1429	4.6411	4.1475	3.7203	3.3512
TI	3.7647	3.4035	3.0607	2.7669	2.5312	6.3101	5.7048	5.1302	4.6377	4.2427
$H_s$	1.9235	1.7356	1.5664	1.4157	1.2813	7.3755	6.6548	6.0061	5.4283	4.9130
$T_p$	12.9974	11.7262	10.5928	9.5759	8.6649	1.8301	1.6511	1.4916	1.3484	1.2201
TR	4.1731	3.7633	3.3983	3.0727	2.7798	4.2407	3.8242	3.4533	3.1224	2.8248
d	1.4311	1.4185	1.4072	1.3959	1.3847	-	-	-	-	-

$p/p_r$	1.5	1.5	1.5	1.5	1.5	1.75	1.75	1.75	1.75	1.75
t	$t_1$	$t_2$	$t_3$	$t_4$	$t_5$	$t_1$	$t_2$	$t_3$	$t_4$	$t_5$
U	5.8223	5.2542	4.6954	4.2118	3.7939	7.9917	7.2118	6.4449	5.7811	5.2075
TI	9.6036	8.6823	7.8078	7.0583	6.4571	12.1656	10.9985	9.8908	8.9412	8.1797
$H_s$	13.1521	11.8669	10.7102	9.6799	8.7609	22.3650	20.1795	18.2125	16.4605	14.8978
$T_p$	1.3682	1.2344	1.1151	1.0081	0.9122	0.8380	0.7561	0.6830	0.6174	0.5587
TR	4.2748	3.8550	3.4811	3.1475	2.8475	4.3079	3.8849	3.5081	3.1720	2.8696
d	-	-	-	-	-	-	-	-	-	-

$p/p_r$	2	2	2	2	2
t	$t_1$	$t_2$	$t_3$	$t_4$	$t_5$
U	8.2884	7.4796	6.6842	5.9957	5.4008
TI	19.1730	17.3336	15.5878	14.0914	12.8911
$H_s$	35.4315	31.9691	28.8530	26.0773	23.6018
$T_p$	0.6820	0.6153	0.5558	0.5024	0.4546
TR	4.3427	3.9162	3.5364	3.1975	2.8928
d	-	-	-	-	-

**Table(s) B.2:** Results of Sensitivity Analyses of simulations  $S_1$  &  $S_2$  in Tool 2.  $p/p_r$  expresses the ratio of 0.25 – 2 that was used for each parameter, as listed in the following 4 sub-tables.

$p/p_r$	0.25	0.25	0.25	0.25	0.25	0.5	0.5	0.5	0.5	0.5
t	$t_1$	$t_2$	$t_3$	$t_4$	$t_5$	$t_1$	$t_2$	$t_3$	$t_4$	$t_5$
U	0.0089	0.0079	0.0071	0.0064	0.0057	0.1868	0.1672	0.1499	0.1347	0.1214
TI	0.0339	0.0305	0.0274	0.0248	0.0227	0.0952	0.0850	0.0761	0.0685	0.0619
$H_s$	1.3153	1.1863	1.0711	0.9681	0.8762	1.3519	1.2195	1.1011	0.9954	0.9009
$T_p$	1.5421	1.3915	1.2568	1.1363	1.0286	2.1329	1.9362	1.7594	1.6005	1.4576
TR	1.4760	1.3303	1.2013	1.0862	0.9827	1.4907	1.3450	1.2148	1.0985	0.9905
D	0.0006	0.0006	0.0006	0.0006	0.0006	0.7677	0.6874	0.6164	0.5534	0.4975
$L_p$	0.0006	0.0006	0.0006	0.0006	0.0006	0.7126	0.6789	0.5894	0.5323	0.4579
$\varphi$	-	-	-	-	-	-	-	-	-	-
$\gamma$	1.5237	1.3753	1.2426	1.1238	1.0176	1.4231	1.3023	1.2102	1.1239	1.0841
$L_s$	1.5237	1.3753	1.2426	1.1238	1.0176	1.5237	1.3753	1.2426	1.1238	1.0176
$Z_p$	0.8757	0.7845	0.7038	0.6320	0.5685	1.0646	0.9557	0.8591	0.7733	0.6970
$L_g$	1.4822	1.3377	1.2084	1.0928	0.9895	1.4673	1.3241	1.1960	1.0815	0.9792
$Z_{TP}$	1.5237	1.3753	1.2426	1.1238	1.0176	1.5237	1.3753	1.2426	1.1238	1.0176

$p/p_r$	0.75	0.75	0.75	0.75	0.75	1.25	1.25	1.25	1.25	1.25
T	$t_1$	$t_2$	$t_3$	$t_4$	$t_5$	$t_1$	$t_2$	$t_3$	$t_4$	$t_5$
U	1.7738	1.6077	1.4587	1.3247	1.2041	1.9847	1.7979	1.6309	1.4814	1.3475
TI	0.4389	0.3906	0.3483	0.3114	0.2792	3.6854	3.3697	3.0838	2.8248	2.5899
$H_s$	1.4175	1.2789	1.1551	1.0443	0.9454	1.6909	1.5275	1.3812	1.2502	1.1328
$T_p$	1.7542	1.5850	1.4334	1.2976	1.1760	1.4283	1.2888	1.1641	1.0526	0.9529
TR	1.5068	1.3598	1.2284	1.1109	1.0056	1.5394	1.3897	1.2558	1.1359	1.0287
D	1.0873	0.9778	0.8795	0.7922	0.7145	2.1091	1.9116	1.7344	1.5750	1.4313
$L_p$	0.9654	0.9458	0.8513	0.7865	0.6850	2.1437	2.0986	1.7987	1.5982	1.4562
$\varphi$	1.5783	1.5623	1.4532	1.2832	1.1932	1.2352	1.1982	1.1384	0.9321	0.8923
$\gamma$	1.5661	1.5602	1.4419	1.2819	1.1873	1.4287	1.3184	1.2839	1.1527	1.0782
$L_p$	1.5237	1.3753	1.2426	1.1238	1.0176	1.5237	1.3753	1.2426	1.1238	1.0176
$Z_p$	1.2796	1.1522	1.0388	0.9367	0.8459	1.7975	1.6265	1.4734	1.3355	1.2115
$L_g$	1.4894	1.3442	1.2143	1.0981	0.9942	1.5587	1.4072	1.2716	1.1502	1.0417
$Z_{TP}$	1.5237	1.3753	1.2426	1.1238	1.0176	1.5237	1.3753	1.2426	1.1238	1.0176

p/p <sub>r</sub>	1.5	1.5	1.5	1.5	1.5	1.75	1.75	1.75	1.75	1.75
T	t <sub>1</sub>	t <sub>2</sub>	t <sub>3</sub>	t <sub>4</sub>	t <sub>5</sub>	t <sub>1</sub>	t <sub>2</sub>	t <sub>3</sub>	t <sub>4</sub>	t <sub>5</sub>
U	3.3499	3.0609	2.8003	2.5651	2.3523	7.9882	7.3661	6.8008	6.2861	5.8169
TI	7.1174	6.5600	6.0526	5.5899	5.1677	12.0022	11.1187	10.3120	9.5741	8.8983
H <sub>s</sub>	1.9479	1.7626	1.5963	1.4471	1.3132	2.3433	2.1261	1.9307	1.7550	1.5968
T <sub>p</sub>	1.3911	1.2551	1.1336	1.0249	0.9278	1.3738	1.2395	1.1194	1.0121	0.9162
TR	1.5558	1.4049	1.2697	1.1486	1.0403	1.5724	1.4201	1.2837	1.1614	1.0520
D	2.8749	2.6165	2.3837	2.1728	1.9825	3.8538	3.5188	3.2165	2.9433	2.6960
L <sub>p</sub>	2.0452	2.0065	1.7753	1.6432	1.4824	1.6982	1.6723	1.6237	1.5239	1.3896
φ	-	-	-	-	-	-	-	-	-	-
γ	2.1452	2.1132	2.0972	1.9235	1.8461	1.7528	1.7421	1.7319	1.7062	1.6982
L <sub>s</sub>	1.5237	1.3753	1.2426	1.1238	1.0176	1.5237	1.3753	1.2426	1.1238	1.0176
Z <sub>p</sub>	2.1038	1.9079	1.7317	1.5734	1.4307	2.4434	2.2206	2.0203	1.8390	1.6757
L <sub>g</sub>	1.5899	1.4356	1.2974	1.1737	1.0631	1.6156	1.4590	1.3187	1.1932	1.0808
Z <sub>TP</sub>	1.5237	1.3753	1.2426	1.1238	1.0176	1.5237	1.3753	1.2426	1.1238	1.0176

p/p <sub>r</sub>	2	2	2	2	2
t	t <sub>1</sub>	t <sub>2</sub>	t <sub>3</sub>	t <sub>4</sub>	t <sub>5</sub>
U	9.6036	8.8790	8.2161	7.6408	7.0533
TI	18.4909	17.1866	15.9935	14.9004	13.8973
H <sub>s</sub>	2.9392	2.6276	2.4390	2.2250	2.0319
T <sub>p</sub>	1.3644	1.2310	1.1117	1.0051	0.9098
TR	1.5902	1.4365	1.2987	1.1751	1.0646
d	5.0707	4.6462	4.2617	3.9118	3.5940
L <sub>p</sub>	1.5623	1.5237	1.4937	1.3492	1.3293
φ	-	-	-	-	-
γ	1.6213	1.6192	1.6034	1.5917	1.5807
L <sub>s</sub>	1.5237	1.3753	1.2426	1.1238	1.0176
Z <sub>p</sub>	2.8201	2.5668	2.3392	2.1341	1.9486
L <sub>g</sub>	1.6357	1.4773	1.3354	1.2084	1.0947
Z <sub>TP</sub>	1.5237	1.3753	1.2426	1.1238	1.0176



## Appendix C – Times of Simulation

**Table C.1:** Time of Simulation as measured in Tool 1 for all lumped cases of the case study.

Simulation in Tool 1	Measured Time for each Simulated Lumped State [s]												
	1	2	3	4	5	6	7	8	9	10	11	12	13
1	1.239	1.447	1.322	1.219	1.334	1.361	1.614	1.255	1.383	1.516	1.355	1.548	1.847
2	1.565	1.346	1.274	1.659	1.238	1.426	1.584	1.128	2.135	1.754	1.187	1.335	1.997
3	1.397	1.907	2.052	1.476	1.252	1.631	1.839	1.272	1.788	1.399	1.159	1.394	1.967
4	1.192	1.922	1.846	1.461	1.204	1.614	1.468	1.520	1.728	1.495	1.394	1.305	2.779
5	1.288	1.315	1.999	1.326	1.141	1.296	1.517	1.254	1.582	1.730	1.242	1.573	1.936
6	1.596	1.477	1.664	1.092	1.246	1.432	1.521	1.296	1.567	1.670	1.112	1.324	2.067
7	1.453	1.367	1.437	1.385	1.253	1.237	1.840	1.601	1.739	1.587	1.570	1.452	2.242
8	1.657	1.092	1.630	1.407	1.048	1.209	1.695	1.181	1.649	1.529	1.287	1.600	1.817
9	1.339	1.531	1.710	1.220	1.237	1.557	1.791	1.422	1.563	1.512	1.419	1.539	2.101
10	1.212	1.428	1.287	1.057	1.046	1.594	1.459	1.464	1.522	1.635	1.246	1.323	2.181

**Table C.2:** Time of Simulation as measured in Tool 2 for the case study.

Simulation in Tool 2	Simulation Time [s]
1	12.174
2	12.248
3	8.653
4	7.842
5	7.481
6	10.419
7	12.502
8	12.288
9	11.477
10	9.684

**Table C.3:** Time of Simulation of the first 7 lumped states of the case study in Tool 3.

Simulation in Tool 3	Measured Time for each Simulated Lumped State [s]						
	1	2	3	4	5	6	7
1	361.128	432.984	478.380	385.338	384.726	361.128	432.984
2	370.350	420.912	421.890	354.756	412.434	415.650	468.828
3	438.912	365.922	425.928	361.176	394.398	434.634	418.986
4	359.118	414.186	419.010	430.410	434.478	408.852	422.094
5	425.364	464.556	483.114	437.640	457.428	474.792	485.706
6	385.554	447.546	410.472	413.664	421.566	410.538	388.236
7	367.776	401.772	402.078	374.766	395.838	397.170	373.224
8	358.992	425.538	304.344	426.012	415.446	442.020	444.552
9	411.360	474.186	476.472	485.514	491.154	458.646	511.986
10	379.266	362.472	409.506	390.186	417.738	412.332	474.210

**Table C.4:** Times of Simulation for the remaining 6 lumped states of the case study in Tool 3.

Simulation in Tool 3	Measured Time for each Simulated Lumped State [s]					
	8	9	10	11	12	13
1	538.380	543.846	335.256	373.290	455.286	491.730
2	482.508	524.544	419.226	425.671	477.486	514.152
3	471.246	477.444	359.166	418.392	418.872	582.186
4	483.366	537.204	411.750	431.731	485.706	605.706
5	419.886	457.806	421.705	386.694	479.106	485.142
6	403.890	419.940	356.046	437.700	414.078	505.716
7	378.078	414.204	380.460	428.916	425.760	474.336
8	478.890	455.646	410.166	483.426	485.772	507.570
9	416.706	362.634	422.886	517.158	504.912	534.306
10	424.548	460.188	412.500	479.352	471.450	539.658

## Appendix D – Operational Times

**Table D.1:** Preprocessing Operational Time [PRT] and Operational Time for each of the first 8 lumped states of the use case throughout all 10 simulations in Tool 1 for the case study.

Simulation in Tool 1	PRT [s]	Operational Time for each of the Lumped States [s]							
		1	2	3	4	5	6	7	8
1	109.31	13.18	13.56	14.08	12.28	13.56	8.55	14.29	14.64
2	108.52	15.09	13.45	14.56	13.55	13.64	9.41	14.23	14.93
3	110.39	16.92	13.23	13.10	12.68	13.39	9.87	14.54	14.78
4	103.67	15.14	14.89	13.89	12.56	13.12	9.34	14.12	13.95
5	101.32	13.23	12.75	12.99	13.35	13.29	9.65	14.07	14.06
6	103.67	16.47	12.94	13.15	13.52	12.71	8.82	13.89	14.38
7	109.43	15.92	12.81	13.50	12.91	13.22	8.91	13.86	15.03
8	99.89	14.65	11.98	13.09	12.85	14.28	9.07	13.47	14.72
9	98.78	13.76	13.04	13.44	12.84	13.36	9.64	13.52	14.55
10	99.45	12.92	13.42	14.09	13.11	14.72	9.03	13.72	14.29

**Table D.2:** Operational Time as measured for the latter 5 lumped cases as well as Post-processing Time (POT) throughout all 10 simulations in Tool 1 for the case study.

Simulation in Tool 1	Operational Time for each of the Lumped States [s]					POT [s]
	9	10	11	12	13	
1	14.95	11.95	13.40	8.98	13.93	20.96
2	15.84	12.24	13.61	8.51	14.43	19.54
3	15.13	12.73	13.57	9.04	14.36	20.01
4	15.01	11.91	13.85	8.54	14.29	19.87
5	13.41	11.75	13.48	9.12	14.76	19.41
6	14.10	12.17	13.74	8.50	14.45	19.36
7	14.79	12.05	13.52	8.06	15.06	19.86
8	14.22	12.01	14.09	8.67	15.47	20.82
9	14.16	11.72	13.54	8.68	14.90	19.97
10	14.51	12.14	12.96	9.33	14.72	18.92

**Table D.3:** Operational Time as measured in Tool 2 for the case study.

Simulation in Tool 2	Operational Time [s]
1	282.07
2	276.05
3	289.14
4	271.68
5	263.93
6	271.50
7	274.89
8	266.52
9	278.14
10	263.51

**Table D.4:** Operational Time as measured for the first 8 lumped cases as well as Preprocessing Time (PRT) throughout all 10 simulations in Tool 3 within the framework of the case study.

Simulation in Tool 3	PRT [s]	Operational Time for each of the Lumped States [s]							
		1	2	3	4	5	6	7	8
1	326.88	30.14	28.01	29.67	28.04	28.89	23.91	27.61	28.81
2	323.97	30.04	29.20	28.55	30.79	30.56	23.93	28.88	27.87
3	334.99	30.40	28.68	28.22	30.06	29.78	23.39	29.39	28.93
4	320.84	29.70	30.00	30.78	30.28	30.03	22.46	27.72	27.68
5	319.53	30.70	29.20	29.08	30.29	29.99	21.45	29.72	27.95
6	318.40	29.03	30.74	30.64	29.10	30.02	22.68	26.70	28.05
7	321.85	30.32	28.39	28.62	28.71	29.65	21.47	27.95	26.34
8	318.16	29.64	29.44	28.42	29.39	28.95	22.88	26.44	26.30
9	318.32	28.73	29.31	29.14	29.42	29.11	23.39	26.03	26.77
10	316.21	28.85	28.20	28.00	28.21	29.05	22.22	26.07	28.52

**Table D.5:** Operational Time as measured for the latter 5 lumped cases as well as Post-processing Time (POT) throughout all 10 simulations in Tool 3 for the case study.

Simulation in Tool 3	Operational Time for each of the Lumped States [s]					POT [s]
	9	10	11	12	13	
1	28.45	26.72	26.15	20.97	27.40	50.21
2	27.68	26.11	25.48	20.61	27.37	49.61
3	26.37	25.30	25.78	19.25	26.39	48.39
4	29.30	26.73	24.07	19.64	25.57	49.27
5	28.10	26.10	25.58	20.51	27.61	52.50
6	29.51	25.02	25.77	20.37	26.82	48.72
7	28.88	27.45	24.28	21.29	27.63	47.13
8	28.67	26.26	26.70	19.97	27.43	48.34
9	29.56	26.67	26.21	19.01	25.77	46.98
10	27.24	27.19	25.90	19.77	26.08	47.47



## Appendix E – Alternative Patterns

$$A_{j,E} = \begin{bmatrix} 1 & 2 & 2 \\ \frac{1}{2} & 1 & 1 \\ \frac{1}{2} & 1 & 1 \end{bmatrix}$$

E.1: Judgmental Matrix for the 3 criteria.

$$A_{jnorm,E} = \begin{bmatrix} \frac{1}{2} & \frac{1}{2} & \frac{1}{2} \\ \frac{1}{4} & \frac{1}{4} & \frac{1}{4} \\ \frac{1}{4} & \frac{1}{4} & \frac{1}{4} \end{bmatrix}$$

E.2: Normalized Judgmental Matrix for the 3 criteria.

$$W_E = [0.5 \quad 0.25 \quad 0.25]$$

E.3: Weighting Vector resulting from  $A_{jnorm,E}$ .

$$ST_E = \begin{bmatrix} 1 & 1 & 9 \\ 1 & 1 & 9 \\ \frac{1}{9} & \frac{1}{9} & 1 \end{bmatrix}$$

E.4: Comparison matrix for  $ST$ .

$$A_E = \begin{bmatrix} 1 & \frac{1}{5} & \frac{1}{9} \\ 5 & 1 & \frac{5}{9} \\ 9 & \frac{9}{5} & 1 \end{bmatrix}$$

E.5: Comparison matrix for Accuracy.

$$D_E = \begin{bmatrix} 1 & \frac{1}{3} & \frac{1}{5} \\ 3 & 1 & \frac{3}{5} \\ 5 & \frac{5}{3} & 1 \end{bmatrix}$$

E.6: Comparison Matrix for Detail.

$$c_{1,E} = \begin{bmatrix} \frac{9}{19} & \frac{9}{19} & \frac{1}{19} \end{bmatrix}$$

E.7: Weighting Vector for ST.

$$c_{2,E} = \begin{bmatrix} \frac{1}{15} & \frac{5}{15} & \frac{9}{15} \end{bmatrix}$$

E.8: Weighting Vector for Accuracy.

$$c_{3,E} = \begin{bmatrix} \frac{1}{9} & \frac{1}{3} & \frac{5}{9} \end{bmatrix}$$

E.9: Weighting Vector for Detail.